Title

Filamentous Fungal Mycelium as an Edible Carrier for Cultivated Meat

Author

Ogawa, Minami

Publication Date

2024

Peer reviewed|Thesis/dissertation

Filamentous Fungal Mycelium as an Edible Carrier for Cultivated Meat

By

MINAMI OGAWA

DISSERTATION

Submitted in partial satisfaction of the requirements for the degree of

DOCTOR OF PHILOSOPHY

in

Food Science and Technology

in the

OFFICE OF GRADUATE STUDIES

of the

UNIVERSITY OF CALIFORNIA

DAVIS

Approved:

_____

David E. Block (Chair)

_____

Keith Baar

_____

Karen McDonald

Committee in Charge

2024

Table of Contents

Acknowledgments

I extend my deepest gratitude to my esteemed advisor, Professor David Block, whose invaluable guidance and mentorship have been pivotal throughout my doctoral journey. His wealth of knowledge, unwavering support, and encouragement have profoundly shaped both my research and personal growth, while providing me with the autonomy to explore new ideas and push the boundaries of innovation in the field of cellular agriculture.

I am also immensely grateful to my committee members, Professor Keith Baar and Professor Karen McDonald, for their insightful feedback, constructive advice, and steadfast support. Their expertise and dedication have been instrumental in refining this work and helping me navigate the many challenges of the research process.

I am immensely thankful to all of my research colleagues in the Block Lab, whose collaborative spirit and scientific rigor have contributed greatly to my development. Special thanks to my undergraduate researchers, Mayrene Huynh and Damian Teria, whose dedication and contributions played a pivotal role in the success of my experiments. I also can't emphasize how proud I am of each of your individual accomplishments!

I extend my heartfelt appreciation to the CMC/iCAMP team, led by Director Kara Leong, for supporting me and disseminating my work at events and conferences around the globe. I am also grateful to the Nitin Lab, Baar Lab, Smith Lab, Leach Lab, McDonald/Nandi Lab, Moreno-Garcia Lab at the University of Córdoba, and Barzee Lab at the University of Kentucky, whose collaborations expanded the breadth of my research.

To my startup and everyone at Optimized Foods, your presence has continuously motivated me to merge academia with innovation and has transformed my research into a tangible and tasty reality! I

also want to thank Supply Change Capital for teaching me valuable insights into the venture capital food technology landscape.

My journey would not have been the same without the camaraderie of my FST cohort and classmates, whose friendship and support made the challenges of graduate life fun and relatable. Especially to Justin Wong, who has been there to empathize with every struggle I've had to overcome. And to Linda Bisson, Lucy Joseph, and Vidhya Ramakrishnan for laying the foundation of my scientific research endeavors.

I am deeply grateful to the funding organizations that made this work possible: NSF, CA State Fund, IIFH, and the UC Davis Food Science Department. Their support allowed me to pursue my research with fewer limitations.

Lastly, to my friends and family—especially my dear mom and loving partner—your unwavering encouragement, care, and patience have been the bedrock of my perseverance. From starting this PhD at the beginning of a pandemic to ending it with two major knee surgeries, you have seen and supported me through it all. This dissertation is as much a reflection of your love as it is of my efforts. For that, I am eternally grateful.

Abstract

This work addresses the challenges of developing edible microcarriers for cultivated meat production, specifically using the biomass of edible filamentous fungi as a material. Leveraging the work of yeast immobilization in the field of wine microbiology, this new application aims to contribute to the hurdles of current cultivated meat production—cost and scalability. Beginning with a proof of concept that filamentous fungal biomass can serve as a support for cell adhesion, it assesses the attachment of yeast and myoblast cells on fungal pellets. Experimental studies explore the proliferation and differentiation of animal cells on the carriers compared with the performance of conventional non-edible microcarriers. Building on these findings, subsequent studies investigate the compatibility of mycelium carriers with bovine satellite cells, using Raman spectroscopy to identify key molecular properties that influence cell attachment. This work advances the field of cellular agriculture by offering insights into edible carrier development, presenting a pathway for cultivated meat production that is one step closer to achieving an integrated bioprocess for animal cell proliferation and differentiation.

CHAPTER 1: Introduction

Whole Cell Immobilization for Cultivated Meat

Expanding the methods for protein production is essential for our future of food systems. Large-scale conventional animal agriculture is the primary source of dietary protein but is associated with the rise of zoonotic diseases, antibiotic resistance, and environmental degradation, including deforestation and biodiversity loss. This together with the world's growing population and climate variability necessitates innovative protein production systems that meet future human consumption and nutritional needs (Karimi et al., 2018). The alternative protein industry aims to improve environmental and human health by reducing the demand for industrial-scale meat production and thereby lowering greenhouse gas emissions and animal waste runoff (Eshel et al., 2014; Nijdam et al., 2012; Steinfeld et al., 2006; Westhoek et al., 2014). Alternative methods for meat production could also protect against supply chain disruptions during epidemics and natural disasters (Biggs et al., 2015). Within this sector, the emerging field of cultured meat, which involves growing meat biomass ex vivo by culturing precursor cells from animals in a bioreactor, offers a complementary approach to meat production. Life cycle assessments (LCA) suggest that cultured meat could significantly reduce land use and greenhouse gas emissions compared to traditional meat production (Mattick et al., 2015; Tomiyama et al., 2020; Tuomisto & Teixeira de Mattos, 2011). However, widespread adoption relies on cultivated meat to have cost parity and sensory and nutrient qualities at scale to meet the predicted demands of consumers.

Tissue engineering and biomaterial approaches, such as 3D printed scaffolds and nanofiber sheets, have enabled the generation of skeletal muscle tissue in vitro at the laboratory scale (Kwee & Mooney, 2017). These advancements have laid the groundwork for the development of cultured meat technologies (Bach et al., 2003; DiEdwardo et al., 1999; Huang et al., 2006; Kim et al., 2018). Producing cultured meat

as a food source requires approximately 10^{11} cells for a single kilogram of animal meat, which requires cells to be grown at large scales in bioreactors (Bodiou et al., 2020). This non-native environment can lead to anoikis—a form of programmed cell death—if cells are not adapted to suspension growth, grown as spheroids, or otherwise tricked into anchorage independence using small molecules such as Rho kinase (ROCK) inhibitors (Frisch & Screaton, 2001). However, in vivo, muscle tissue cells (including precursor myoblasts, satellite muscle cells, and myotubes) attach to the extracellular matrix (ECM), which plays a critical role in the formation and development of skeletal muscle (Ahmad et al., 2023). The ECM localizes growth factors that influence the proliferation and differentiation of muscle satellite cells (Thomas et al., 2015). In vitro experiments have shown that substrate surface topology impacts C2C12 muscle cell proliferation and differentiation, while substrate stiffness regulates myoblast differentiation and skeletal muscle stem cell expansion (Cooper et al., 2010). A commonly used method to bypass anoikis in suspension-based bioreactors while still providing ECM-like cues involves using microcarriers.

Microcarriers are small bead-like structures that allow cells to attach by mimicking ECM characteristics such as stiffness, topography, and porosity (McKee & Chaudhry, 2017; Rafiq et al., 2013). They offer several advantages in bioreactor cultures, including a large surface area to volume ratio, which permits high cell densities relative to 2D culture. They are controllable and can be used in flexible bioprocessing pipelines (e.g., batch, fed-batch, perfusion). Cell expansion using microcarriers can occur in several ways. Cells are seeded and proliferate on carriers. Upon reaching confluency, cells can be enzymatically dissociated from the carriers and passaged to larger vessels with new carriers via a seed train process (Oh et al., 2007; Rafiq et al., 2013). Another method is bead-to-bead transfer, where cells migrate to new microcarriers that are added mid-culture, allowing a continuous cultivation process (Verbruggen et al., 2018). Microcarriers can support differentiation triggered by changes in media components, microcarrier characteristics, or shear forces through mechanotransduction (A. K.-L. Chen et al., 2014).

Thus, microcarriers offer immense potential for scaling relevant stem cell populations and providing differentiated cell types for cultivated meat production by leveraging bioengineering principles.

Microcarrier use in cultivated meat production has been demonstrated using bovine myoblasts in a spinner flask bioreactor with inert, synthetic microcarriers like dextran (Cytodex) beads (Verbruggen et al., 2018). These non-edible microcarriers are commonly utilized because they have a growth surface that supports the proliferation and differentiation of various animal cells, mainly for use in cell therapy and pharmaceutical applications. However, dissociating cells from inedible microcarriers complicate downstream processing for cultured meat applications (Bodiou et al., 2020). In most cases, complete dissociation is nearly impossible and can lead to downstream processing complications(Bomkamp et al., 2022). Cells that did not completely dissociate remain on discarded microcarriers, leading to product loss. Microcarriers can also only be reused a finite number of times, and used carriers will generate unrecyclable solid waste or be a point of contamination if not properly sterilized between uses. In a more hazardous situation, incomplete removal of carriers could introduce health risks such as microplastic ingestion.

Another option to circumvent the use of nonedible microcarriers is to use dissolvable materials. Dissolvable carriers are constructed from degradable materials like denatured collagen, cross-linked polygalacturonic acid, and alginate, which can be dissolved after the microcarrier cells have reached confluency(Ng et al., 2021; Rodrigues et al., 2019; Yan et al., 2020). Corning has commercialized a dissolvable carrier made of crosslinked polygalacturonic acid (PGA) that is dissolved using an EDTA solution, which works by destabilizing the PGA crosslinking in combination with pectinase that digests the polymer. Alginate beads are also shown to be dissolvable with 0.1M phosphate-buffer solution (Gray & Dowsett, 1988). However, like synthetic carriers, the dissolution process introduces additional complexity and costs to cell culture. Because dissolvability is dependent on microcarrier contact with the dissolving solution, carriers may not properly dissolve if beads are completely confluent and covered

entirely with cells. How the cells handle stress experienced in the dissolving process, sometimes induced by changes in temperature, has yet to be determined. Thermal and photodegradation methods are generally unsuitable for cell culture due to their harsh conditions. The high temperatures required for thermal polymer degradation and the ultraviolet radiation needed for photolytic, photo-oxidative, and thermo-oxidative reactions can denature proteins and damage DNA, particularly within the UVC (200–280 nm) and UVB (280–320 nm) ranges(Pathak & Navneet, 2017; Yousif & Haddad, 2013).

Process efficiency is best achieved with edible carriers that can be incorporated directly into the final product, simplifying the bioprocess by eliminating the need for dissociation or dissolution steps and contributing to the overall mass yield (Bodiou et al., 2020; Pajčin et al., 2022). Several edible materials have been developed and proven compatible with cell growth. These include rice grains coated with fish gelatin and decellurized plant cell tissue from asparagus (Murugan et al., 2024; Park et al., 2024). Spherical or grooved gelatin microcarriers have also been shown to support the proliferation and differentiation of C2C12 cells (Norris et al., 2022). These 3D-printed carriers incorporate specific spatial patterns compatible with cells to control tissue formation. Similarly, 3T3-L1 preadipocytes and primary porcine satellite cells were grown on commercially available porous gelatin microcarriers (Y. Liu et al., 2022). Various cell types, i.e., C2C12, 3T3-L1, primary porcine satellite, and commercially available chicken satellite cells, proliferate on alginate microcarriers coated with gelatin, and this surface also supports the differentiation of C2C12 cells (Kong et al., 2022). Many of these carriers can be incorporated or used as scaffolds to create fibrous structures for cultivated meat products that mimic the native striated architecture of skeletal muscle. Centimeter-scale pieces of cultured meat can be produced using edible scaffolds and cooked to achieve desired sensory properties (Tsuruwaka & Shimada, 2022).

Edible food-grade carriers, which require the least processing steps, are abundantly available, scalable, and cost-efficient are best suited as a material for cultivated meat microcarriers. Filamentous fungal

biomass, or mycelium, is a candidate biomaterial that fits these criteria. In addition to being a food-grade, raw ingredient in alternative proteins known as mycoprotein, mycelium can grow rapidly on low-cost feedstocks such as agricultural waste residues, adding to the sustainability component that other edible biomaterials lack. The following section explains how to use mycelium as a support to immobilize whole cells, and this dissertation covers the development of mycelium carriers as a tool for cultivated meat production.

Mycelium as an edible material for whole-cell immobilization

Ubiquitous in nature as decomposers with complex enzyme systems, filamentous fungi possess unique attributes and relationships with macro- and microorganisms in the environment. They can convert substrates such as agricultural waste from food processing byproducts to higher-value products. Filamentous fungi also form complex relationships with other microbes in the environment, for instance, in soil (i.e., mycorrhizal fungus and rhizobia bacteria) and lichen (i.e., filamentous fungus, microalgae, and/or yeast (Frey-Klett et al., 2011; Hawksworth, 1988; Spribille et al., 2016). Filamentous fungi are valuable in industrial biotechnology as cell factories for producing useful molecules worth billions of dollars annually (Füting et al., 2021). The biomass of filamentous fungi has emerged as a new generation of biological, abundant, and nutritional material with diverse applications.

Immobilizing cells on support materials is an important technique in various bioprocesses. Cellular immobilization can improve the performance of microbial fermentations and wastewater treatment systems by increasing cell densities in bioreactors, insulating cells from rapid or harmful changes in the external environment, increasing reactor stability, and separating cells from bulk media to facilitate cellular harvest and reuse(García-Martínez et al., 2012; Karel et al., 1985; Mehrotra et al., 2021; Moreno-García, García-Martínez, et al., 2018; Ravi Kumar, 2000; Zhu, 2007). The attachment of cells to supports or “scaffolds” is also required to properly develop cells into desired materials, such as tissue

formation (Bomkamp et al., 2022; Fish et al., 2020). Supporting materials become necessary for anchorage-dependent cell types or require a surface to adhere to maintain viability and biological activity. Materials used in cellular immobilization can utilize natural organic polymers (e.g., alginate, gelatin, agar, chitosan) and synthetic polymers (e.g., polyvinyl alcohol (PVA), polyacrylamide (PAM), polyethylene (PE), and polyvinyl chloride (PVC)). Applications of these systems are well reviewed elsewhere (Bomkamp et al., 2022; Mehrotra et al., 2021; Moreno-García, García-Martínez, et al., 2018).

Filamentous fungal biomass can be an ideal support for whole-cell attachment of various organisms without additional synthetic supports. It is composed of a network of self-growing, fibrous, elongated cells (hyphae), and their chemical and physical properties can be adjusted depending on the growth conditions and the substrate they are fed. In submerged fermentation, mycelia can form various macromorphologies, including dispersed hyphae, compact pellets, or loose clumps, which are influenced by the physicochemical culture conditions and the fungal species (J. Zhang & Zhang, 2016; Zhou et al., 2012). Spherical pellets are conventionally produced on an industrial scale and offer a favorable morphology for biotechnological applications. They have several advantageous characteristics, including ease of harvest and recycling, long-term storability, low broth viscosity, improved culture rheology resulting in better mass and oxygen transfer, and lower energy input (Nyman et al., 2013; Zhou et al., 2012). The dense, porous, and flexible hyphal structure of these pellets enables them to withstand mechanical forces and facilitates efficient mass transfer. In addition, it can enhance and prolong the production of specific metabolites (Baptista et al., 2006; Groboillot et al., 1994; Nedović et al., 2015; Sakurai et al., 2000; Williams & Munnecke, 1981).

The composition of fungal cell walls, which consists of proteins, glucans, and chitin, provides anchor points for flocculating cell receptor ligands, making fungal pellets an excellent platform for scalable cell immobilization in large-scale fermentation and cultivation processes (Moreira et al., 1996; Ogawa et al., 2019). By adjusting the culture conditions, such as reducing peptone concentration, promoting autolysis,

or intensifying agitation, fungi can form spherical masses called pellets and accumulate a larger population of encapsulated cells within (Fu et al., 2014; Metz & Kossen, 1977; Truong et al., 2004). In addition, filamentous fungal biomass is a sustainable and biodegradable alternative to other immobilization supports, which may otherwise contain ingredients that are animal-derived, highly processed, and/or non-renewable. They have carbon sequestering capabilities, which can help offset greenhouse gas release into the atmosphere - all of which support the circular bioeconomy (Clemmensen et al., 2013).

Various cell types (e.g., animal, yeast, microalgae, and bacteria cells) have been immobilized in many species of filamentous fungal biomass (e.g., *Aspergillus* sp., *Penicillium* sp., *Pleurotus* sp.) and studied over the past two decades (Figure 1). The number of immobilized cells on mycelium (reported per mass, volume, pellet, etc, depending on application) typically measures the performance of whole-cell immobilization carriers (Moreno-García, García-Martínez, et al., 2018). In general, higher cell densities equal higher final mass yield and/or improved titers for metabolites. Because of this, many studies focus on improving cell adherence or increasing cell growth in mycelium carriers through modifications of preculture steps. Two main methods have been reported for immobilizing cells on mycelial biomass (J. Chen et al., 2018). While details and nuances vary across studies and applications, the immobilization method generally falls under fungal spore-assisted (FSA) or fungal pellet-assisted (FPA), both illustrated in Figure 2. FSA involves the co-culture of fungal spores and another microbe. Fungal spores and microbes are precultured separately in their respective growth medium until the desired cell mass is achieved. The fungal spores and cells are then co-cultivated where fungal mycelium typically develops into small pellets with cells immobilized in a complex mycelial matrix. This method entraps cells within the pellets, and immobilized cells can be found in and around the pellet biomass. The FPA method, on the other hand, similarly precultures fungal spores and cultures separately, but fungal culture is grown until mycelial pellets form. At this stage, the mycelial pellets are inactivated, when seeding animal cells,

or left active, when working with yeast cells and microalgae. The fungal pellets and immobilization cells are then added to a nutrient-rich medium and incubated. During this time, the cells adhere to the fungal pellets. Various mechanisms have been hypothesized to describe the attachment and adherence of cells to pellets. The mechanisms are likely system-specific but are thought to broadly include protein-mediated, hydrophobic, electrostatic, and van der Waals interactions along with salt bridging or cross-linking of biopolymers (Ogawa et al., 2019). A summary of interactions that have been hypothesized and/or demonstrated with different cellular immobilization systems is shown in Figure 3.

The use of whole-cell immobilization on a mycelial biomass has multiple functions, including intensified fermentations, production of mycoprotein and alternative meat, production of biofuels, and wastewater treatment. This dissertation explores the use of mycelium biomass as a support material for whole-cell immobilization in food applications. Cell immobilization in the food and beverage industry was first reported on yeast, particularly for alcoholic fermentations like wine and beer. The techniques and knowledge gained from yeast immobilization have laid the groundwork for more innovative uses, including the more recent application of immobilizing animal cells for cultivated meat, which is the primary focus of this work.

Mycelium as a carrier for food applications

Yeast cell immobilization for alcoholic beverage fermentations

Yeast immobilized on mycelium pellets function as a tool to facilitate the production of alcoholic beverages. Compared with other immobilization systems, cell confinement within mycelial pellets does not necessitate the addition of chemicals or inert external support to the wort (Peinado et al., 2006). The porous and flexible fungal hyphae network can withstand severe mechanical strain in bioreactors, while other conventional systems cannot. Alginate beads, a conventionally used yeast immobilization technology, can burst during fermentation due to high shear stress and vigorous gas production and

cause the release of carrier particles and yeast cells from the alginate immobilizer into the medium, which can obstruct filters during the downstream process (Duarte et al., 2013). In a case where alginate beads vs. fungal yeast cell immobilization were used to produce sparkling wine, alginate was reported to increase calcium and sodium ions in the finished wine and cause crystal precipitation and undesired flavors. Riddling, or the process of settling and removing precipitates from wine, was possible with yeast biocapsules in two minutes, whereas a typical riddling lasts for about 24 days (López de Lerma et al., 2018; Puig-Pujol et al., 2013).

Sensory improvements were reported when using the yeast-fungal pellet system to produce natural sweet wine, IPA-beer brewing, young white wine, Sherry wine, and red raspberry wine; versus the conventional immobilization method: i.e., alginate beads and/or suspended yeast cells (García-Martínez et al., 2015; Lu, Liu, et al., 2024; Ogawa, Carmona-Jiménez, et al., 2022; Pastor-Vega et al., 2023; Rojas López-Menchero et al., 2021). These finished alcoholic beverages, such as beer, resulted in improved sensory profiles when yeast biocapsules were used but cell retention through alcoholic fermentation of the beer wort was lower when compared with alginate beads. This lowers the clarification efficiency. More recently, biocapsules were used to make wine out of red raspberries (M. Liu et al., 2022). These authors reported that yeast immobilized in fungal pellets exhibit superior fermentation capabilities compared to free yeast. It effectively preserves the anthocyanins, polyphenols, and active compounds in red raspberries, thereby enhancing the quality of wine. This yeast immobilization method not only improves aroma components such as alcohols and esters, contributing to a more pleasant sensory experience but also maintains consistent fermentation performance even after three consecutive fermentations. Yeast biocapsules could also be used as a bioactive or drug-delivery vehicle for functional foods. In a study immobilizing curcumin-loaded yeasts on fungal pellets, curcumin, the model bioactive compound, resulted in gradual, more controlled release during the gastrointestinal phase, showing promising results as a tool to increase the bioaccessibility of micronutrients (Lu, Ogawa, et al., 2024).

Yeast cells attached to mycelium carriers work well due to their high immobilization efficiency, reporting up to 93.2% immobilization in some cases (García-Martínez et al., 2012; Moreno-García, García-Martinez, et al., 2018). However, cell leakage from the carrier and cell proliferation in the surrounding medium have been observed during alcoholic fermentations. Different approaches have been attempted to circumvent this limitation. Moreno-Garcia et al. demonstrated a 2.5-fold improvement through the use of specific biofilm forming yeast strains (Moreno-García, García-Martinez, et al., 2018). Additionally, the overexpression of the FLO11 gene (involved in yeast biofilm formation) led to a remarkable 5-fold improvement in immobilization (Moreno-García, Martín-García, et al., 2018). Moreover, alginate coating of the yeast-fungal pellet system has also been tested, showing a 4 and 6-fold cell retention improvement after fermentation (Rojas López-Menchero et al., 2021). Other proposed modifications to enhance yeast cell-hyphae attachment are to utilize filamentous fungi with the ability to synthesize significant amounts of hydrophobins and oxylipins, overexpressing yeast biofilm formation genes, and incorporating polycations while lowering the pH of the cell immobilization medium (Ogawa et al., 2019). In Chapter 2 of this dissertation, we discuss inactivation methods to increase the immobilization rate, which was achieved in 3 days compared to the former method, which took a 12-day cycle.

More recently, a novel FPA approach to immobilize yeast cells into fungal pellets has been attempted and applied for a patent (GARCÍA et al., 2024). It consists of: (1) separate culture of yeasts and fungal pellets to avoid competition and promote biomass productivity; (2) mixing the fungal pellet and yeast cells; (3) infusion of yeast cells into pellets through a vacuum step; and finally, (4) fungal pellet-yeast cell culture in a medium that promotes additional growth. Compared to the FSA method, this procedure improves cell retention 2-fold and offers several advantages including better scalability, lower contamination risk, and improved productivity. In addition, the methodology is not only limited to the

immobilization of yeast cells but also can be applied to encapsulate different types of microorganisms, such as bacteria or microalgae; or even cells from pluricellular organisms.

Animalia cell immobilization for cultivated meat production

Filamentous fungi, such as *Aspergillus oryzae* and *Rhizopus oligosporus*, have a long history of use in food production, particularly in traditional fermented foods such as soy sauce, tempeh, and koji. These fungi have gained attention as a promising source of alternative proteins for food and feed applications due to their ability to produce a wide range of functional and nutritious proteins with desirable characteristics such as high solubility, digestibility, and amino acid profiles (Zeng et al., 2022). Fungal mycelium is also attractive for sustainable food systems because it can be grown on various substrates such as agricultural residues, food waste, and lignocellulosic biomass to produce mycoprotein. This protein-rich biomass can be processed into various meat alternatives and plant-based foods (Barzee et al., 2021, 2022). However, most of these food applications mainly use mycelium as an ingredient in food products and do not yet leverage mycelium's functional attributes as an immobilization support. An exception to this is the use of filamentous fungi as both a support and ingredient for cultivated meat production, as they offer several advantages such as fast growth rates, high yields, and the ability to produce a variety of meat-like textures and flavors (Letcher et al., 2022; Ogawa, Carmona-Jiménez, et al., 2022).

Recent studies have reported on the successful attachment of animal cells to mycelium biomass compared to commercially available nonedible supports. Studies that reported on animal cell growth on mycelium biomass are compiled and presented in Table 1. In particular, Letcher et al. increased lipid accumulation in immobilized insect cells, which could be suitable for fat-based foods. Manduca sexta (tobacco hornworm) embryonic primary cell growth was shown on decellularized ExcellTM mycelium scaffolds (Letcher et al., 2022). Mycelia scaffold supported lipid accumulation and displayed mechanics

amenable for fat-based foods, providing a tool to enhance flavor, texture, and nutritional properties to cultured meat. Other studies that look at using mycelia as edible microcarriers are the focus of this dissertation and are discussed in depth in the following chapters.

Review of Dissertation

This dissertation is about the development of mycelium as an edible microcarrier for cultivated meat applications. Chapter 2, published in MDPI Foods, introduced the proof of concept, fabricating mycelial pellets from food-grade fungi, inactivating them, and using yeast and C2C12 myoblasts as model cell types to establish a successful attachment to the carrier. Chapter 3, published in npj Science of Food, built upon the POC, exploring proliferation and differentiation potential on mycelium carriers and extending the technology to include the culture of bovine satellite cells, a cell type more amenable to cultivated meat. Chapter 4 explores the attachment mechanism between Animalia cells and mycelium carriers, which identifies critical molecular vibrations of the surface chemistry of mycelium pellets using Raman spectroscopy to predict the best bSC attachment performance. The practical implications of this research have garnered interest beyond the academic setting, leading to the filing of a provisional patent, which was subsequently converted into an international PCT patent in 2024. This patent has since been exclusively licensed to a spinoff company based in Davis, CA. As a result, this work is already making tangible contributions to the rapidly expanding field of alternative proteins, solidifying its place in the ongoing advancements within this innovative sector. This dissertation delves deeply into the development of mycelium carriers, offering a scientific perspective on how to adapt existing food-grade materials for application in the emerging sector of cultivated meat.

Tables & Figures

Table 1. Immobilization of animal cells in filamentous fungal supports.

Filamentous Fungus Strain	Immobilized Cell Strain	Purpose	Scale	Reference

Aspergillus sp.	Human keratinocyte cell line (CRL-2310)	Mycelium as a scaffold for keratinocytes proliferation and differentiation with applications in tissue engineering, regenerative medicine, and wound healing	1mL in 24 well plates	(Narayanan et al., 2020)
Pleurotus ostreatus DSM1119 *Ganoderma lucidum* DSM962	Primary human dermal fibroblasts (HDFa, Thermo Fisher Scientific)	Mycelium as a scaffold for human fibroblasts biocompatibility and interaction. Applications are intended to be as an alternative to traditional tissue engineering scaffolds	1mL in 24 well plates 1mL in 24 well plates	(Antinori et al., 2021)
Excell scaffold	*Drosophila melanogaster* embryonic cells *Maduca sexta* (tabacco hornworm)	Mycelium as a scaffold for insect fat cell attachment and growth. The applications are intended to develop a low-cost, scalable and nutritious method for cultured fat production for cellular agriculture and cultivated meat.	96 well plate	(Letcher et al., 2022)
Aspergillus oryzae	C2C12 murine myoblast	Mycelium as a support for mammalian cell attachment and growth. The proposed application is to use mycelium as an edible carrier or scaffold for cellular agriculture and cultivated meat.	200 uL in 96 well plates	(Ogawa, Moreno García, et al., 2022)
Aspergillus oryzae *Aspergillus awamori* *Aspergillus sojae* *Aspergillus nishimurae* *Aspergillus tubingensis* *Rhizopus oligosporus* *Penicillium chysogenum*	C2C12 murine myoblast & bovine satellite cells	Mycelium as a support for mammalian cell attachment and growth for cultivated meat research. Different combinations of various fungal strains and mammalian cells were explored. Differentiation of mammalian cells on mycelium was studied.	200 uL in 96 well plates	(Ogawa, 2024)

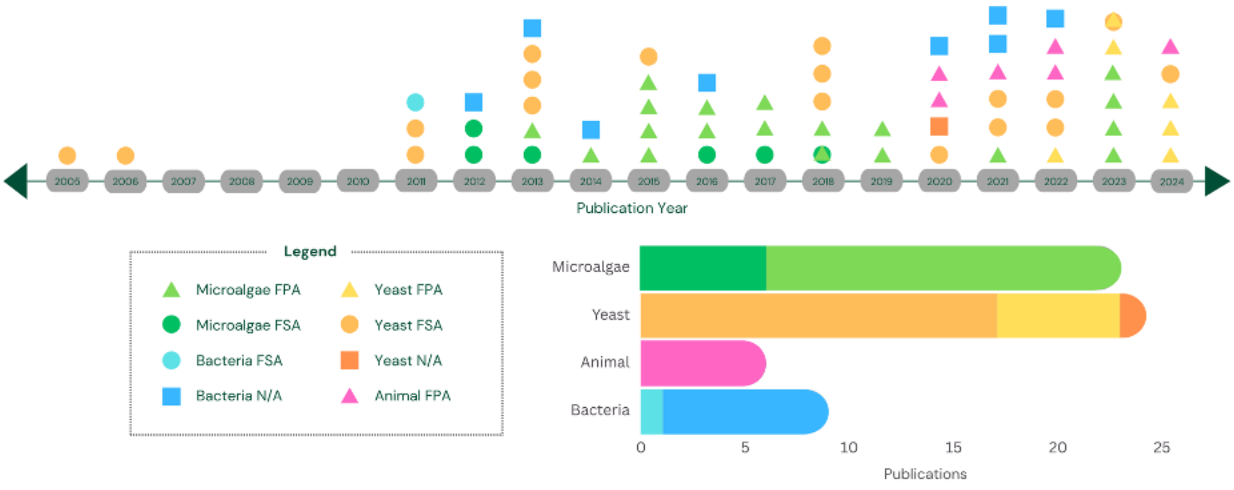

Figure 1. Timeline of manuscripts published by year and stacked bar graph of publications grouped by immobilized cell (microalgae, yeast, animal and bacteria cells) and differentiated by color. Method of immobilization: Fungal Spore-Assisted (FSA) method, Fungal Pellet-Assisted (FPA) method, or not available (N/A) is grouped by shapes. Overlapping shapes such as the circle with triangle signifies that both FSA and FPA methods were used in the same paper. N/A refers to those manuscripts which did not clearly define if FSA or FPA method was utilized.

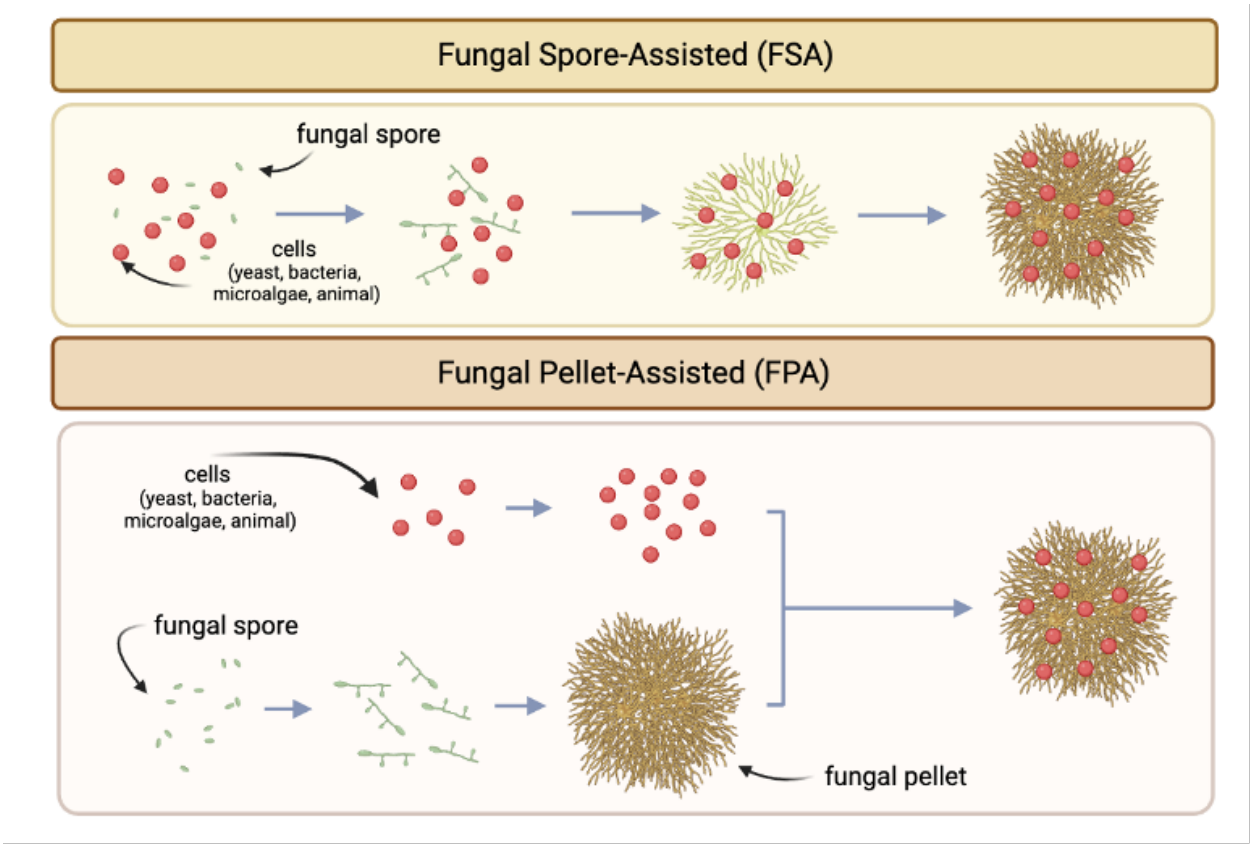

Figure 2. Summary of methodology of cellular immobilization in hyphal matrix of fungal pellets. Fungal Spore-Assisted (FSA) method vs Fungal Pellet-Assisted (FPA) method.

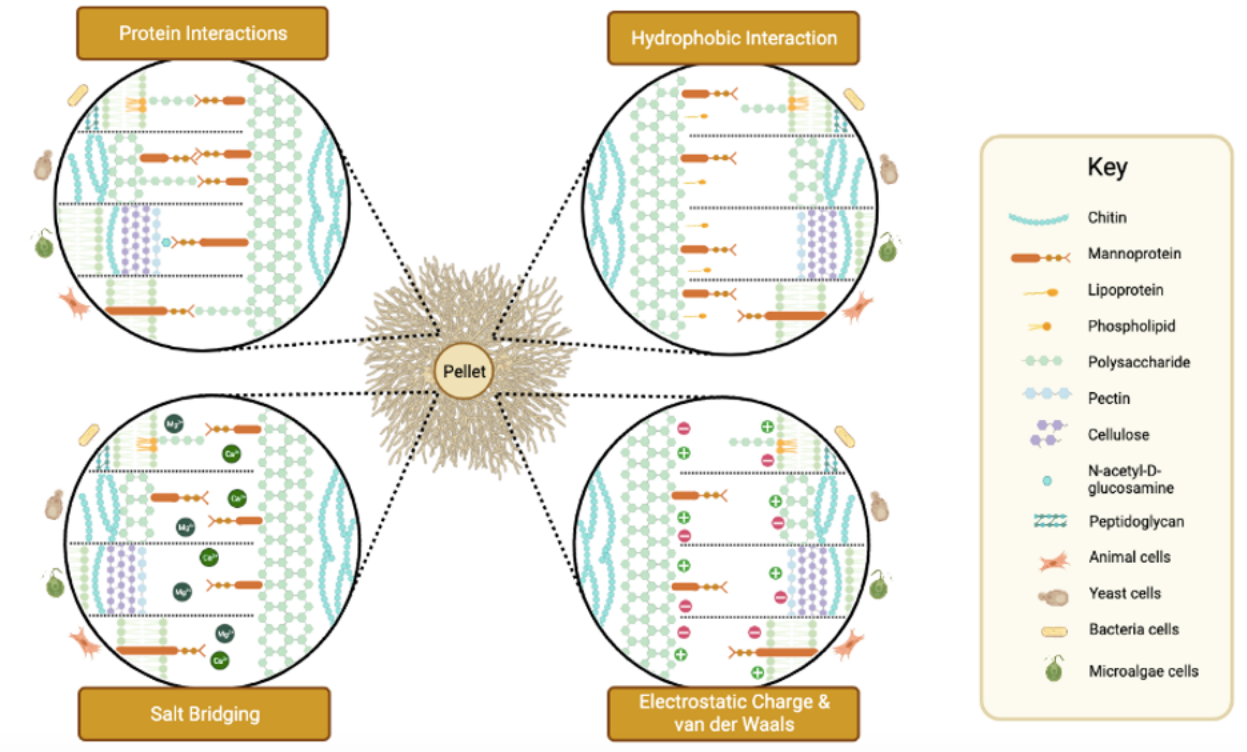

Figure 3. Hypothesized and proposed mechanism of attachment between filamentous fungus and whole cells (animal, yeast, bacteria, and microalgae). Cell walls are representative of the organism that has been most studied. The interactions depicted here are speculative based on the attachment mechanism of each organism.

CHAPTER 2: Assessing Edible Filamentous Fungal Carriers as Cell Supports for Growth of Yeast and Cultivated Meat

This manuscript was published in: MDPI Foods 11, 3142 (2022).

Co-authors: Jaime Moreno García, Nitin Nitin, Keith Baar, David E. Block

Abstract:

The growth and activity of adherent cells can be enabled or enhanced through attachment to a solid surface. For food and beverage production processes, these solid supports should be food-grade, low-cost, and biocompatible with the cell of interest. Solid supports that are edible can be a part of the final product, thus simplifying downstream operations in the production of fermented beverages and lab grown meat. We provide proof of concept that edible filamentous fungal pellets can function as a solid support by assessing the attachment and growth of two model cell types: yeast, and myoblast cells. The filamentous fungus Aspergillus oryzae was cultured to produce pellets with 0.9 mm diameter. These fungal pellets were inactivated by heat or chemical methods and characterized physicochemically. Chemically inactivated pellets had the lowest dry mass and were the most hydrophobic. Scanning electron microscope images showed that both yeast and myoblast cells naturally adhered to the fungal pellets. Over 48 h of incubation, immobilized yeast increased five-fold on active pellets and six-fold on heat-inactivated pellets. Myoblast cells proliferated best on heat-treated pellets, where viable cell activity increased almost two-fold, whereas on chemically inactivated pellets myoblasts did not increase in the cell mass. These results support the use of filamentous fungi as a novel cell immobilization biomaterial for food technology applications.

Introduction

Whole-cell immobilization technology aims to attach intact cells to a support material that supports cell growth and differentiation (Karel et al., 1985). This system of immobilizing cells to a carrier can be advantageous over freely suspended cells because immobilization frequently facilitates an increase in metabolic product yield, product recovery, cell stability, cell recovery, and reactor performance during fermentation, as well as allowing sus-pended culture for adherent cells (Moreno-García, García-Martínez, et al., 2018; Ravi Kumar, 2000; Zhu, 2007). The discovery of novel materials that support the growth and differentiation of cells is crucial, especially for the sustainable food technology sector, where food grade requirements must be met. An ideal edible support material must have favorable chemical and mechanical stability, wide applicability, high bio-compatibility, and low-cost(Moreno-García, García-Martínez, et al., 2018; Ravi Kumar, 2000; van de Velde et al., 2002; Zhu, 2007; Žnidaršič-Plazl, 2021).

Several emerging biomaterials have been developed in recent years for cell im-mobilization support that meet some or all of these criteria (Vasilieva et al., 2020; H.-T. Wang et al., 2019). Filamentous fungal biomass is one of these promising technologies as it can be edible and is produced through a food-grade fermentation process. By utilizing GRAS fungal strains such as Aspergillus oryzae, the fungal support can be consumed whole, as an integral part of a food product, and therefore has applications in the beverage and food production sectors. One of the most defining features of filamentous fungus (FF) is its ability to grow quickly on simple, low-cost carbon sources and several FF species are able to spontaneously form spherical masses, called pellets (J. Zhang & Zhang, 2016). Pellets are a matrix of intertwining hyphae and have a hollow or sparse interior core (Veiter et al., 2018). From an immobilization perspective, the pellet geometry is beneficial because the hyphae layer is dense and flexible enough to maintain structure and withstand high mechanical forces to provide a robust platform for cell attachment while having a porous wall that allows mass transfer of nutrients, high sur-face-area-to-volume ratio, and low overall density. These properties allow pellets to remain mechanically resilient while suspended in bioreactors under gentle agitation (Moreira et al., 1996). Structurally, the fungal cell

wall is composed of layers of proteins, glucans, and chitin, which not only gives FF high-protein and high-fiber nutritional value but provides anchorage points to which flocculating cell receptor ligands can adhere (Ogawa et al., 2019). Because of these characteristics, fungal pellets can be an ideal cell immobilization platform that is scalable and useful for large-scale fermentation and cultivation practices.

In this experiment, we explore two different types of cells immobilized onto FF as a support: Saccharomyces cerevisiae yeast and C2C12 murine myoblast cells. These two cell types were selected to provide insight into the factors that impact cell attachment and growth with specific application to food industry sectors. Yeast immobilization to fungal biomass has been studied previously and is utilized for alcoholic fermentation such as for the production of beer, wine, and bioethanol (Chacón-Navarrete et al., 2021; García-Martínez et al., 2011; Peinado Amores & Garcia Mauricio, n.d.). The attachment of yeast to FF is termed a yeast biocapsule. Yeast biocapsulation improves cell stability; allows for continuous operation, operational flexibility, and control of fermentation; and facilitates cell recovery and reuse(Moreno-García, García-Martínez, et al., 2018; Peinado et al., 2006). In the past, yeast biocapsule formation required careful control of fermentation conditions and long incubation times for both the FF and yeast to remain viable. The method proposed in this study looks to accelerate biocapsule formation by adhering yeast to already inactivated fungal pellets, a technique that also improves the quality of biocapsule formation.

The second novel application of fungal pellet supports is as edible microcarriers in cultivated meat production. Edible filamentous fungal supports may be able to replace conventional non-edible microcarriers, which are used to produce high cell density for anchorage-dependent animal cells. Since traditional microcarriers are nonedible and need to be removed from the final product to meet taste and sensory requirements, there are extensive downstream operational costs associated with the dissociation of the meat cells from the carriers, the separation of the meat cells, and the elimination of microcarriers (Bodiou et al., 2020). Edible filamentous microcarriers, by contrast, could remain an

integral part of the final product, simplifying downstream processing and formulation and providing opportunities to improve the nutritional and/or organoleptic qualities of the final product. In muscle cell cultivation, the FF edible support would need to be inert to avoid interference with the cultivation and growth of the more slowly growing myoblasts.

In both applications, cell attachment is the critical first step in assessing the validity and efficiency of the immobilization technology. Low attachment efficiency would lead to low productivity [20]. Support surface properties can impact cell attachment (Bodiou et al., 2020; Moreno-García, García-Martínez, et al., 2018; Ogawa et al., 2019). These properties include chemical traits such as the charge or hydrophilicity, and physical attributes such as the size, shape, and topography of the carrier. In this study, we grow fungal pellets and inactivate them using conventional sterilization techniques common in the food sector. The active and inactive pellets are then characterized, and the impact of these properties on cell attachment are assessed using *S. cerevisiae* yeast and C2C12 myoblast cells as a proof of concept. In the case of myoblast cells, only inactive fungal pellets were studied to provide an inert support, and yield was compared with a non-edible microcarrier, Cytodex 3. The activity of both model systems post-attachment was also assessed. With this study, we test whether we can use established scalable fer-mentation processes to produce edible fungal pellets to support the growth of adherent cells for cultivated meat and fermentation practices.

Materials and Methods

Cells and Media Components

The FF used in this study was *A. oryzae* UCD 76-2 (UC Davis Phaff Culture Collection, Davis, CA, USA), selected for its GRAS status and the history of its biomass consumed and used as a food source [21]. The FF was grown on sporulation agar plates (1.7% (w/v) corn meal agar (BD, Franklin Lakes, NJ, USA), 0.1% (w/v) yeast extract (BD, Franklin Lakes, NJ, USA), 0.2 % (w/v) glucose (Spectrum Chemicals, New

Brunswick, NJ, USA) and 2 % (w/v) bactoagar (BD, Franklin Lakes, NJ, USA)) and FF pellet medium (6% (w/v) glucose, 0.3% (w/v) yeast extract, 0.3% (w/v) NaNO3 (Sigma-Aldrich, St. Louis, MO, USA), 0.1% (w/v) K2HPO4 (Thermo Fisher Scientific, Waltham, MA, USA), 0.05% (w/v) MgSO4, (RPI, Mount Prospect, IL, USA) 0.05% (w/v) KCl (Thermo Fisher Scientific, Waltham, MA, USA), and 0.001% (w/v) FeSO4 (Thermo Fisher Scientific, Waltham, MA, USA). The yeast *S. cerevisiae* G1 (ATCC: MYA-2451) (UC Davis Viticulture and Enology Culture Collection and University of Cordoba, Spain) was selected because of its high affinity to FF in previous yeast immobilization studies [18]. The yeast was pre-grown on YPD agar (yeast extract 1% (w/v), peptone 2% (w/v), glucose 2% (w/v), and bacto-agar 2% (w/v)) and YPD liquid. C2C12 cells (mouse myoblasts; ATCC: CRL-1772) were used for the animal cell immobilization and cultivated in complete proliferation media: 89% (v/v) DMEM (Thermo Scientific, Rochester, NY, USA) 10% (v/v), fetal bovine serum (Thermo Scientific, Roch-ester, NY, USA), and 1% (v/v) Penicillin-Streptomycin (Sigma-Aldrich, St. Louis, MO, USA).

Fungal Pellet Formation and Inactivation

FF was pre-grown on sporulation agar plates for 7 days at 28 °C. Spores were then suspended in sterile distilled water, the suspension vortexed and sonicated for 5 min, and a volume inoculated to reach a final concentration of 1×10^6 spores/mL in 50 mL of FF pellet medium with pH adjusted to 5.5 in 250 mL Erlenmeyer flasks covered with hydrophobic cotton. The flasks were incubated under high agitation (250 rpm at 30 °C). After 3 days, the active fungal pellets (AFP) were harvested and washed with sterile DI water. For inactive pellet conditions, heat-treated fungal pellets (HFP) were autoclaved in sterile DI water at 121 °C for 20 min and chemically treated fungal pellets (CFP) were placed in 50 mL of 70% (v/v) ethanol in 250 mL flask and incubated for 20 min at 100 rpm and washed with sterile DI water. Both inactivation methods were performed immediately after pellet formation was complete. The viability of pellets was confirmed by taking single pellets, assessing the growth on YPD plates, and incubating for 5 days at 28 °C. Each viability check was repeated with 12 randomly chosen pellets.

Measurement of Pellet Parameters

After the formation of active and inactivated pellets, individual pellet mass was measured by wet weight and dried in a 100 °C oven overnight to obtain the dry weight. The diameters of pellets were measured in their wet state from digital images using the particle analyzer feature in ImajeJ2 software 2.3.0 (Bethesda, MD, USA) (Schindelin et al., 2012). The volume of pellets was measured by measuring displacement in volume after and before sub-mersion for 1 mL of settled pellets. Further, some other traits that influence cell immo-bilization were quantified: charge, elemental composition, and hydrophobicity. The charge of the pellets was analyzed using a Zetasizer (Malvern Panalytical, Worcester-shire, UK). Since this instrument measures particle sizes of up to 100 microns, pellets were mechanically broken into smaller hyphae fragments using a homogenizer (IKA, Staufen, Germany) at a 14 k setting for 3 min. The mixture was filtered using a 300 micron filter and subsequently through an 80 micron filter to remove larger particles, and the re-maining suspension was measured for zeta potential. Carbon percentage was analyzed by Thermo Fisher Quattro S. Environmental scanning electron microscope (Thermo Scientific, Rochester, NY, USA) equipped with a QUANTAX EDS detector (Bruker, Billerica, MA, USA). The hydrophobicity of the pellets was measured using a phase-partition method described by Rosenberg et al. (Rosenberg et al., 1980). Briefly, pellets were washed with phosphate buffer saline (PBS), and 0.5 mL of settled pellets was placed in 9.5 mL of PBS. The optical density of the cell suspension was measured at 640 nm (A1) using a Genesys 10 s UV-Vis spectrophotometer (Thermo Scientific, Rochester, NY, USA). Next, 1.4 mL of octane (Alfa Aesar, Haverhill, MA, USA) was added to the 10 mL of fungal suspension, mixed with a vortex mixer for 2 min, and allowed to stand for 10–15 min until phase separation was observed. The upper hydrocarbon phase was discarded, and the lower aqueous phase was collected and measured for optical density at 640 nm (A2). The hydrophobicity index (HPBI) was determined as

$$HPBI = (A1 - A2)/A1 \times 100$$

Measurement of Yeast Cell Immobilization Potential

S. cerevisiae G1 was pre-grown on YPD agar, and a colony was inoculated in 50 mL of YPD liquid medium in a 250 mL flask at 175 rpm, 28 °C for 3 days. The suspension was centrifuged for 10 min at 4200 rpm and the supernatant discarded. Yeasts were weighed and combined with AFP, HFP, or CFP at a weight ratio of 1:10 in a sterile container. YPD liquid was added to the same container to submerge pellets and gently shaken to homogenize the solution. The container was left loose-capped, and yeasts were left to grow for 72 h at 28 °C under static condition. At this point, the yeast cells began attaching to fungal mycelium to form the yeast-fungus structure referred to as yeast biocapsules, which can be applied to alcoholic fermentation production such as beer, wine, and bio-ethanol. Once the yeast biocapsule incubation was finished, the supernatant was decanted and yeast biocapsules were washed twice with sterile DI water.

Samples were taken at 24 h and 72 h, and the immobilization yield was counted directly after sampling. For the immobilized yeast counting, ten biocapsules out of the total from each flask were disrupted with salt to separate yeast cells from the fungal hyphae. Biocapsules were broken by placing them into a NaCl solution (100 mM), grinding them with a tissue grinder for 2 min, and then transferring them to a test tube and sonicating for 20 min. As a result, a mixture of yeast cells and fungal hypha segments was obtained. The immobilized yeast number was determined by direct counting using a hemacytometer grid under the microscope at 40× objective.

Microscopic Imaging Analysis

To analyze the fungal pellet structure, pellets were observed using a Thermo Fisher Quattro S Environmental scanning electron microscope (Thermo Scientific, Rochester, NY, USA) in high vacuum mode using 5 kV accelerating voltage to capture pellets before a brief increase to 15 kV for imaging. Prior to imaging, pellets and yeast biocapsules were freeze-dried and gold-sputter-coated. To observe

the inner area of the fungal pellets or yeast biocapsules, pellets were cut in half with a scalpel. Yeast cells in images obtained from SEM were later colored using Adobe Photoshop CS6 13.1.3 by Adobe Inc. (San Jose, CA, USA).

Measurement of Animal Cell Immobilization Potential

C2C12 cells were immobilized on fungal pellets and Cytodex 3 (Cytiva, Marlborough, MA, USA), a nonedible conventional microcarrier. Cytodex 3 was used as a positive control and prepared prior to seeding according to the manufacturer's instructions. Fungal microcarriers (HFP and CFP) were prepared by placing 20 inactivated pellets in each well of a 96 well plate (Corning, Somerville, MA, USA), washing twice with DPBS, and submerging them in complete proliferation media for 15 min at 37 °C with 5 % CO2. AFP were not tested, with the reasoning that fungal metabolism will outcompete the animal cell metabolism and prevent animal cell growth. C2C12 cells were seeded at 3000 cells/cm2 in 96 well plates coated with anti-adherent solution (StemCell, Vancouver, WA, Canada) to prevent cell attachment to the bottom of the wells. No microcarriers were placed in negative control wells, and a second positive control, cells growing on a standard tissue culture-treated 96 well plate that promotes cell adhesion, was run in parallel. All wells contained 200 µL total of complete proliferation media, incubated at 37 °C, 5% CO2 and assessed at 24 h and 72 h for cell viability. AlamarBlue® Cell Viability Assay Reagent (AB) (Invitrogen, Waltham, MA, USA) was used to quantify cellular metabolic activity and in turn determine the concentration of viable cells in a given sample. Briefly, the dye incorporates an oxidation-reduction (REDOX) indicator that both fluoresces and changes color in response to chemical reduction within active mitochondria. In total, 20 µL of AB was administered in each well at each time point. After 4 h, the absorbance of each well was measured at 570 nm and 600 nm with SpectraMax iD5 Multi-Mode Microplate Reader (Molecular Devices, San Jose, CA, USA). The percent reduction of AB was calculated using Equation 2.

Percent reduction of AB = ((O2 x A1) - (O1 x A2))/((R1 x N2) - (R2 x N1)) x 100

where O1 is the molar extinction coefficient (E) of oxidized AB at 570 nm, O2 is the E of oxidized AB at 600 nm, R1 is the E of reduced AB at 570 nm, R2 is the E of reduced AB at 600 nm, A1 is the absorbance of test wells at 570 nm, A2 is the absorbance of test wells at 600 nm, N1 is the absorbance of negative control well (media plus microcarriers and AB but no cells) at 570 nm, and N2 is the absorbance of negative control well at 600 nm. The higher the percentage reduction of media, the more metabolically active cells are present.

Statistical Analysis

Statistical analysis was performed using the software package Statgraphics ® Cen-turion XVI from Stat Points Technologies, Inc. (Warrenton, VI, USA) for the following methods: ANOVA (Analysis Of Variance) and Fisher test for the establishment of Homogeneous Groups (HG) at a significance level $p \leq 0.05$. Standard deviation was calculated for all values for pellet diameter, pellet number, and cell immobilizations.

Results

Fungal Pellet Growth and Characterization

Fungal pellets were first produced in flasks in order to characterize their growth and final properties. Fungal pellets were grown over the course of 72 h, during which time the pellet diameter and number of individual pellets per flask increased, particularly between 24 and 48 h (Figure 4). Inactivation was achieved by HFP at 121 °C for 20 min or CFP with 70% (v/v) ethanol for 20 min. Following inactivation, the physiological characteristics of fungal pellets did not change significantly when compared to the AFP. Pellets retained their spherical shape and diameter (Figure 5 and Table 2), even after inactivation treatments. All pellets appear to have a compact spherical structure, with a clearly defined outer wall

containing hyphae that protrude from the surface in HFP. In all conditions, the outer surface of the pellets is microtextured with intertwining layers of fungal hyphae with an individual diameter of 2 to 3 microns. The void spaces between hyphae are present in within the pellets, emphasizing the porous nature of the pellet geometry.

Other measured parameters, which were significantly different between the activated and inactivated fungal pellet conditions, were (1) the dry mass, where AFP was 0.4 ± 0.01 mg/fungal pellet compared to HFP with 0.3 ± 0.01 mg/fungal pellet and CFP 0.01 ± 0.01 mg/fungal pellet; (2) the hydrophobicity, with HPBI varying from AFP at 4.7 ± 0.1, to 2.1 ± 0.5 and 0.7 ± 0.1 in the HFP and CFP, respectively (Table 2); and (3) the charge of the pellet (AFP had a stronger negative charge compared to the inactivated HFP and CFP; however, all conditions presented zeta potentials that are fairly close to neutral). The carbon composition of fungal pellets did not show significant differences: AFP was 61 ± 10%, HFP was 53 ± 9%, and AFP was 50 ± 8% carbon by mass. Materials with high carbon content or carbonaceous material can improve cell activity and growth and assist inter-species electron transfer, buffering capacity, and nutrient adsorption onto their surface (Kyriakou et al., 2019; J. Zhang et al., 2018).

Yeast Cell Immobilization

The immobilization of yeast cells onto fungal pellets was confirmed both by direct counting of yeast and by SEM imaging. In the SEM images, yeast cells can be seen attached both on the outer surface of the pellet and the inner area of the pellets, with more cells adhering to the outer surface compared to the inner (Figure 6a). At higher magnification, it is clear that the yeast cells are firmly attached to the hyphae walls, as if they are embedded into the fungal matrix. Some yeasts bud and show signs of replicating while remaining adhered onto the hyphae. The newly formed daughter cells may be using the same natural process of adhesion as the parental cells. This observation is consistent with previous literature

where authors saw an increase in immobilized cells after the yeast biocapsules were incubated in a nutrient rich media (Moreno-García, García-Martinez, et al., 2018).

The yeast immobilization yields, or yeast cell mass, increased over time for all conditions, where AFP and HFP showed a higher increase in yield from 24 h to 72 h incubation compared to CFP. AFP increased from $56.8 \pm 12.3 \times 10^6$ cells/g wet weight to $291.8 \pm 26.2 \times 10^6$ cells/g wet weight, HFP increased from $51.0 \pm 18.5 \times 10^6$ cells/g wet weight to $306.4 \pm 40.1 \times 10^6$ cells/g wet weight, and CFP increased from $69.4 \pm 32.6 \times 10^6$ cells/g wet weight to $121.3 \pm 2.2 \times 10^6$ cells/g wet weight (Figure 6b). The decreased immobilization efficiency of CFP may be related to the loss of hydrophobicity since hydrophobic cell surface components that may be important in yeast-FF attraction were lost with ethanol treatment.

Animal Cell Immobilization

C2C12 murine myoblast cells were used to study animal cell attachment and growth on fungal pellets as an edible carrier. The attachment of C2C12 to microcarriers was visualized by SEM images (Figure 7a), where a mass of cells can be seen to cover the surface of both CFP and HFP pellets. C2C12 cells are anchorage-dependent, in other words, they require attachment to an inert surface in order to remain viable and proliferate. This was demonstrated in the negative control conditions, where C2C12 cells were seeded in wells coated with an anti-adherent solution and no microcarriers. When forced to remain in suspension, no growth was observed between 24 and 72 h (Figure 7b). In contrast, the positive control, where cells were seeded on tissue culture treated plates, proliferated, as indicated by the increase in AB reduction from 26 ± 1% to 70 ± 2% in 72 h. Cytodex 3 showed similar growth to the positive control, showing an increase from 35 ± 0.3% to 73 ± 7% over the same time period. The fungal pellets showed slightly different proliferation trends depending on the treatment. CFP exhibited no growth from 24 to 72 h going from 35 ± 2% to 37 ± 11% reduction. On the other hand, on HFP myoblasts went from 34 ± 0.5% to 59 ± 2% reduction in AB, indicating growth or increased metabolic activity

comparable to the positive controls. These data give a clear indication that heat-treated fungal pellets could be a viable edible microcarrier for the scaling up of cultivated meat relevant cell lines.

Discussion

This study provides a proof of concept that inactive fungal pellets can function as a support for cell attachment and growth, with the focus placed on two model cell types, *S. cerevisiae* and the C2C12 muscle cell line. We were successfully able to culture edible FF to achieve small pellet sizes, confirming the method reported by (Jeennor et al., 2019). In the same study, Jeenor et al. reported the scalability of the method by culturing *A. oryzae* in bioreactors with a 5 L capacity. Fungal pellet fermentation was also performed at a commercial scale to produce industrially relevant enzymes and compounds (L. Li et al., 2020; Z. J. Li et al., 2000; Veiter et al., 2018). Our aim was to utilize an existing scalable process, to determine whether these pellets have the potential to be used for yeast or animal cell adhesion and growth. The development of edible microcarriers would reduce the number of operations and downstream processing and improve the economics of cellular agriculture by reducing raw material cost/unit operation. We were able to validate fungal microcarriers for cell culture by confirming cell attachment and the growth of cells on the engineered pellets. For the animal cells, these data suggest edible fungal pellet microcarriers are a viable path to creating animal cell mass at commercial scale.

Following inactivation, there were no significant differences physically, such as pellet size and surface texture of the pellets; however, dry weight and hydrophobicity varied with inactivation technique. Dry weight was the lowest in the CFP group, which may be explained by action of ethyl alcohol on the pellets. Because ethyl alcohol is amphiphilic, it denatures proteins and solubilizes lipids and hydrophobic proteins, such as oxylipins and hydrophobins [30]. The result is damage to cell membrane and cell wall components, followed by the solubilization of cytosolic components by the aqueous part of the solution and a reduction in dry weight of the fungal biomass. HFP are inactivated by autoclaving. Autoclaving

causes irreversible coagulation and the denaturation of enzymes and structural proteins by quickly raising the heat to 121 °C using saturated steam at 1 atm overpressure (*Steam Sterilization | Disinfection & Sterilization Guidelines | Guidelines Library | Infection Control | CDC*, n.d.). This caused FF surface properties such as hydrophobicity and charge to decrease; however, the mass of the pellets was not significantly affected.

For yeast cell immobilization, yeast were seen to immobilize both on active pellets and inactive pellets. In prior studies, yeast immobilization on mycelium occurred by co-culturing FF and yeast, where both microorganisms remained viable. Using this method, the growth of both FF and yeast was observed simultaneously in liquid culture over the course of 7 days, resulting in the immobilization of 200×10^6 yeast cells/g wet weight. These results match previous studies comparing yeast biocapsules to alginate beads, the conventional yeast immobilization system, where yeast biocapsules had similar or higher yeast density per wet weight (López-Menchero et al., 2021). By contrast, in the current study, we observed the direct attachment of yeast to already formed filamentous fungal pellets, and similar yeast immobilization was achieved after 3 days of incubation. Further, in order to inactivate only the FF while keeping yeast alive, prior methods required an additional 12-day cycle of incubation in high-sugar medium (YP + 25% dextrose), which caused the yeast to multiply, ferment, and produce ethanol concentrations high enough to inactivate the FF but not the yeast.

A novel finding of the current work is that yeast cell growth was lower on CFP compared to the other conditions. Yeast cell attachment is mediated by cell surface proteins, called flocculins, that directly participate in adhesion of cells to each other or other substrates (Ogawa et al., 2019; Verstrepen & Klis, 2006). The flocculins recognize and bind to α-mannan residues (receptors) of neighboring cells and other flocculins embedded in the rich outer mannoprotein layer of the cell wall (Verstrepen et al., 2003; Verstrepen & Klis, 2006). As described earlier, ethyl alcohol treatment may denature these receptors on the FF, leaving fewer anchorage points and limiting binding to a peak at 24 h of incubation [36]. Further,

the CFPs were also significantly less hydrophobic than the other conditions, most likely due to the solubilization of fatty acid components and the removal of hydrophobins. Hydrophobicity plays a part in yeast-FF attraction since flocculation proteins responsible for yeast attachment have hydrophobic domains and are attracted to other hydrophobic surfaces. The loss of hydrophobicity may therefore have contributed to the decrease in yeast cell immobilization yield for CFP.

The C2C12 muscle cell line also exhibited attachment and growth on fungal pellets, with HFP showing comparable growth to the commercial Cytodex 3, the conventional cell immobilization technology for in vitro animal cells [37]. Most conventional microcarriers such as Cytodex 3 are composed of non-edible materials such as cross-linked dextran and coated with animal derived ECM such as pig skin gelatin (McKee & Chaudhry, 2017). Even though the fungal pellets were not coated with specific ECM proteins, cell attachment and viability were still observed. The physicochemical properties of the fungal pellets were sufficient to promote cell attachment and allow immobilization yields comparable to Cytodex 3 microcarriers. The fungal pellets are four times larger than Cytodex microcarriers. Schmidt et al. (Schmidt et al., 2011) reported that microcarrier size affects cell behavior, where microcarriers between 1500 and 3000 µm promote cell attachment compared to smaller 500 µm microcarriers. Fungal pellets also have microtextured surface typology. C2C12 cells have been shown to adhere better to micropatterned surfaces because they more closely resemble the native ECM (Cha et al., 2017). Interestingly, HFP showed increased C2C12 viability and metabolic activity compared to CFP despite the size and surface typology remaining similar. The difference may be attributed to the difference in pellet stiffness, which has been reported to be a crucial parameter for cell attachment affecting protein expression, cytoskeleton modification, and cell viability (Boonen et al., 2009; Choquet et al., 1997; Cukierman et al., 2001). The change in dry weight in the absence of a change in pellet size as a consequence of inactivation treatments suggests that the density (or stiffness) of fungal pellets was modified. While these characteristic changes may impact cell attachment, there are also reports that

proliferation, alignment, and fusion are promoted on micro-carriers that are smaller and have smoother surfaces (Cha et al., 2017; Schmidt et al., 2011). In order to assess the full efficacy of cell growth on fungal pellets, longer proliferation and differentiation studies are required. Nonetheless, the data from this study confirms mammalian cell attachment and growth on FF pellets, a prerequisite for further investigation as an edible microcarrier for cultivated meat.

Conclusions

The data presented in this study demonstrate that inactive fungal biomass can be used to attach and grow very different cell types and is a proof of concept of tunable and edible fungal pellets for cellular agriculture. In future experiments, cell attachment can be enhanced by modifying the fungal pellet, changing fermentation conditions, utilizing different species/strains of FF, or engineering FF with other desired properties. It should also be possible to introduce qualities that not only improve cell immobilization but boost the flavor, taste, and nutritional properties of the final product, for example, studying the change in aromatic profiles when using yeast biocapsules for alcoholic fermentations or the effect on texture and taste when fungal microcarriers are incorporated into cultivated meat products. The data presented in this study unlock the potential of fungal pellet technology and serve as a foundation for future cell immobilization studies.

Tables and Figures

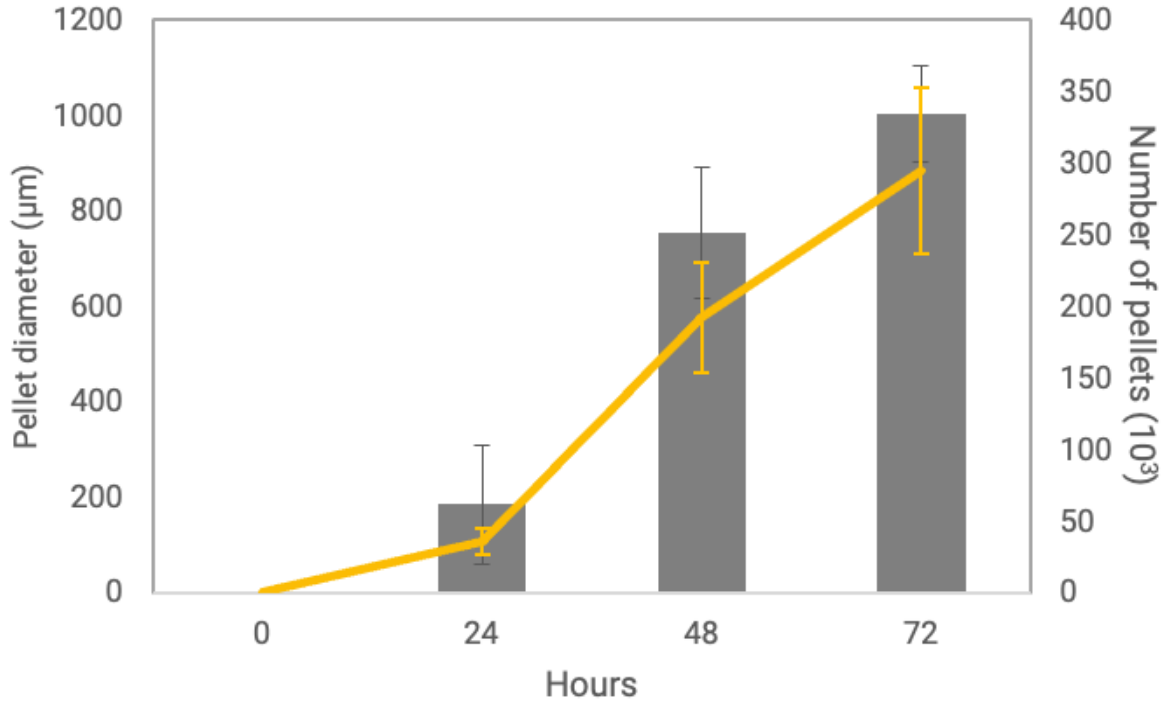

Figure 4. Pellet diameter and number of pellets per flask measured over the course of 72 h from the point of inoculation. The bars represent the number of pellets, and yellow line represents pellet diameter.

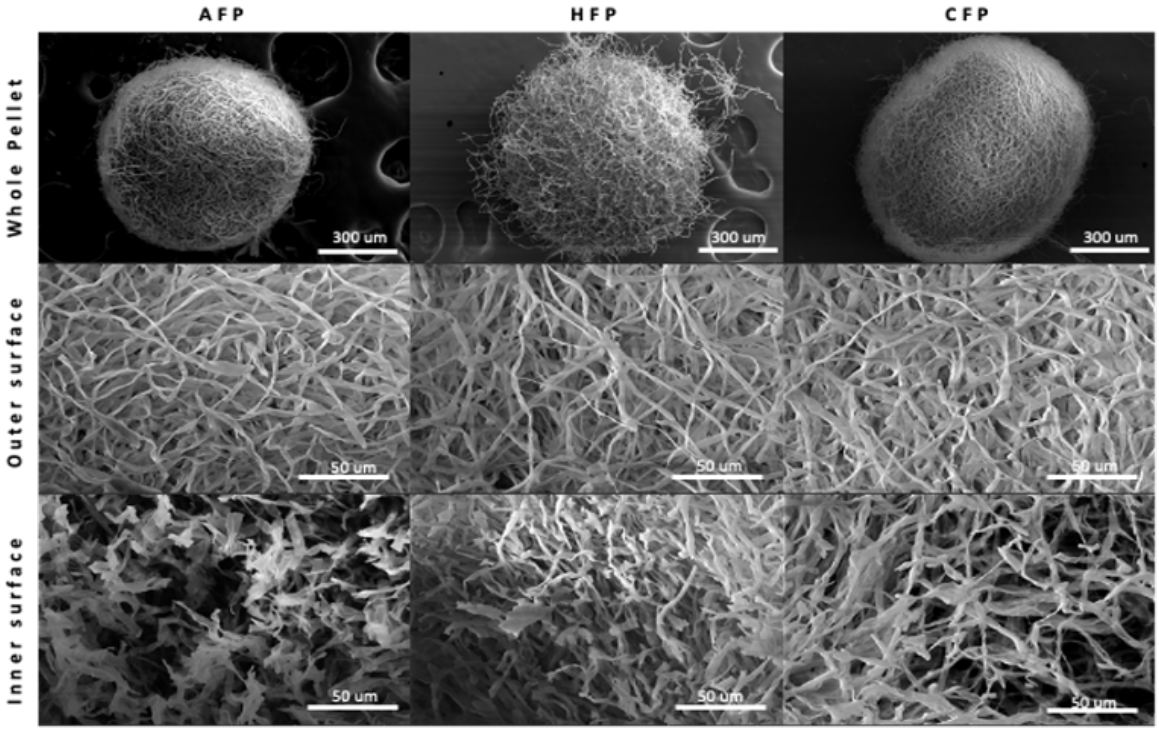

Figure 5. SEM of whole pellet, outer surface, and inner surface of fungal pellets. Active fungal pellets (AFP), heat-treated fungal pellets (HFP), and chemically treated fungal pellets (CFP).

Table 2. Characteristics of fungal pellets for active fungal pellets (AFP), heat-treated fungal pellets (HFP), and chemically treated fungal pellets (CFP). Superscript letters (a–d) indicate statistically significant homogenous groups differing in the parameters among the strains ($p < 0.05$, F-test).

	AFP	HFP	CFP
Viability (%)	100 ± 0 ^{b}	0 ± 0 ^{a}	17 ± 2 ^{a}
Diameter (mm)	0.90 ± 0.10 ^{a}	0.97 ± 0.21 ^{a}	1.03 ± 0.25 ^{a}
Wet weight (mg/fungal pellet)	0.37 ± 0.05 ^{a}	0.27 ± 0.06 ^{ab}	0.21 ± 0.04 ^{a}
Dry mass (mg/fungal pellet)	0.04 ± 0.01 ^{b}	0.03 ± 0.01 ^{b}	0.01 ± 0.01 ^{a}
Volume (mm^3/fungal pellet)	0.017 ± 0.005 ^{a}	0.014 ± 0.002 ^{a}	0.017 ± 0.001 ^{a}
Charge or zeta potential (mV)	−4.3 ± 0.6 ^{a}	−2.5 ± 0.3 ^{b}	−2.4 ± 0.2 ^{b}
Carbon % on pellet surface	61 ± 10 ^{a}	53 ± 9 ^{a}	50 ± 8 ^{a}
HPBI [1]	4.7 ± 0.1 ^{c}	2.1 ± 0.5 ^{b}	0.7 ± 0.1 ^{a}

[1] Hydrophobicity index.

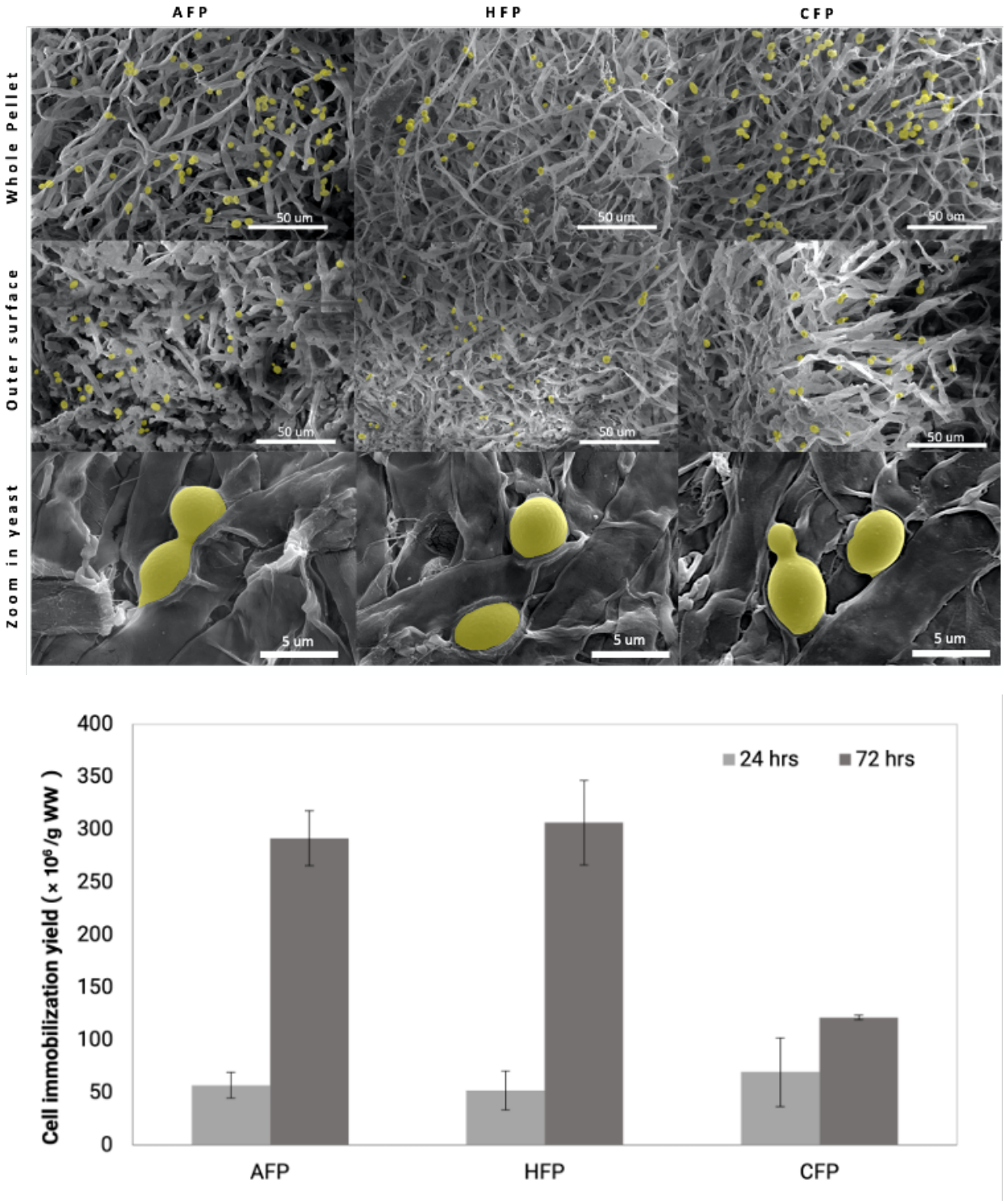

Figure 6. (a) SEM of yeast biocapsules with yeast cells (colored in yellow manually) on the outer surface and inner surface of fungal pellets. Yeasts immobilized on active fungal pellets (AFP), heat-treated fungal pellets (HFP), and chemically treated fungal pellets (CFP). (b) Cell immobilization yield at 24 h and 72 h incubation.

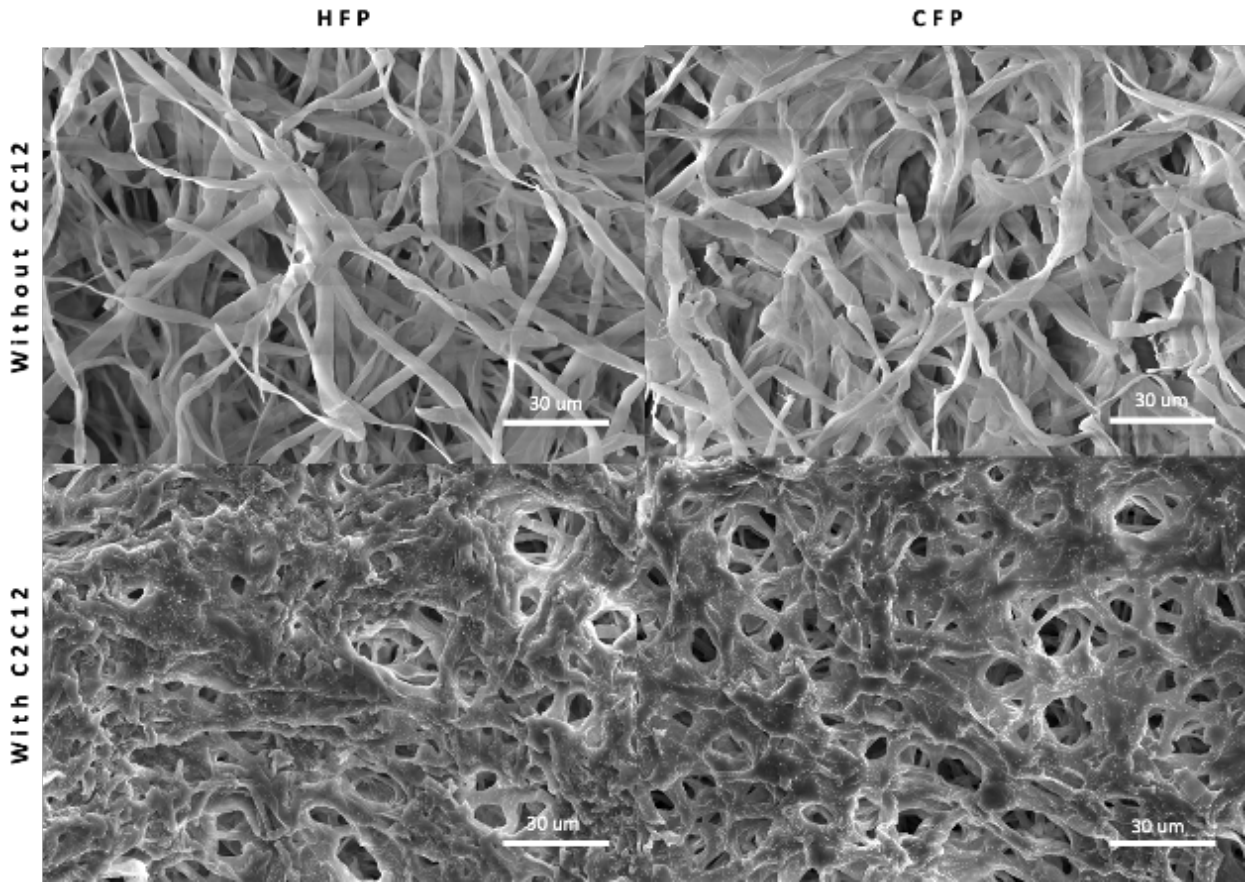
HFP
CFP
Without C2C12
With C2C12
30 um
30 um
30 um
30 um

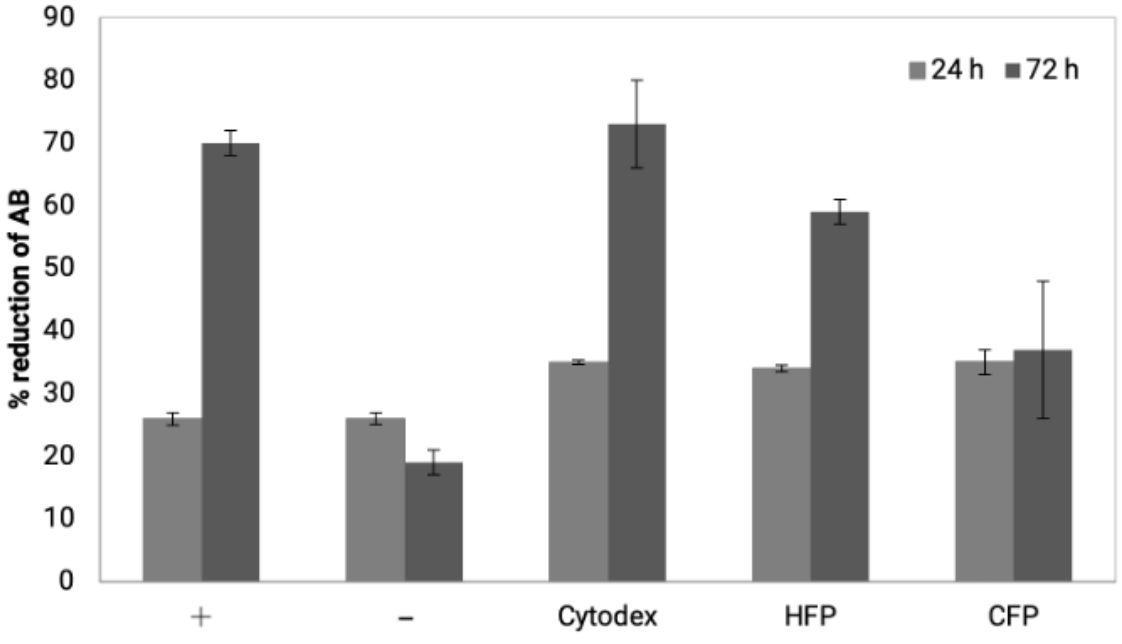
90
80
70
60
50
40
30
20
10
0
% reduction of AB
24 h
72 h
+
–
Cytodex
HFP
CFP

Figure 7. (a) SEM of raw fungal pellet surface and with C2C12. (b) Viability of C2C12 on micro-carriers using percent reduction of alamar blue (AB) as an indicator of cell number. Light grey bars are samples at 24hrs incubation and dark grey bars are 72hrs incubation after seeding. Positive control is C2C12 grown on tissue culture treated plates, negative control is C2C12 forced to grow in suspension on low attachment plates, HFP are C2C12 cells cultivated on heat-treated fungal pellets, and CFP are C2C12 cells cultivated on chemically treated fungal pellets.

CHAPTER 3: Edible Mycelium as Proliferation and Differentiation Support for Anchorage-dependent Animal Cells in Cultivated Meat Production

This manuscript was published in: npj Science of Foods 8, 23 (2024).

Coauthors: Alex S. Kermani, Mayrene J. Huynh, Keith Baar, J. Kent Leach, David E. Block

Abstract

Cultivated meat production requires bioprocess optimization to achieve cell densities that are multiple orders of magnitude higher compared to conventional cell culture techniques. These processes must maximize resource efficiency and cost-effectiveness by attaining high cell growth productivity per unit of medium. Microcarriers, or carriers, are compatible with large-scale bioreactor use, and offer a large surface-area-to-volume ratio for the adhesion and proliferation of anchorage-dependent animal cells. An ongoing challenge persists in the efficient retrieval of cells from the carriers, with conflicting reports on the effectiveness of trypsinization and the need for additional optimization measures such as sieving procedures. To surmount this issue, edible carriers have been proposed, offering the advantage of integration into the final food product while providing opportunities for texture, flavor, and nutritional incorporation. Recently, a proof of concept (POC) utilizing inactivated mycelium biomass derived from edible filamentous fungus demonstrated its potential as a support structure for myoblasts. However, this POC relied on a model mammalian cell line combination with a single mycelium species, limiting realistic applicability to cultivated meat production. This study aims to advance the POC. We found that the species of fungi composing the carriers impacts C2C12 myoblast cell attachment—with carriers derived from Aspergillus oryzae promoting the best proliferation. C2C12 myoblasts effectively differentiated on mycelium carriers when induced in myogenic differentiation media. Mycelium carriers also supported proliferation and differentiation of bovine satellite cells. These findings demonstrate the

potential of edible mycelium carrier technology to be readily adapted in product development within the cultivated meat industry.

Introduction

Large-scale culture of anchorage-dependent animal cells is necessary for regenerative medicine, tissue engineering, and biopharmaceutical manufacturing. However, if cellular agriculture is to meet the rising need for animal protein, it must scale orders of magnitude beyond established methods (Moritz et al., 2015). In addition, achieving a high productivity of cell growth per unit of medium is essential to maximize resource efficiency and reach price parity with conventional meat (Negulescu et al., 2023; Post & van der Weele, 2014; Rowley et al., 2012; van der Weele & Tramper, 2014). To address the scalability and productivity bottlenecks, microcarriers can be used to achieve higher cell densities for anchorage-dependent cells5. Microcarriers are suspended scaffolds commonly used in bioreactors or stirred tank reactors. They act as physical supports that provide a surface for cells to adhere and proliferate on (Blüml, 2007; Bodiou et al., 2020; GE Healthcare/Amersham Biosciences, 2005; McKee & Chaudhry, 2017). The microcarriers remain suspended in medium under gentle agitation, allowing adherent cells to be cultivated in suspension and offering a large surface-area-to-volume ratio to support high cell-density cultures relative to standard 2D planar cell culture practices (Bomkamp et al., 2022; Lee & Yang, 2012). In addition, the growth surface can easily be expanded by “bead-to-bead transfer,” where cells on microcarriers can migrate to newly added microcarriers in a near-confluent culture and cells maintain a longer exponential growth phase (Baraniak et al., 2012). Microcarriers also allow smooth transition from 2D surface growth to 3D culture and can be adapted to be used in a variety of culture vessel geometries and existing cell culture infrastructure. Therefore, compared to other culturing methods such as aggregates and fixed bed reactors, microcarriers are easier to control, monitor, implement, and more cost effective—leading to reduced training, capital expenditure, and setup costs (Leber et al., 2017).

Current commercial microcarriers are mostly composed of nonedible, synthetic materials (e.g., polystyrene, cross-linked dextran, cross-linked cellulose, and high-density polyethylene silica) and/or consist of animal-derived components. These microcarriers are optimized for use in cell culture to produce monoclonal antibodies, vaccines, and proteins of interest (Rafiq et al., 2013). Few applications focus on maximizing cell mass. A key challenge of these microcarriers is cell harvesting. The efficiency of trypsinization remains controversial, and additional microcarrier sieving procedures are needed to improve cell retrieval from the carriers (Goh et al., 2013; B. Li et al., 2015). Furthermore, harvesting at the required 200-250 m^3 scale is likely not practical and will generate large amounts of solid waste in the form of used synthetic microcarriers or introduce hazards such as microplastic ingestion if not completely removed from the final product (Negulescu et al., 2023). To circumvent this issue, carriers can be composed of edible or dissolvable material. Dissolvable carriers are made of degradable materials (e.g., denatured collagen, cross-linked polygalacturonic acid, alginate, etc.) that can be dissolved once the cells on microcarriers have reached confluency (Caruso et al., 2014; Ng et al., 2021). However, like the synthetic carriers, dissolving operations add complexity and cost to cell culture and degradation must be very carefully controlled to retain cell function. Edible carriers, on the other hand, can be incorporated into a final product, simplifying the bioprocess by eliminating dissociation or dissolving steps and adding to the gross mass yield. For food applications like cultivated meat, this provides an additional avenue to incorporate texture, flavor, and nutrition (Z. Wang et al., 2023). The discovery of edible materials which support proliferation and differentiation of cells is crucial, especially for the sustainable food technology sector, where food-grade requirements must be met. However, there is a research gap pertaining to edible materials compatible with cell culture. There are very few edible carriers that are readily available commercially in the market and for those that are available, data on cell proliferation and differentiation are scarce.

Recently, we provided proof of concept (POC) that edible, inactive biomass of *Aspergillus oryzae* can function as a support for myoblast cells (Derakhti et al., 2019; Ogawa, Moreno García, et al., 2022). *Aspergillus oryzae* is a Generally Recognized As Safe (GRAS) fungal species commonly used in food fermentation and its biomass is consumed as an alternative protein (known as mycoprotein) (Barzee et al., 2021; Block & Ogawa, 2024; Huling, 2023). Filamentous fungi are fast growing, robust microorganisms that can grow on simple, low-cost carbon sources, including agricultural waste (Caruso et al., 2014). These important properties can contribute to reducing the overall cost of cultivated meat products and increase sustainability. The morphological and biochemical properties of these fungi can be tuned by fermentation bioprocesses, with know-how that has already been optimized for large scale fermentation vessels (Berger et al., 2022). Mycoprotein contains all essential amino acids and has a protein digestibility-corrected amino acid score (PDCAAS) of 0.996, making it a complete protein source with a bioavailability similar to that of dairy milk and better than that of wheat-based or soy-based protein (Derbyshire, 2022; Edwards & Cummings, 2010; Lopez & Mohiuddin, 2023). Therefore, edible filamentous fungi are an ideal, sustainable biomaterial for cultivated meat microcarriers.

Previous work on mycelium carriers supporting C2C12 attachment and growth was limited by investigating biocompatibility of a single edible fungal strain and a model animal cell line20,21. In this study, we expand on the POC and hypothesize that mycelium can be a carrier for animal cell growth and differentiation by assessing cell viability and gene expression with combinations of multiple filamentous fungal species and cultivated meat relevant muscle cell types. We chose to work with bovine satellite cells suitable for cultivated meat. Moreover, the inclusion of cell seeding conditions and differentiation compatibility extends our work's impact. In short, this mycelium carrier technology could provide nutrition, flavor, and versatility for cultivated meat product development.

Methods

Fungal Strains and Media Components

Filamentous fungal strains were obtained from the UC Davis Viticulture and Enology Department Culture Collection (Davis, CA, USA), UC Davis Phaff Yeast Culture Collection (Davis, CA, USA), and the University of Cordoba Culture Collection (Cordoba, Spain). The strains are *Aspergillus oryzae* FST 76-2, *Aspergillus oryzae* UCD 8*, Aspergillus awamori* FST 40-400, *Aspergillus sojae* FST 76-1, *Aspergillus nishimurae* UCD 15, *Aspergillus tubingensis* UCD 12, *Rhizopus oligosporus* FST 72-2, and *Penicillium chrysogenum* H3 (Table 3).

Filamentous fungi were pre-grown on a common sporulation agar media (1.7% (w/v) corn meal agar (BD, Franklin Lakes, NJ, USA), 0.1% (w/v) yeast extract (BD, Franklin Lakes, NJ, USA), 0.2 % (w/v) glucose (Spectrum Chemicals, New Brunswick, NJ, USA) and 2% (w/v) bactoagar (BD, Franklin Lakes, NJ, USA)) and filamentous fungal pellet medium (6% (w/v) glucose, 0.3% (w/v) yeast extract, 0.3% (w/v) NaNO3 (Sigma-Aldrich, St. Louis, MO, USA), 0.1% (w/v) K2HPO4 (Thermo Fisher Scientific, Waltham, MA, USA), 0.05% (w/v) MgSO4, (RPI, Mount Prospect, IL, USA) 0.05% (w/v) KCl (Thermo Fisher Scientific, Waltham, MA, USA), and 0.001% (w/v) FeSO4 (Thermo Fisher Scientific, Waltham, MA, USA). Inactivation check was performed on YPD plates (yeast extract 1% (w/v), peptone 2% (w/v), glucose 2% (w/v), bactoagar 2% (w/v)).

Animal Cells and Culture Media

C2C12 cells (mouse myoblasts; ATCC: CRL-1772) and bovine satellite cells (bSC) were studied for proliferation and differentiation potential on microcarriers. To aid with microscopy, C2C12 cells were transduced with tdTomato (C2C12 TD) using a Lentivirus construct. Lentiviral particles encapsulating tdTomato-encoding plasmid were acquired from the UC Davis Health Vector Core. Approximately 105 C2C12 cells were incubated with lentivirus at a multiplicity of infection (MOI) of ~7.5 for 24 h. Cells were expanded after clonal selection of tdTomato-positive cells, using a cloning cylinder and validated for

reporter gene expression by fluorescence miscroscopy49,50. C2C12 cells were then cultivated in complete proliferation media: 89% (v/v) DMEM (Thermo Scientific, Rochester, NY, USA), 10% (v/v), fetal bovine serum (Thermo Scientific, Rochester, NY, USA), 1% (v/v) Penicillin-Streptomycin (Sigma-Aldrich, St. Louis, MO, USA) and differentiation media: 97% (v/v) DMEM (Thermo Scientific, Rochester, NY, USA) 2% (v/v), horse serum (Thermo Scientific, Rochester, NY, USA), 1% (v/v) Penicillin-Streptomycin (Sigma-Aldrich, St. Louis, MO, USA). bSC were isolated from fresh leg skeletal muscle of XX/XXY Holstein Cow at Animal Science Department the University of California, Davis. Briefly, the biopsy was cut into 0.5cm or smaller bundles and digested with 2% penicillin/streptomycin/amphotericin (Lonza 12-745E) and 200 units/mL collagenase (Worthington, Lakewood, NJ, USA) for 2 hours. Debris was removed by repeated centrifugation, washing, and filtering through a 100 µm filter and 40 µm filter. Cells were incubated with a FcR blocking reagent, labeled with micromagnetic brands in the satellite cell isolation kit (Miltenyi), and passed through a MACS column and separator (Miltenyi) with bSC sorted out via negative selection. bSC was cultivated in complete proliferation media: 79% (v/v) F10 (Thermo Scientific, Rochester, NY, USA), 20% (v/v) fetal bovine serum (Thermo Scientific, Rochester, NY, USA), 1% (v/v) Penicillin-Streptomycin (Sigma-Aldrich, St. Louis, MO, USA) supplemented with 5 ng/mL FGF2 (Thermo Scientific, Rochester, NY, USA) and differentiation media: 93% (v/v), DMEM (Thermo Scientific, Rochester, NY, USA), 2% (v/v) fetal bovine serum (Thermo Scientific, Rochester, NY, USA), 1% (v/v) Penicillin-Streptomycin (Sigma-Aldrich, St. Louis, MO, USA).

Mycelium carrier formation and inactivation

All fungi used in this study were grown under the same conditions as the initial POC (Derakhti et al., 2019; Ogawa, Moreno García, et al., 2022). Filamentous fungal strains were pre-grown on sporulation agar plates for 7 days at 28 °C. Conidia and spore formation was confirmed via confocal and light microscope. The spores were then suspended in sterile distilled water and vortexed, then sonicated for 5 minutes. The suspension was inoculated into 50 mL of filamentous fungal pellet medium, adjusted to a

pH of 5.5, in 250 mL Erlenmeyer flasks covered with hydrophobic cotton, with the final spore concentration reaching 1×10^6 spores/mL. The flasks were placed under high agitation at 250 rpm and a temperature of 30 °C in an Innova 4000 Incubator Shaker (New Brunswick Scientific Co., Edison, New Jersey). This produced spherical, porous biomasses, called pellets (except *R. oligosporus*). These pellets spontaneously form with certain species of fungi when cultivated in this condition. After 3 days, the fungal pellets were harvested, washed with sterile DI water, then immediately autoclaved in sterile DI water at a temperature of 121 °C for 20 minutes. Inactivation was confirmed by taking 20 random pellets and assessing growth on YPD agar plates at 28 °C for at least 1 week. No growth was observed, which confirmed that the pellets were inactive. Brightfield images of the pellets were characterized using the particle analysis feature in FIJI (Bethesda, Rockville, MD, USA)(Schindelin et al., 2012).

Biocompatibility, initial seeding concentration, and proliferation potential

Several species of mycelium carriers were screened for biocompatibility with C2C12 cells. Carriers were pretreated by washing twice with Dulbecco's phosphate-buffered saline (DPBS) (Gibco, Thermo Fisher Scientific, Waltham, MA, USA) and submerging in complete proliferation media for 3 hours prior to seeding. Cytodex 3 (Cytiva, Marlborough, MA, USA), the commercial standard non-edible carrier, was used as a positive control. Cytodex 3 are non-porous, type I porcine collagen-coated beads, composed of cross-linked dextran and a diameter of 141-211 µm and 2700 cm2/g dry weight specific surface area. Cytodex 3 was prepared at 3 g/L per replicate then hydrated and pre-treated according to the manufacturer's instructions before seeding. Mycelium carrier conditions were standardized by assessing fungal strain differences in diameter and approximating to match the available surface area to that of the Cytodex conditions. One strain in particular, *R. oligosporus*, did not form spherical pellets but a flat, matt-like structure. For this condition, a circular cutout with approximately 7 mm diameter and 1 mm thickness was placed at the bottom of the 96 well with cells seeded above it for biocompatibility testing. After pretreatment of carriers, the C2C12 cells were seeded in 96-well plates coated with anti-adherent

solution (StemCell Technologies, Vancouver, BC) to prevent them from anchoring to the bottom of the wells. Negative control wells had no microcarriers. Wells that contained only media or only microcarriers were prepared as blanks. Each replicate had its own dedicated well on the 96-well plates. The cells were incubated at 37 °C with 5 % CO2 in a HERAcell VIOS 160i incubator (Thermo Fisher Scientific, Waltham, MA, USA).

AlamarBlue® (AB) Cell Viability Assay Reagent (Invitrogen, Waltham, MA, USA) was used to determine the number of viable cells. This dye incorporates an oxidation-reduction indicator that fluoresces and changes color in response to chemical reduction within active mitochondria. A 20 µL AB solution was added to each replicate 48 hours after seeding. After four hours of incubation, 100 µL of media with AB solution was transferred to a clear bottom 96-well plate, and absorbance was measured at 570 nm and 600 nm using the SpectraMax iD5 Multi-Mode Microplate Reader (Molecular Devices, San Jose, CA, USA). The percentage reduction of AB was calculated per the manufacturer's instructions. Previous work from our lab has found that the higher the percentage reduction of media, the more metabolically active cells present34. Assuming a uniform (average) metabolic activity for each cell, this percent reduction is linearly correlated with cell concentration. This simple assessment gives us a way of comparing between groups with this proxy for biocompatibility and proliferation potential.

The fungal species, *A. oryzae* 1, which showed the highest percent reduction in AB, was chosen for a seeding concentration study. Cytodex and mycelium carriers were prepared as described above and each replicate used the same cell concentration. Seeding conditions for C2C12 cells were 5×10^2, 5×10^3, 5×10^4, 5×10^5, 5×10^6 cells/mL and for bSC were 1×10^5, 2.5×10^5, 5×10^5, 1×10^6, 2.5×10^6 cells/mL. At 24 and 72 hours after seeding, the cell number was analyzed by AB following the methods described above.

Differentiation Potential

Differentiation potential of C2C12 cells on microcarriers was tested by taking carriers with cells at >90% confluence, washing twice with DPBS, and adding 200 µL of differentiation media. The cells were incubated at 37 °C with 5 % CO2. The entire sample volume was collected at 48 hours (T1), 96 hours (T2), and 168 hours (T3) after switching to differentiation media. Each time-point replicate was a dedicated well on the 96-well plate coated with anti-adherent solution (StemCell, Vancouver, WA, Canada). Each time point was performed at least in triplicate.

The collected samples were immediately placed in TRIzol reagent (Invitrogen, Carlsbad, CA) and frozen at -80 °C. Defrosted samples were mixed with chloroform and RNA was separated from cell proteins and DNA in a liquid-liquid phase separation per manufacturer instructions. The RNA was precipitated and purified with IPA/EtOH/H2O then re-dissolved in RNase-free water (Qiagen, Hilden, Germany). The concentration of RNA was measured with a NanoDrop (Thermo Fisher Scientific, Waltham, Massachusetts, USA) and diluted to a uniform concentration between 20 and 50 ng/µL. The extracted and purified RNA was reverse transcribed using Quantiscript Reverse Transcriptase, Quantiscript RT Buffer, and RT Primer Mix (Qiagen, Hilden, Germany) using the manufacturer's instructions.

The TaqMan PCR reaction was performed in a final volume of 10 µL using 7 µL of Quantitect Probe PCR mix (Qiagen, Hilden, Germany), 30 ng cDNA, and 0.5 µL of each TaqMan probe with FAM reporter dye. The amplifications were performed on an Applied Biosystems™ QuantStudio™ 6 Pro Real-Time PCR System, 96-well, 0.1 mL block (Thermo Fisher Scientific, Waltham, Massachusetts, USA). The thermal cycling protocol was 95 °C for 3 min, followed by 45 cycles of 95 °C for 3 sec and 60 °C for 30 sec. Mouse-specific TaqMan Assays for *GAPDH* (Mm99999915_g1), *MYOD1* (Mm00440387_m1), *MYOG* (Mm00446194_m1), *MYH2* (Mm01332564_m1), and *PAX7* (Mm01354484_m1) were used. Bovine-specific TaqMan Assays for *GAPDH* (Bt03210913_g1), *MYOD1* (Bt03244740_m1), *MYOG* (Bt03258929_m1), *MYH1/2* (Bt03223147_gH), and *MYH3* (B03258391_m1). Rabbit *PAX7* (Oc06751922_s1) was used for bSC differentiation analysis because of a lack of bovine-specific assay and

likely cross-species reactivity, but no expression was observed. All TaqMan Assays were purchased from Thermo Fisher Scientific. Results were normalized to the corresponding sample's endogenous control, *GAPDH*. Reactions were thrice replicated and plate wells that did not amplify were not plotted. The data are presented in Figure 11 and Figure 13 as the single delta fold-change in gene expression compared to *GAPDH* 1e3 or 1e6, depending on the gene of interest.

Microscope Imaging Analysis

Fluorescent microscopy was used to visualize cells on Cytodex and mycelium carriers as well as in suspension. For C2C12 cells, the myoblasts were transfected with TdTomato and imaged in the TRITC channel with a 10× objective. Transfection methods are described in Smith et al.50. bSC were immunostained with Hoechst 33342 (1:2000; Invitrogen A32766) and imaged in the DAPI channel with a 20× objective. All samples were imaged using an ImagePICO (Molecular Devices, San Jose, CA, USA) with z stack.

Statistical Analysis

Statistical analysis was performed using the software R (v4.2.1; R Core Team, 2022) and the agricolae package (v1.3-5; de Mendiburu, 2021) for the following methods: ANOVA (Analysis of Variance) and Fisher's LSD test for the establishment of homogeneous groups (HG) and two-tailed unpaired t-test. Any statistically significant difference was implied by $p \leq 0.05$ unless otherwise stated in the figures. At least three biological replicates were performed for every condition and time point, with each biological replicate corresponding to a dedicated well on a 96-well plate.

Results

Fungal species impacts C2C12 attachment on mycelium carriers

Different fungal species were made into mycelium carriers under the same fermentation conditions, inactivated, and seeded with C2C12 cells to observe the impact of fungal species differences on mycelium-cell interactions. Both food grade and non-food grade fungi were selected to broaden the range of species which may be compatible with animal cell attachment and growth (Table 3). Fungal morphology differed between species even when cultured under the same conditions due to their genetic difference (Table 3). Species such as *Rizosporus oligosporus* did not form spherical pellets but produced a matted structure, while other species spontaneously formed differently sized pellets. Pellet diameter ranged from 1101 ± 580 µm for *A. oryzae* 1 and to 3050 ± 17 µm for *A. oryzae* 2. Carrier concentration was selected so that all conditions had similar approximate available surface area per well, but all metabolic activity results were normalized to the actual calculated surface area. The metabolic activity of cells, expressed as percent reduction of AB, was assessed at 48 hours after seeding, when C2C12 cells have attached to microcarriers (Figure 8) and are in the exponential phase of growth. Any cells that did not attach have very low metabolic activity, which can be seen in the negative control condition (no microcarriers) where cells are forced to grow in suspension. Cytodex 3, a non-edible commercial microcarrier, was used for comparison. When used as carriers, different fungal species impacted C2C12 metabolic activity. C2C12 cells on *A. oryzae* 1, *A. oryzae* 2, and *A. awamori* showed strong reduction in AB: 29.00 ± 0.03 %, 24.06 ± 0.11%, and 23.80 ± 0.07%, respectively. *R. oligosporus* (3.00 ± 0.01%), *A. nishimurae* (5.38 ± 0.02%), *P. chrysogenum* (5.19 ± 0.01%), and *A. tubingensis* (4.29 ± 0.01%) did not support C2C12 metabolism and were not significantly different from cells not attached to anything, or the negative control—implying that these species did not support cell metabolic activity most likely because cells did not attach to these carriers. *Aspergillus sojae* at 9.4 ± 0.02% reduction in AB supported evidence of weak cell attachment, but the metabolic activity was less than half that of C2C12 cells on Cytodex. Therefore, *A. oryzae* 1 was chosen for subsequent experiments.

C2C12 proliferation is impacted by seeding concentration for mycelium carriers

To assess optimal seeding densities, carriers were seeded with C2C12 cells at concentrations of 5 x 10^2, 5 x 10^3, 5 x 10^4, 5 x 10^5, and 5 x 10^6 cells/mL, and percent reduction of AB was measured at two time points (24 hours and 72 hours after seeding) to determine cell proliferation after 48 hours in culture. Fluorescent microscope images of C2C12 TD cells were taken at 72 hours to visualize cells on carriers or formation of cell clumps (Figure 9). When C2C12 cells are forced to grow in suspension, they aggregate with each other at concentrations of 5 x 10^4 cells/mL and above. In the non-edible Cytodex microcarrier condition, C2C12 cells can be seen to evenly cover the entire surface of the beads. These high-density conditions showed saturation of C2C12 cells on the Cytodex beads where C2C12 were at 100% confluency in the 5 x 10^5 cells/mL condition and formed large aggregates at the 5 x 10^6 cells/mL condition. C2C12 cells cover the surface of the mycelium carriers at 5 x 10^6 cells/mL with some small cell clumps attached to the strands of hyphae coming out of the center of the pellet. The group without microcarriers showed low AB percent reduction and little to no change in metabolic activity between the two time points except for the 5 x 10^6 cell/mL condition, where some cells appeared viable at 24 hours, but metabolic activity decreased from 15.7 ± 1.1% to 8.4 ± 0.6% at 72 hours (Figure 10). Cytodex carriers showed the highest increase in metabolic activity at 5 x 10^4 cells/mL seeding density, where percent AB increased from 7.6 ± 0.2% to 21.3 ± 1.8%. Low-density seeding conditions (i.e., 10^2 and 10^3 cells/mL) did not exhibit signs of proliferation with Cytodex and were lower in AB reduction or not significantly different from No MC conditions (Supplementary Figure 1S). High-density seeding conditions (5 x 10^5 and 5 x 10^6 cells/mL) showed sizeable AB percent reduction at the 24-hour time point and modest proliferation over the course of 48 hours. On the other hand, these high-density seeding conditions supported the largest increase in metabolic activity for C2C12 cells on mycelium carriers, increasing from 8.3 ± 1.0% to 33.7 ± 5.5% for 5 x 10^5 cells/mL and 9.4 ± 2.2% to 33.2 ± 1.9% for 5 x 10^6 cells/mL. At a seeding density of 10^4 cells/well, C2C12 cells proliferated, albeit not as well, with 6.6 ±

0.7% AB reduction at 24 hours and 17.0 ± 0.8% at 72 hours. Low-density seeding conditions (5 x 10^2 and 5 x 10^3 cells/mL) did not exhibit signs of proliferation on mycelium carriers.

C2C12 on mycelium carriers express differentiation markers

Cell differentiation on microcarriers is an integral part of the cultivated meat production process, especially if the microcarriers are edible and cells remain on the carriers until the final product formulation. As a measure of the capacity of cells to differentiate on microcarriers, C2C12 cells on microcarriers were placed in differentiation medium for 7 days, and myoblast maturation markers, *PAX7, MYOD1, MYOG*, and *MYH2* were studied at three time points (Figure 11). *PAX7* gene expression (associated with proliferation) decreased significantly from T1 to T2 for C2C12 on Cytodex carriers, while expression was detected but did not change significantly across timepoints on mycelium carriers. *MYOD1* expression showed a decreasing trend with time on Cytodex with significant decrease between T2 and T3. For mycelium however, *MYOD1* expression increased significantly between T1 and T2 and remained approximately the same at T3. *MYOG* expression fluctuated for Cytodex, increasing from T1 to T2 then decreasing slightly at T3. On the other hand, *MYOG* expression for cells grown on mycelium was less strong but showed steady and significant increases at each time point. Lastly, MYH2 expressed strongly across all time points and with a substantial magnitude range, reflected using a logarithmic y-axis. Therefore, MYH2 expression did not change significantly in the case of Cytodex or mycelium. Overall, differentiation gene expression was present, indicating C2C12 can differentiate on mycelium carriers.

bSC attached and proliferated on mycelium carriers

To test the biocompatibility of mycelium carriers with relevant cell types, bSC attachment and proliferation was assessed. bSC are anchorage-dependent cells, as evidenced by the low metabolic activity when they are forced to grow in suspension and high metabolic activity when cells are anchored

to carriers. bSC attachment on Cytodex and mycelium carriers can be confirmed with microscopy images (Figure 12a). Proliferation of bSC was assessed by determining the bSC metabolic activity at 24 hours and 72 hours after seeding and seeding densities ranging from 1 x 10^5 to 2.5 x 10^6 cells/mL (Figure 12b). bSC on Cytodex proliferated most when seeded at 1 x 10^6 cells/mL, where percent reduction of AB increased from 7.0 ± 0.2% at the 24-hour time point to 16.7 ± 0.6% at the 72-hour time point. Cells on mycelium carriers proliferated at all seeding densities. At the 24-hour time point, mycelium carriers had similar AB reduction as no microcarrier conditions except for 3 x 10^6 cells/mL (Supplementary Figure 2S). However, AB reduction increased significantly at the 72-hour time point, surpassing Cytodex conditions in some cases. Cells on mycelium carriers reached AB percent reduction higher than Cytodex for 5 x 10^5 and 1 x 10^6 cells/mL at T3; the greatest change was seen at the 1 x 10^6 cells/mL condition where AB percent reduction increased from 4.0 ± 0.5% to 18.4 ± 1.4%.

bSC on mycelium carriers express some differentiation markers

Similar to C2C12, bSC differentiation capacity on microcarriers was evaluated at three time points over 7 days following a change from proliferation to differentiation media. Gene expression associated with myogenic differentiation was studied using *MYOD1*, *MYOG*, *MYH1/2*, and *MYH3* (Figure 13). Bovine satellite cell expression of MYOD1 decreased over time on both Cytodex and mycelium carriers, though the expression of genes tested was not significantly reduced. MYOG expression also decreased over time for bSC on Cytodex from T1 to T3. Expression of *MYOG* was weak and not significantly different for bSC cells on mycelium carriers for T1 and T2 with no detectable expression at T3. Several samples expressed MYH1/2 on both Cytodex and mycelium carriers, though like with *MYOG*, many samples failed to amplify. However, *MYH3* expression was clearly detected for cells on both Cytodex and mycelium carriers. The only significant difference is a reduction from T1 to T2 on Cytodex. Therefore, observed differentiation gene expression indicates that bSC can differentiate on mycelium carriers.

Discussion

In this study, we demonstrated the potential of mycelium carrier technology by surveying several fungal species that can be compatibly used to culture cells relevant to cultivated meat. We further tested the differentiation capacity of cells on mycelium carriers, which is an important feature of edible carriers for cultivated meat production. Our results demonstrate wide utility of mycelium carrier technology, advancing our previously published POC and corroborating the carrier's mammalian cell biocompatibility (Derakhti et al., 2019).

Animal cells have differential metabolic activity and attachment in response to fungal species variation. The cell-carrier interface largely governs cell attachment. Surface hydrophobicity, charge, stiffness, elasticity, size, shape, topography and chemical composition are also known characteristics of cell-surface interface that impact the ability of a cell to anchor (reviewed in (Bodiou et al., 2020)). We saw that different fungal species yielded different sized pellets. This was expected because the genetic makeup of the species determines mycelium morphology (Berger et al., 2022; Veiter et al., 2018). We also observed that different strains produced more or less compact pellets (data not shown). This implies that surface topography, stiffness and elasticity is likely to differ between strains, thereby impacting attachment. In a previous study, we observed that heat-treated mycelium carriers showed better proliferation than chemical-treated mycelium carriers20. The heat-treated carriers weighed less and were slightly more hydrophobic than chemical-treated carriers. The impact of fungal species on attachment was also reported by (Antinori et al., 2021) where two fungi of different genus were made into scaffolds to attach human dermal fibroblasts (Antinori et al., 2021). The authors speculated that residual extracts or fungal metabolites (which may be beneficial or toxic to cells) could be secreted, impacting cell attachment and viability. Our goal in this targeted strain screening was to select food-related fungal strains that were biocompatible with C2C12 cells, then move forward with the strain that showed the most promise for cell proliferation and differentiation. One limitation to our analysis is that

it fails to quantitatively measure available area for cell attachment on fungal pellets. Numerous attempts were made to quantify fungal pellet specific surface area, without any improvement on the smooth spherical pellet assumption. Thus, we did not quantitatively characterize strain topology in detail. Our focus was on the efficacy of this edible and sustainable biomaterial to support mammalian skeletal muscle culture. In this study, our results show that fungal microcarriers perform promisingly and could be used in alternative protein products. To improve this technology, it is necessary to adapt it to specific cell culture practices and characterize fungal pellet strains in detail, including specific surface area analysis. A characterization dataset for fungal strains can inform high-throughput screening that aligns cell types with compatible fungal strains. Moreover, optimizing the technology involves fine-tuning process parameters like dissolved oxygen control, pH control, and nutrient feeds to enhance productivity of animal cell-mycelium carrier systems and maximize cell density in the media (Z. Cosenza et al., 2023; Z. A. Cosenza, 2022; O'Neill et al., 2021).

For mycelium carriers, seeding density optimization clearly showed a benefit to a high seeding density (5 x 10^5 cells/mL and 5 x 10^6 cells/mL), resulting in better C2C12 cell proliferation. Seeding optimization is commonly performed in cell culture, since cell-cell contact inhibition is a factor that impacts cell signaling for proliferation and other biological cascades(Kimura et al., 1991). The same high cell densities for Cytodex and suspension (no microcarrier) culture system resulted in large aggregates with low metabolic activity. In many cases, large (>500 μm diameter) cell aggregates are difficult to control because of heterogeneous cell clumps and mass transfer limitations that yield necrotic cores (Kwee & Mooney, 2017; McMurtrey, 2016). On the other hand, small aggregates—which are not limited by diffusion—can maintain cell viability. Norris et al. showed that small cell aggregates, named microtissues, support myogenic cell growth and differentiation, and can be a promising solution to address scalability of cultivated meat production at bioreactor scale. For mycelium carriers, fluorescence images showed numerous small aggregates surrounding the surface of the mycelium carriers (Norris et

al., 2022). These aggregates were much smaller than those observed in suspension (no microcarrier) and Cytodex conditions, and they did not clump into large aggregates even at high cell seeding densities. These findings suggest that mycelium carriers have potential to control aggregate size and could be used for scalable cultivated meat production using a single bioreactor. It also suggests a strong interaction between the cells and the Cytodex surface, and a weaker interaction between the cells and the mycelium surface. Cadherin-mediated cell clumping on mycelium may enable the fungal filaments to entrap cell aggregates near the pellet surface.

Further, we demonstrated that C2C12 on carriers expressed key markers of myogenesis in response to media-induced differentiation. *MYOD1*, *MYOG*, and *MYH* are myogenic regulatory factors that regulate the development of functional embryonic skeletal fiber muscle differentiation (Asfour et al., 2018; Bi et al., 2022). *MYH1* and *MYH2* are genes that encode MyHC-2X and MyHC-2A, respectively. Both proteins are found in fast-twitch adult skeletal muscle. *MYH3* encodes MyHC-emb, an embryonic skeletal muscle protein (N. Zhang et al., 2020). While the expression of these transcription factors functions as a switch in the differentiation of myoblasts, *PAX7* is a proliferation regulator of muscle stem cells and is activated during muscle regeneration 43. We observed increase in expression of *MYOD1* and *MYOG* over time and expression of *MYH2* for C2C12 on mycelium carriers. The expression of these key markers, especially the strong expression of *MYH2*, indicate that C2C12 are going through differentiation on microcarriers such as Cytodex44. Interestingly, *PAX7* expression was observed without significant decrease in expression on mycelium carriers over time indicating that some C2C12 cells may still be maintaining their proliferative state while others are differentiating. Compared to the smooth, monolayered surface of Cytodex, the mycelium is structurally intricate and compositionally complex, consisting of a porous matrix of various protein, glucans, and chitin. *MYH2* expression is detectable, though the wide range of expression renders no comparison significantly different. Nevertheless, we consistently detected late myogenic gene expression in both the Cytodex and mycelium carriers.

Since the focal application of this technology is cultivated meat production, it was imperative to demonstrate cell growth potential using a cell type suitable for cultivated meat. We chose bSC, which can proliferate and maintain stemness. Satellite cells are mononuclear cells located between the basal membrane and the sarcolemma of adjacent muscle fibers in mammalian skeletal muscles (Mauro, 1961). Unlike embryonic stem cells, induced pluripotent stem cells, and mesenchymal stem cells that have multilineage differentiation capacity, satellite cells are lineage-restricted and differentiate into myocytes upon activation from quiescence (Yablonka-Reuveni, 2011). This unique property makes them ideal for facilitating the bioprocess of muscle cell production. Our results demonstrate bSC attachment to mycelium carriers and increased proliferation compared to Cytodex at the same seeding density. Trends in differentiation gene expression were difficult to assess. However, *MYOD1* and *MYH3* expression was clear across all sampling points. This coupled with the fact that *PAX7* expression was undetectable, suggests that spontaneous differentiation may be occurring early on and stemness of bSC is lost perhaps even before differentiation was induced by media change. Nonetheless, bSC appear to have similar differentiation potential on mycelium as they do on Cytodex carriers. These are promising initial observations that a one-step proliferation/differentiation bioprocess on edible microcarriers may be possible. In cultivated meat, such a simplified process where the microcarrier formation, cell proliferation, and cell differentiation could occur in a single bioreactor is highly advantageous. Such a process would reduce manufacturing time, contamination risk, and the cost for other specialized equipment. The bSC cell type is also favorable, as they have been observed to proliferate in spinner flasks on Cytodex and edible carriers composed of gelatin and eggshell membrane with collagen (Andreassen et al., 2022; Norris et al., 2022). Verbruggen et al. demonstrated bovine myoblast proliferation and differentiation on Cytodex in spinner flasks (Verbruggen et al., 2018). Thus, we further hypothesize that bSC on mycelium carriers have potential to grow and differentiate in culture with agitation at larger scales.

In summary, we were able to demonstrate the applicability of mycelium carriers for cultivated meat production. While the experiments of this study were limited to microwell plates in static conditions, the data presented here are necessary foundational knowledge to fuel future investigations of this edible biomaterial for cellular agriculture applications. For example, future and ongoing work to advance the technology can tailor mycelium fermentation and cell culture conditions to the respective cell type and enhance productivity. Scaling up cell culture to larger volumes and validating bead-to-bead transfer under agitation conditions represent immediate, evident progressions. Investigating the impact of mycelium and different strains of fungi on the flavor, texture, and nutritional attributes of the final cultivated meat or seafood remains a valuable avenue for product refinement and development. Furthermore, leveraging biological organisms like filamentous fungi as biomaterials holds promise not only due to their edible qualities but also their genetic modifiability. The use of genetic modification in cultivated meat is still uncertain, however, engineering filamentous fungi is technically feasible. Using this approach, we can create mycelium carriers superior at facilitating animal cell proliferation and differentiation or amplify sensory attributes to be more appetizing. Even if not directly applicable to cellular agriculture, this avenue of research contributes to comprehending the fundamental science underpinning cell-mycelium interactions and can find applications in sectors like medical and pharmaceutical cell culture, where genetic modification is less restrictive.

Tables and Figures

Table 3. Filamentous fungal species used to create carriers and their morphological characteristics

Strain	Strain Details	Morphology	Pellet Diameter (µm)	Origin
FST 76-2	*Aspergillus oryzae* (*A. oryzae 1*)	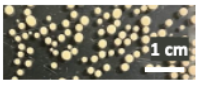	1101 ± 580[c]	UC Davis Phaff Culture Collection, Davis, CA, USA
UCD 8	*Aspergillus oryzae* (*A. oryzae 2*)	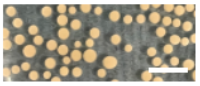	3050 ± 17[a]	UC Davis Viticulture and Enology Culture Collection, Davis, CA, USA
FST 40-400	*Aspergillus awamori*	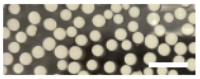	2990 ± 650[a]	UC Davis Phaff Culture Collection, Davis, CA, USA
FST 76-1	*Aspergillus sojae*		1720 ± 427[bc]	UC Davis Phaff Culture Collection, Davis, CA, USA
UCD15	*Aspergillus nishimurae*	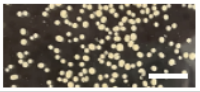	1200 ± 78[c]	UC Davis Viticulture and Enology Culture Collection, Davis, CA, USA
UCD12	*Aspergillus tubingensis*	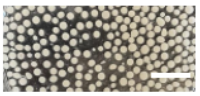	2097 ± 162[b]	UC Davis Viticulture and Enology Culture Collection, Davis, CA, USA
FST 72-2	*Rhizopus oligosporus*		-	UC Davis Phaff Culture Collection, Davis, CA, USA
H3	*Penicillium chrysogenum*	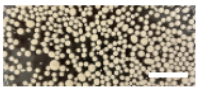	2270 ± 71[b]	University of Cordoba, Department of Microbiology, Spain

*Superscript letters (a–c) indicate statistically significant homogenous groups differing in the parameters among the strains ($p < 0.05$, *F*-test).

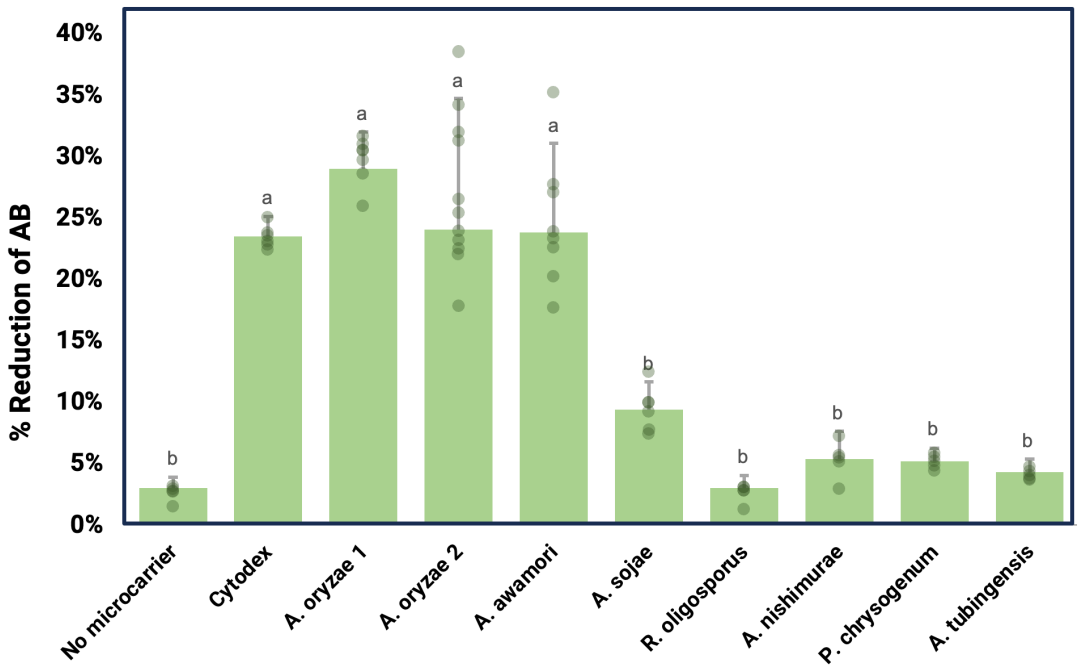

Figure 8. C2C12 metabolic activity expressed as percent reduction of alamarblue (AB) on different fungal species as carriers at 48 hours after time of seeding. No microcarrier as the negative control and nonedible carrier Cytodex as the positive control. Superscript letters (a–c) indicate statistically significant homogenous groups differing in the parameters among the strains ($p < 0.05$, *F*-test).

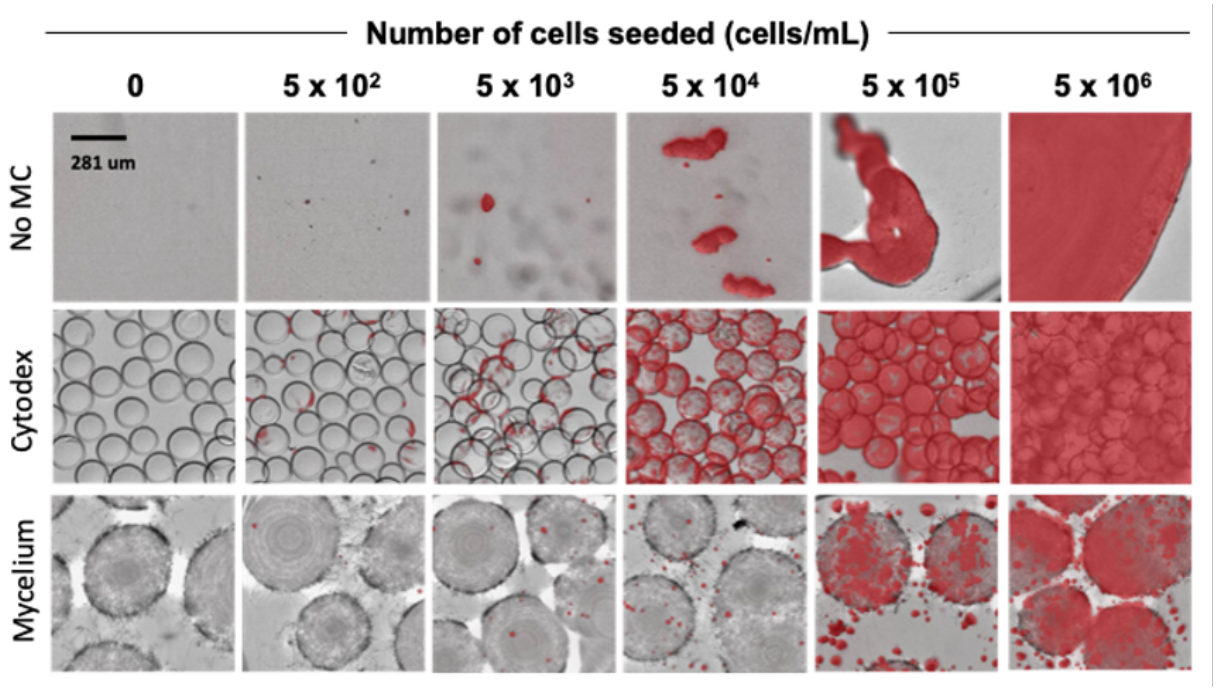

Figure 9. C2C12 transfected with TdTomato (red fluorescent) on Cytodex, Mycelium carrier, and no microcarrier (MC) at 72 hours after seeding.

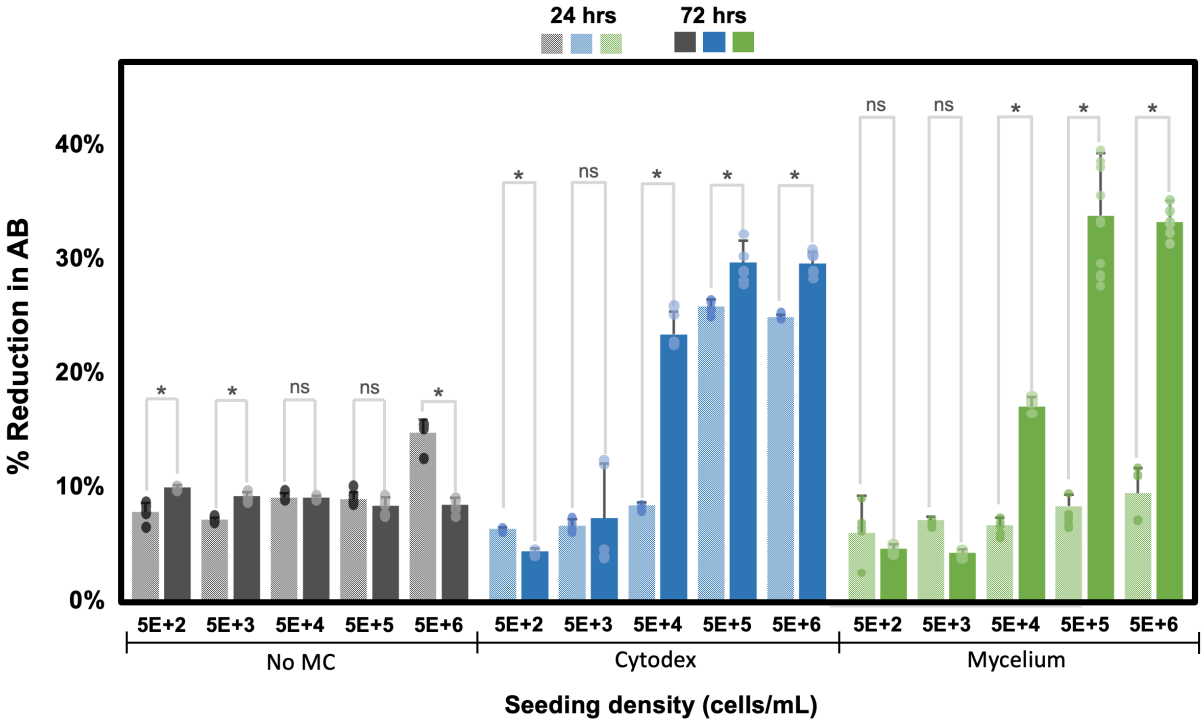

Figure 10. C2C12 metabolic activity represented as % reduction of alamarblue (AB) on Cytodex, mycelium carriers and no microcarrier (MC) at 24 hours from time of seeding (represented in lighter colored bars) and 72 hours from time of seeding (represented in darker color bars). * indicates significant differences at $p \leq 0.05$ with $n \geq 3$ and ns indicates no significant differences

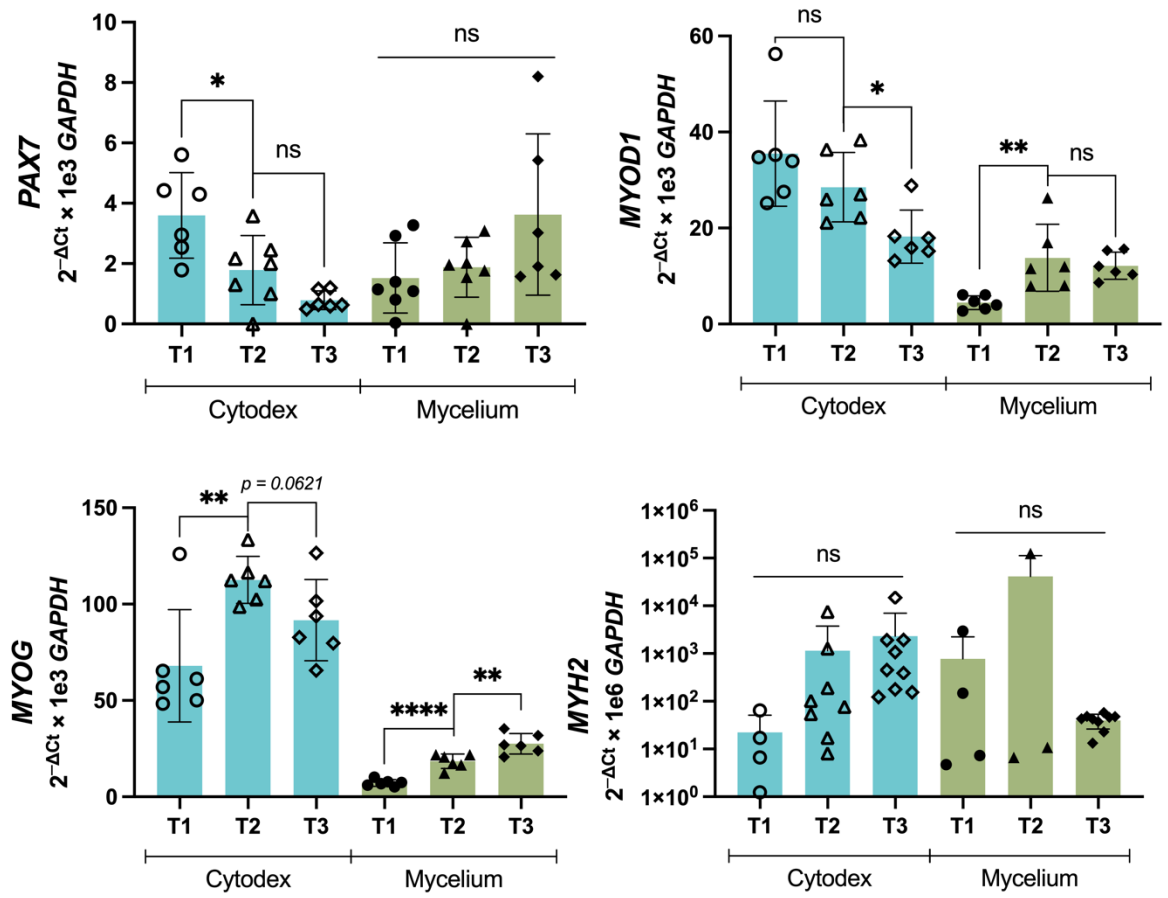

Figure 11. Relative expression of differentiation markers PAX7, MYOD1, MYOG, MHC for C2C12 at four different sampling time points on Cytodex and Mycelium carriers. Samples were collected right after switching to differentiation media (time point 0, T0) and at 48 hrs (time point 1, T1), 96 hrs (time point 2, T2), and 168 hrs (time point 3, T3).

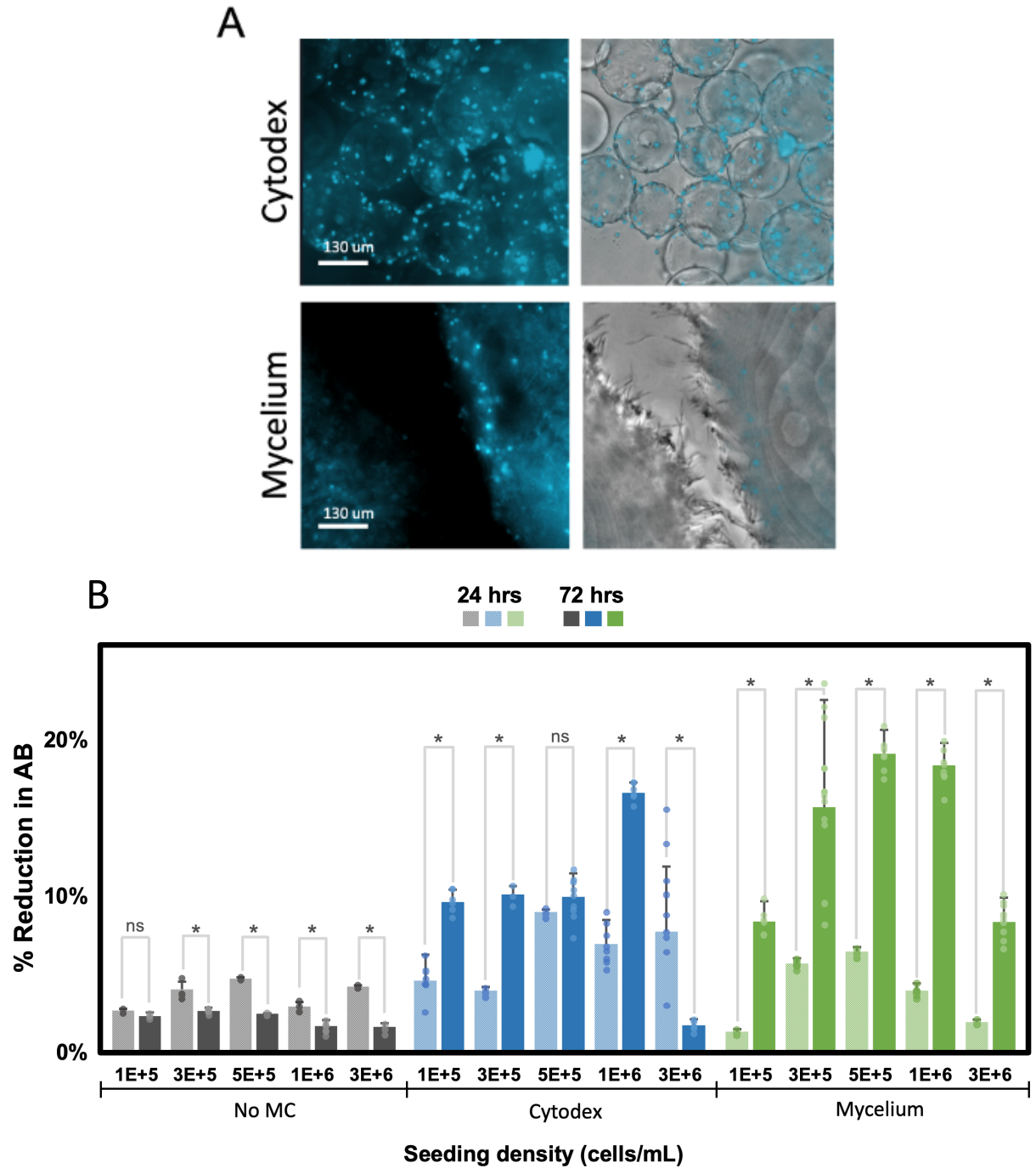

Figure 12. A) bSC immunostained with Hoescht (blue fluorescent) on Cytodex microcarriers and mycelium carriers after 72 hour incubation. B) bSC metabolic activity represented as % reduction of alamarblue (AB) on Cytodex, mycelium carriers and no microcarrier (MC) at 24 hours from time of seeding (represented in lighter colored bars) and 72 hours from time of seeding (represented in darker color bars). * indicates significant differences at $p \leq 0.05$ with $n \geq 3$ and ns indicates no significant differences

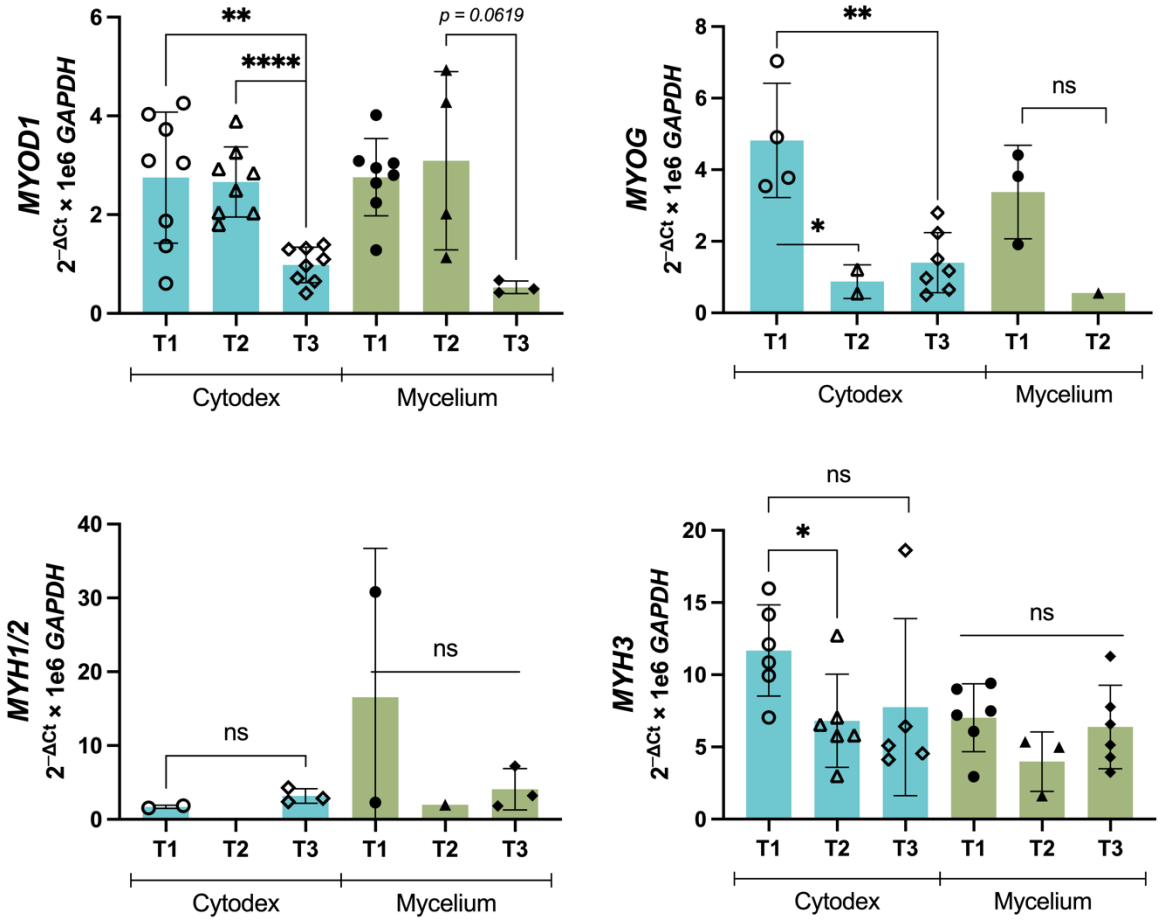

Figure 13. Relative expression of differentiation markers MYOD1, MYOG, MYH1/2, and MYH3 for bSC at three time points on Cytodex and Mycelium carriers. Samples were collected 48 hours (time point 1, T1), 96 hours (time point 2, T2), and 168 hours (time point 3, T3). * indicates significant differences at $p \leq 0.05$, ** at $p \leq 0.01$, **** at $p \leq 0.0001$, with n indicated by individual data points and ns indicates no significant differences. Plate wells that did not amplify are not shown.

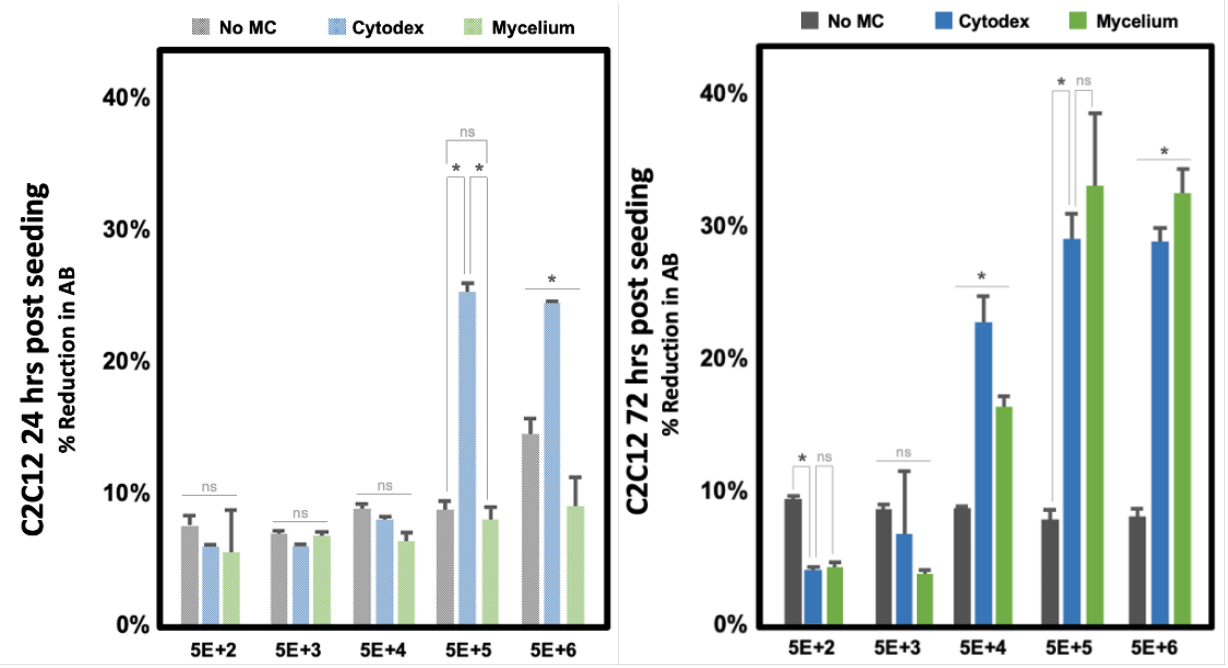

Figure 1S. C2C12 metabolic activity represented as % reduction of alamarblue (AB) on Cytodex, mycelium carriers and no microcarrier (MC) at (A) 24 hours from time of seeding, and (B) 72 hours from time of seeding.

* indicates significant differences at $p \leq 0.05$ with $n \geq 3$ and ns indicates no significant difference

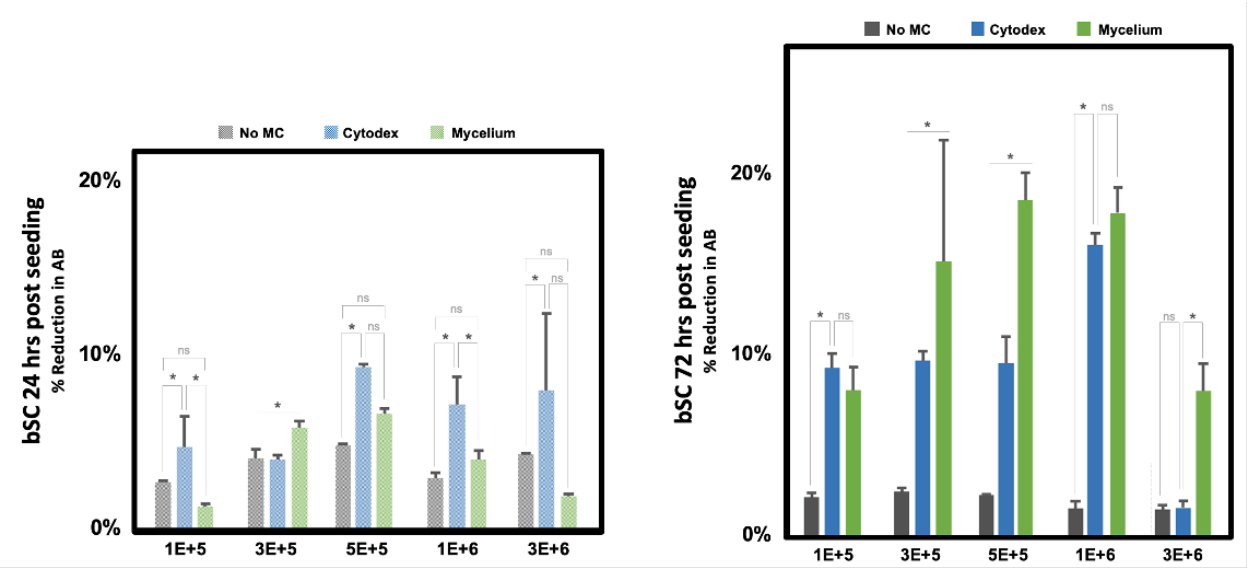

Figure 2S. bSC metabolic activity represented as % reduction of alamarblue (AB) on Cytodex, mycelium carriers and no microcarrier (MC) at (A) 24 hours from time of seeding, and (B) 72 hours from time of seeding.

* indicates significant differences at $p \leq 0.05$ with $n \geq 3$ and ns indicates no significant differences

CHAPTER 4: The Impact of Mycelium Carrier Characteristics on Animal Cell Attachment for Cultivated Meat Production

Abstract

Cell biocompatibility and the mechanism of attachment are crucial information needed to develop new edible microcarriers for cultivated meat production. This study investigates mycelium biomass as an edible material and its biocompatibility with bovine satellite cells (bSC). Inactive mycelial biomasses, called pellets, were characterized using Raman spectroscopy, and physical properties such as dry weight, volume, density, and elastic modulus were analyzed. Using multivariate statistical analysis, key pellet characteristics and their relationship with bSC adhesion were uncovered using AlamarBlue metabolic activity as a proxy for cell attachment. Cell components of the mycelium carriers attributed to C-C and C-O stretching and N-H deformation were most correlated with in cell-carrier interaction and bSC attachment. Physical properties also contributed to supporting bSC viability but were not clearly correlated. Pellet volume and density surpassed the variable importance threshold of 1 and correlated significantly with bSC viability but dry mass and elastic modulus did not supass the threshold. In general, smaller, lighter, and less dense pellets favored supporting bSC metabolic activity. The findings demonstrate that Raman spectroscopy can effectively identify key molecular vibrations associated with high cell compatibility, making it a promising initial screening tool for selecting biocompatible carriers. Furthermore, an enhanced understanding of mycelium-cell interactions facilitates the rapid scale-up and bead-to-bead transfer potential of these carriers, bringing the field closer to developing edible mycelium carriers suitable for cultivated meat production.

Introduction

The industry of cultivated meat—growing animal cells in a bioreactor to produce meat— has experienced rapid growth, attracting over $3.1 billion in investments over the past decade, with 83% of

that total occurring in just the last three years (*US Approval of Lab-Grown Meat to Unleash "stifled" Sector - PitchBook*, n.d.). Since the announcement of the first cultivated meat company in 2016, nearly 200 companies worldwide have publicly entered the field (*State of the Industry Reports - The Good Food Institute*, 2024). This remarkable expansion is fueled by rising consumer demand for sustainable and nutritious food options and increasing concerns about the environmental and ethical implications of traditional animal agriculture and the current food system.

Despite the increasing interest in cultivated meat, and the recent initial approval of two products for sale in the U.S., the industry still faces challenges that prevent it from achieving large-scale commercialization (Kirsch et al., 2023). One major challenge is developing a process that maximizes cell growth productivity per unit of medium volume, to enhance resource efficiency and cost-effectiveness (Negulescu et al., 2023; Post & van der Weele, 2014; van der Weele & Tramper, 2014). For anchorage-dependent cells, microcarriers can be used to attain higher cell densities (Bodiou et al., 2020). Traditional microcarriers are inedible polymer beads. The removal of cells from their surface post harvest makes these beads prohibitively expensive and operationally difficult at scale (Caruso et al., 2014; Goh et al., 2013). Edible carriers and supports, which are incorporated into the final food product, can negate these issues and are the most promising approach to increasing process efficiency while providing opportunities to improve the nutritional and sensory properties of the final cultivated meat (Derakhti et al., 2019).

The development of cell-culture carriers starts with understanding cell biocompatibility and the mechanism of attachment to the support. Cells attach to a surface using mechanosensitive signaling pathways that are dependent on the extracellular environment. These cell-matrix interactions impact cell polarity, migration, and differentiation (Ahmad et al., 2023). Several important matrix properties mediate the cellular response to the material, including stiffness; topography; and surface chemical composition (Dyachuk, 2013; Handorf et al., 2015; Odintsova et al., 2010; Sun et al., 2016). These factors

also impact bead-to-bead (B2B) transfer, a process where cells migrate from cell-seeded beads to newly added beads, a necessary process for microcarrier use in cell culture for continuous culturing as well as seed train expansion for batch or fed-batch cultures at large scales (Verbruggen et al., 2018).

Filamentous fungal biomass has recently been shown to support anchorage-dependent cell proliferation and differentiation and is a strong candidate edible biomaterial for cultivated meat (Block & Ogawa, 2024; Ogawa, Moreno García, et al., 2022). Both C2C12 and transformed mouse myoblasts primary bovine satellite cells (bSC) attached and grew on deactivated mycelium carriers at a comparable rate to the commercially standard inedible carrier (Block & Ogawa, 2024; Ogawa, 2024). While these initial results are promising, the attachment mechanism remains unclear, and optimizing the process remains challenging. Biocompatibility with animal cells appears to be impacted by mycelium carrier characteristics, which can differ based on the selected fungal species and the inactivation methods. Pellet morphology and characteristics also depend highly on fermentation parameters (Papagianni, 2004; Veiter et al., 2018). Thus, there are thousands of ways to modify the material properties when working with mycelium biomass. To characterize the pellet, especially the cell-carrier interface, which directly impacts mechanical properties of the biomass, a non-destructive, rapid, and highly chemical-specific method is necessary.

Raman spectroscopy is a technique that is particularly useful in providing detailed and comprehensive information by measuring the broad chemical profiles of filamentous fungal biomass (Dzurendová et al., 2021; Saif et al., 2021; Shigeto & Takeshita, 2022). This technique is highly suitable for biotechnology applications because it does not require special sample pretreatment or labeling, is non-destructive, cost-effective, and provides rapid results (Noothalapati et al., 2016; Okada et al., 2012; Schuster et al., 2000). Raman spectroscopy relies on the inelastic scattering of light, known as the Raman effect, and involves identifying molecular vibrations resulting from the interaction between the sample and excitation radiation, typically provided by a laser in the ultraviolet, visible, or near-infrared

regions of the electromagnetic spectrum (Raman & Krishnan, 1928). The resulting Raman spectrum in biological samples reveals a wide range of signals corresponding to different cellular components, such as lipids, proteins, pigments, and carbohydrates (De Gelder et al., 2007; Stöckel et al., 2016). Using this technique, the chemical profile of mycelial pellets can be rapidly elucidated and correlated with animal cell attachment.

This study aims to understand the properties of mycelium carriers that impact cell-carrier biocompatibility and attachment. A select combination of eight fungal species with two growth media was chosen to produce mycelium pellets with different physicochemical properties. These pellets were characterized as to their physical traits and using Raman spectroscopy to establish the chemical composition of the fungal biomass. The same pellets were then used as carriers of bSC and assessed for biocompatibility. Using multivariate analysis, the carrier characteristics that impact bSC attachment were elucidated. Following the determination of attachment, a subset of mycelium carriers was used to determine the potential for bead-to-bead (B2B) transfer and scaling up into spinner flask scales. The main goal of this study was to uncover the mycelium properties driving the attachment of bSCs cells to improve their capacity to serve as an edible carrier for cell types that are relevant to cultivated meat.

Material and Methods

Fungal Strains and Media Components

Filamentous fungal strains were obtained from the UC Davis Viticulture and Enology Department Culture Collection (Davis, CA, USA), UC Davis Phaff Yeast Culture Collection (Davis, CA, USA), and the University of Cordoba Culture Collection (Cordoba, Spain). The strains are *Aspergillus oryzae* FST 76-2, *Aspergillus oryzae* UCD 8, *Aspergillus awamori* FST 40-400, *Aspergillus sojae* FST 76-1, *Aspergillus nishimurae* UCD 15, *Aspergillus tubingensis* UCD 12, *Rhizopus oligosporus* FST 72-2, and *Penicillium chrysogenum* H3 (Table 4).

Filamentous fungi were pre-grown on a common sporulation agar media (1.7% (w/v) corn meal agar (BD, Franklin Lakes, NJ, USA), 0.1% (w/v) yeast extract (BD, Franklin Lakes, NJ, USA), 0.2 % (w/v) glucose (Spectrum Chemicals, New Brunswick, NJ, USA) and 2% (w/v) bactoagar (BD, Franklin Lakes, NJ, USA)). Two media were used to grow the filamentous fungi. The first media, filamentous fungal pellet medium (FPM) consisted of 6% (w/v) glucose, 0.3% (w/v) yeast extract, 0.3% (w/v) $NaNO_3$ (Sigma-Aldrich, St. Louis, MO, USA), 0.1% (w/v) K_2HPO_4 (Thermo Fisher Scientific, Waltham, MA, USA), 0.05% (w/v) $MgSO_4$, (RPI, Mount Prospect, IL, USA) 0.05% (w/v) KCl (Thermo Fisher Scientific, Waltham, MA, USA), and 0.001% (w/v) $FeSO_4$ (Thermo Fisher Scientific, Waltham, MA, USA). An inactivation check was performed on YPD plates (yeast extract 1% (w/v), peptone 2% (w/v), glucose 2% (w/v), bactoagar 2% (w/v)). The second media, potato dextrose broth (PDB), consisted of potato dextrose broth 2.4% (w/v) (Sigma-Aldrich, St. Louis, MO, USA) (which consists of dextrose 2% (w/v) and potato infusion 0.4% (w/v)).

Animal Cells and Culture Media

Bovine satellite cells (bSC) were studied for attachment and proliferation potential on mycelium carriers. bSC were isolated from fresh leg skeletal muscle of XX/XXY Holstein Cows at the Animal Science Department of the University of California, Davis. Briefly, the biopsy was cut into 0.5 cm or smaller bundles and digested in DMEM with 2% penicillin/streptomycin/amphotericin (Lonza 12-745E) and 200 units/mL collagenase (Worthington, Lakewood, NJ, USA) for 2 hours. Debris was removed by repeated centrifugation, washing, and filtering through a 100 µm filter and a 40 µm filter. Cells were incubated with an FcR blocking reagent, labeled with micromagnetic brands in the satellite cell isolation kit (Miltenyi), and passed through a MACS column and separator (Miltenyi) with bSC sorted out via negative selection. bSCswere cultivated in complete proliferation media: 79% (v/v) F10 (Thermo Scientific, Rochester, NY, USA), 20% (v/v) fetal bovine serum (Thermo Scientific, Rochester, NY, USA), 1% (v/v)

Penicillin-Streptomycin (Sigma-Aldrich, St. Louis, MO, USA) supplemented with five ng/mL FGF2 (Thermo Scientific, Rochester, NY, USA) and differentiation media: 93% (v/v), DMEM (Thermo Scientific, Rochester, NY, USA), 2% (v/v) fetal bovine serum (Thermo Scientific, Rochester, NY, USA), 1% (v/v) Penicillin-Streptomycin (Sigma-Aldrich, St. Louis, MO, USA).

C2C12 cells (mouse myoblasts; ATCC: CRL-1772) were used for B2B transfer potential and scale-up experiments. C2C12 cells were cultivated in complete proliferation media: 89% (*v*/*v*) DMEM (Thermo Scientific, Rochester, NY, USA), 10% (*v*/*v*), fetal bovine serum (Thermo Scientific, Rochester, NY, USA), 1% (*v*/*v*) Penicillin-Streptomycin (Sigma-Aldrich, St. Louis, MO, USA)

Mycelium Carrier Formation and Inactivation

All fungi used in this study were grown under the same conditions as the initial POC (Block & Ogawa, 2024; Ogawa, Moreno García, et al., 2022). A list of fungi used with their respective sample names are presented in Table 4. Filamentous fungal strains were pre-grown on sporulation agar plates for seven days at 28 °C. Conidia and spore formation were confirmed via confocal and light microscope. The spores were then suspended in sterile distilled water and vortexed, then sonicated for 5 minutes. The suspension was inoculated into 50 mL of FPM medium and adjusted to a pH of 5.5. A subset of fungi (species A, E, and J) were grown in 50 mL of PDB medium. All conditions were grown in 250 mL Erlenmeyer flasks covered with hydrophobic cotton, with the final spore concentration reaching 1×10^6 spores/mL. The flasks were placed under high agitation at 250 rpm and a temperature of 30 °C in an Innova 4000 Incubator Shaker (New Brunswick Scientific Co., Edison, New Jersey). This produced spherical, porous biomasses called pellets (except *R. oligosporus*). These pellets spontaneously form when certain species of fungi are cultivated in this manner. After three days, the fungal pellets were harvested, washed with sterile DI water, and then immediately autoclaved in sterile DI water at a

temperature of 121 °C for 20 minutes. Inactivation was confirmed by taking 20 random pellets and assessing growth on YPD agar plates at 28 °C for at least one week. No growth was observed, which confirmed that the pellets were inactive.

Pellet Physical Characterization

Characteristics of inactivated pellets were measured for each condition A to K. After pellet formation and inactivation, pellets in one flask (one biological replicate) were used to determine pellet volume and mass. For volume, the pellets were placed in a petri dish and DI water was added until all pellets were submerged under water. Brightfield images using an inverted microscope with a camera attached were taken. The images were later processed to obtain pellet diameter using the particle analysis feature in FIJI (Bethesda, Rockville, MD, USA). Under the assumption that all pellets are spherical in shape, the average volume of pellets in each condition was calculated using the volume of a sphere $4/3\ \pi r^3$ with the exception of condition I, which was cylindrical in shape and was calculated using the volume of a cylinder $h\ \pi r^2$. The pellets were then strained so minimum water was left, placed on pre-weighed aluminum boats, and oven-dried at 40 °C overnight. The pellets were then weighed the next day continuously every hour until the weight remained constant and the final mass was recorded.

The elastic modulus of each pellet was measured using the MicroTester G2 from CellScale Biomaterials Testing (Waterloo, Ontario, Canada). The test method involved a 30 second linear ramp to achieve a compressive strain of at least 20%. Depending on the fungal species, the testing beam had a diameter ranging between 0.15 and 0.56 mm. The elastic modulus is reported at 10% nominal compressive strain. Prior to analysis, force vs. displacement data were reviewed for quality before proceeding with calculations in Python. The stiffness values for the compression tests were calculated using a modified Hertz model for a sphere described by Kim et al., using equations 1-4

$$\phi = cos^{-1}\left[\frac{R-\delta}{R}\right] \quad (1)$$

$$a = (R-\delta)\, tan\, tan\, \phi \quad (2)$$

$$f(a) = \frac{2(1+v)R^2}{(a^2+4R^2)^{3/2}} + \frac{1-v^2}{(a^2+4R^2)^{1/2}} \quad (3)$$

$$E = \frac{3(1-v^2)F}{(4\delta a)} - \frac{f(a)F}{\pi\delta} \quad (4)$$

Where R is the distance from the sphere center to the outer edge of contact area (in µm), δ is the compressive displacement (in µm), a is the radius of sphere contact area (in µm), $f(a)$ is the force applied to the sphere contact area (in N), v is Poisson's ratio which is assumed to be 0.5 for incompressible materials, F is the force applied to the sphere (in N), and E is the Young's modulus (in Pa) of the material under compression.

Raman Analysis

Raman spectra were taken by Renishaw Raman spectrometer (Renishaw, Wotton-under-Edge, UK) with Leica microscopy using NIR laser emitting light at a wavelength of 785 nm. The light was focused on the fungal biomass from each sample condition A to K. On a glass coverslip covered with aluminum foil, pellets of each condition were placed so a monolayer of biomass covered the middle of the coverslip of approximately 1 cm x 1 cm. Raman spectra were collected in the range of 100–1800 cm^{-1}, with a spectral resolution of 4 cm^{-1}. The spectra were recorded with a total of 128 scans, using Blackman–Harris 4-term apodization, with a digital resolution of 1.928 cm^{-1} at a 500 mW laser power. The Windows-based Raman Environment software (Renishaw, Wotton-under-Edge, UK) was used for data acquisition and instrument control.

Spectral processing was done using the Spectragryph Software (Oberstdof, Germany). Raman-spectrawere smoothed by using a Savitzky-Golay (SG) algorithm (polynomial 3, window size 10,

derivative order 0), followed by an adaptive baseline correction (coarseness 15, offset 0), and normalization by extended multiplicative signal correction (EMSC). Spectra were averaged per sample. Key Raman shift ranges (v#) specific to filamentous fungi are compiled in Table 5 The intensities for each v# were integrated under the curve and analyzed using multivariate statistical analysis explained in detail later in this section.

bSC growth on mycelium carriers

Carriers were pretreated by washing twice with Dulbecco's phosphate-buffered saline (DPBS) (Gibco, Thermo Fisher Scientific, Waltham, MA, USA) and submerging in complete proliferation media for 3 hours prior to seeding. Cytodex 3 (Cytiva, Marlborough, MA, USA), the commercial standard non-edible carrier, was used as a positive control. Cytodex 3 isnon-porous, type I porcine collagen-coated beads composed of cross-linked dextran and a diameter of 141-211 µm and 2700 cm^2/g dry weight specific surface area. Cytodex 3 was prepared at 3 g/L per replicate then hydrated and pre-treated according to the manufacturer's instructions before seeding. Mycelium carrier conditions were standardized by assessing fungal strain differences in diameter and approximating to match the available surface area to that of the Cytodex conditions. One strain in particular, *R. oligosporus*, did not form spherical pellets but a flat, matt-like structure. For this condition, a circular cutout with approximately 7 mm diameter and 1 mm thickness was placed at the bottom of the plate well with cells seeded aboveon top of it for biocompatibility testing. After pretreatment of carriers, the C2C12 cells were seeded in 96-well plates coated with anti-adherent solution (StemCell Technologies, Vancouver, BC) to prevent them from anchoring to the bottom of the wells. Negative control wells had no microcarriers. Wells that contained only media or only microcarriers were prepared as blanks. Each replicate was a single well of the 96-well plates. The cells were seeded at 2.5 x 10^5 cells/mL and incubated at 37 °C with 5 % CO_2 in a HERAcell VIOS 160i incubator (Thermo Fisher Scientific, Waltham, MA, USA). 48 hours after seeding, the

metabolic activity of the attached cells was analyzed by AlamarBlue (AB) following the methods described below.

AlamarBlue® Cell Viability Assay Reagent (Invitrogen, Waltham, MA, USA) was used to determine the number of viable cells. in each well This dye incorporates an oxidation-reduction indicator that changes color in response to chemical reduction within active mitochondria. Since dividing cells have similar mitochondrial mass, this measure is often used to estimate cell number. For the assay, 20 µL of AB solution was added to each replicate 48 hours after seeding. After four hours of incubation, 100 µL of media with AB solution was transferred to a clear bottom 96-well plate, and absorbance was measured at 570 nm and 600 nm using the SpectraMax iD5 Multi-Mode Microplate Reader (Molecular Devices, San Jose, CA, USA). The percentage reduction of AB was calculated per the manufacturer's instructions. Previous work from our lab has found that the higher the percentage reduction of media, the more metabolically active cells are present in the well[34]. Assuming a uniform (average) metabolic activity for each cell, this percent reduction is linearly correlated with viable cell concentration. This simple assessment gives us a way of comparing between groups with this proxy for biocompatibility and proliferation potential.

Multivariate Statistical Analysis

The effect of different pellet characteristics on bSC attachment was analyzed by Principal Component Analysis (PCA) using Prism 10 software (GraphPad Software, San Diego, CA). All data were centered and standardized for analysis. Those principle components with the largest eigenvalues, which together represent over 75% of the variance in the data set were selected. The loading and PC score plots were prepared for the first two PCs.

Partial Least Squares (PLS) regression analysis was conducted using JMP 17 software (SAS Institute, Cary, NC) to examine the effect of Raman analysis data on bSC attachment to carriers, with the percent reduction of AB as the response variable. The data were scaled and centered, employing the SIMPLS algorithm with fast singular value decomposition SVD (REF). A holdback cross-validation method was used with 33% proportion. The initial search consisted of 11 factors and the minimum root mean predicted residual error sum of squares (PRESS) occurred with 8 factors. To evaluate model quality, the root mean PRESS, van der Voet T^2 statistic, correlation coefficient (R^2), and correlation coefficient (Q^2) values for factors ranging from 0 to 11 were used. Raman intensity (X) loadings were analyzed to determine their influence on the PLS model and to identify the chemical components most likely affecting cell culture performance.

Bead To Bead Transfer and Scale Up

The B2B potential of mycelium carriers was studied in a subset of experiments. The controls and culturing conditions are the same as described above for bSC growth on mycelium carriers, but these studies used C2C12 cells. Pellet A was selected for this study because this mycelium carrier resulted in the best proliferation for C2C12 in previous studies (Ogawa, 2024). B2B conditions for Cytodex and mycelium were studied by adding new carriers to the culture on day 2 after seeding. These conditions were compared and done in parallel to cultures where no additional carriers were added. Samples were collected on day 1 and day 3 after bead addition, and % AB reduction was analyzed at those time points.

All work on mycelium carriers with cells was done in static, microwell plates up until this point. To scale up this system, 100 mL working volume spinner flasks (Chemglass Life Sciences, Vineland NJ) were used. Cytodex carriers at 3 g/mL (concentration recommended by the manufacturer) and 0.8 g (dry weight) of mycelium carriers were used in each spinner flask within 45 ml of growth medium. Cells were seeded at

1.8 x 10^5 cells/mL. The spinner flask containing carriers and cells were placed on a stirring plate in an incubator for 8 days. For the first 24 hours, the cells were subjected to an intermittent stirring schedule, alternating between 30 minutes of rest and 3 minutes of stirring at 30 rpm, 37 °C and 5% CO_2. After this period, an additional 50 ml of growth medium was added, and the agitation rate was set to 50 rpm. Samples were taken daily and cells on microcarriers were dissociated with trypsin and counted on a hemacytometer.

Statistical Analysis

Statistical analysis was performed using the software R (v4.2.1; R Core Team, 2022) and the agricolae package (v1.3-5; de Mendiburu, 2021) for the following methods: ANOVA (Analysis of Variance) and Fisher's LSD test for the establishment of homogeneous groups (HG) and two-tailed unpaired t-test. Any statistically significant difference was implied by $p \leq 0.05$ unless otherwise stated in the figures. At least three biological replicates were performed for every condition and time point, with each biological replicate corresponding to a dedicated well on a 96-well plate.

Results

Both fungal strain and media type influenced pellet physical properties

Filamentous fungi were made into mycelium carriers under the same fermentation conditions, inactivated, and characterized for physical properties, which were dry weight, volume, density, and elastic modulus. Both food-grade and non-food-grade fungi were selected to broaden the range of species (Table 4). A subset of fungi (*A. oryzae* FST 76-2, *A. sojae* FST 76-1, and *A. oryzae* UCD8) were grown in two different growth media, but with all other carrier formation conditions the same in both media. This was done to assess the impact of growth media on pellet characteristics and subsequent bSC attachment.

Results showed that fungal physical properties differed in all conditions. The dry weight ranged between 0.0001 to 0.0013 g per pellet, with pellet D averaging the lightest and pellet K averaging the heaviest (Figure 14a). Those pellets produced with PDB media weighed more than the pellets with FPM media, even within the same species. For species E and J, their PDB counterparts weighed over two fold more. The media differences were also apparent in the volume where PDB pellets were larger than the FPM pellets (Figure 14B). The smallest pellets were pellets A and D, 1.2 mm^2 and 0.91 mm^2, respectively. The largest were pellets B and D, 22.1 mm^2 and 25.1 mm^2, respectively. The resulting density of pellet A being the greatest at 0.00014 g/mm^3 and pellet I being the least at 0.000011 g/mm^3 (Figure 14c). The elastic modulus (ratio between the compressive stress and strain or the stiffness of each pellet) is presented in Figure 14d. Pellets, indicated that sample A and K were the stiffest, averaging 7101 Pa and 6451 Pa, respectively. The least stiff was pellet I with a modulus of 130 Pa.

Raman fingerprinting showed distinct chemical composition of each pellet

The Raman spectra of eleven samples of mycelium pellets, conditions A to K were taken in the range of 1800 cm^{-1} to 100 cm^{-1}, and the spectra are shown in Figure 15 with wavenumbers and their respective molecular vibration and cell components defined in Table 5. In Figure 15, the spectra are grouped by fungal species and media conditions. Samples C, D, G, H, and I which are pellets of different species made under the same fermentation conditions. Figure 15 groups samples A&B, E&F, and J&K which are pairs of pellets of the same fungal strain, but made in either FPM or PDB media. These spectra provide biochemical insights into molecular structures of the mycelial pellet mass. Specific peaks observed in the spectra are attributed to biological molecules such as proteins, lipids, and carbohydrates. The Raman bands along with the characteristic infrared bands are listed in Table 5.

Peaks corresponding to carbohydrates include 1680 cm^{-1} - 1620 cm^{-1} range indicating -C=C stretching, signaling Amide I and chitin, 1755 cm^{-1} is -C=O stretching for glucuronan, 1620 cm^{-1} - 1570 cm^{-1} is NH2

deformation, indicating chitosan. 1460 cm^{-1} - 1440 cm^{-1} are CH2 and Ch3 deformation. 1377 cm^{-1} and 1327 cm^{-1} are CH2, CH, and COH deformation. 1256 cm^{-1} indicates C-C, C-O, CH, CH2. 1200 cm^{-1} - 1150 cm^{-1} are C-O-C stretching, 1150 cm^{-1} - 1050 cm^{-1} is C-N stretching, C-C stretching, and C-O-C stretching and deformation. 950 cm^{-1} - 850 cm^{-1} indicates COH deformation, 715 cm^{-1} is O-C-O stretching and CH deformation, 1158 cm^{-1} - 1130 cm^{-1} is C-C and C-O stretching, 999 cm^{-1} - 902 cm^{-1} are C-O-C stretching, 896 cm^{-1} - 840 cm^{-1} are C-C stretching, 567 cm^{-1} - 461 cm^{-1} is COC glycosidic ring, CCC deformation signifying chitin, and 424 cm^{-1} - 413 cm^{-1} signifies beta(1,3)-D-glucan.

The Raman spectral regions of 1639 cm^{-1}–1609 cm^{-1} and 1576 cm^{-1}–1547 cm^{-1} correspond to the C–N, C–C stretching, and N–H deformation groups of Amide I and Amide II, respectively, indicating the presence of proteins. The varying intensities of these regions across different species suggest differences in protein content. Peaks at 1302, 1313, and 1314 cm^{-1} indicate contributions from amide III for proteins. Furthermore, samples A, E and J grown in FPM media show higher Raman bands in the 1287 cm^{-1}–1214 cm^{-1} range, while samples B, F and K grown in PDB are low. These bands are linked to Amide III protein components. Intensities at 1279 cm^{-1} and 1276 cm^{-1} are high in some samples, highlighting differences in protein content. Bands corresponding to nucleic acids are observed in the regions 670 cm^{-1}–622 cm^{-1} and 835 cm^{-1}–702 cm^{-1}, representing adenine, cytosine, thymine, and phosphodiester groups in DNA and RNA. The region 1158 cm^{-1}–1130 cm^{-1} corresponds to C–C and C–O stretching groups in polysaccharides, observed in all samples.

Lipid contributions are indicated by the 1469 cm^{-1}–1402 cm^{-1} range due to CH2 deformation groups, 750 cm^{-1} is C=O stretching in esters, 1660 cm^{-1} is C=C stretching, and 1080–1060 cm^{-1} is C-C and C-O stretching. These all point to differences in lipid quantities among the samples.

To determine those Raman shifts that corresponded best with bSC number, represented by percent reduction in AB, PLS regression followed by PCA was performed and is discussed more in detail below.

bSC cell metabolism differed when grown on pellets with different characteristics

bSC cells were seeded onto the pellets to assess carrier-cell biocompatibility and growth potential (Figure 16). All conditions were assessed in parallel with the negative control, where cells are forced to grow in suspension without a support, and positive control, using the commercial standard Cytodex 3 microcarriers. Carrier concentration was selected so that all conditions had similar approximate available surface area per well, but all metabolic activity results were normalized to the actual calculated surface area. The metabolic activity of cells, expressed as a percent reduction of AB, was assessed at 48 hours after seeding when bSC cells have attached to microcarriers and are in the exponential phase of growth. Any cells that did not attach have very low metabolic activity, which can be seen in the negative control. Three pellet conditions A, D, and E were significantly better or the same in % AB reduction as the Cytodex positive control: 21.80 ± 0.33 %, 25.01 ± 3.02%, and 28.24 ± 2.45%, respectively. Pellets B, C, F, G, H, J, and K did not support bSCcell attachment and growth as well as the control but were significantly better than the negative control. They were 13.01 ± 2.68%, 18.81 ± 1.82%, 17.64 ± 1.54%, 17.47 ± 1.44%, 12.68%, and 12.66 ± 0.68%. Pellet I resulted in the lowest %AB reduction with 0.3%.

Partial least squares regression analysis pointed to distinct chemical profiles of mycelium carriers that influenced bSC viability

Table 6 shows the PLS regression holdback cross-validation performed on the intensities at Raman shifts relevant for filamentous fungal biomass. The lowest root mean PRESS was found at 2 factors, with a cumulative Q2 value of -0.8. The cumulative percent variation explained for X effects (intensities of Raman shifts) by the two factors used in the model was 83.36%, and Y responses (% AB reduction) were 67%.

Figure 17a shows the X effects loading plot for the first factor of the PLS regression analysis. The first factor accounts for 48.7% of the variation. Raman shifts with positive loadings correlate positively

with %AB reduction, thus benefiting bSC viability and growth. Raman shift at v4, v5, v12, v20, v24, and v33 were positively correlated while the rest were negatively correlated.

Figure 17b shows the variable importance plot (VIP) of the X effects in the model. The conventional threshold value is 0.8 (Errikson et al 2016). Of the 36 Raman shifts, 19 had variable importance values above the conventional threshold, indicating that those molecular variations in the mycelium biomass significantly influenced bSC metabolic activity. Raman shifts that have both a low VIP value and low PLS coefficient indicate that there is minimal influence on explaining the variability among the X effects or Y responses (Figure 18). Those wavelengths that scored VIP of 1 or more were selected to assess further impact on bSC metabolic activity for the principal component analysis.

Principal component analysis showed clustering of pellets supporting bSC viability

The PCA scores plot for the first two principal components in Figure 19 show distinct groupings of pellets that supported bSC attachment and growth (high % reduction in AB). The colors as well as the size of the circles representing each sample in the PC scores plot corresponds to the percent reduction in AB, where larger circles that are closer to the yellow end of the color spectrum are high in percent reduction of AB and smaller circles that are closer to the purple color on the spectrum are low in percent reduction of AB. Pellets that supported higher % reduction of AB, pellets D and E, were clustered in quadrant III, the lower left of the plot. The pellet that supported bSC metabolism the worst was pellet I, which is isolated in quadrant I, the upper right of the plot. All other pellets are grouped in the middle of the PC scores plot along the zero axis of PC1, except for pellet B which is in the bottom right corner.

The PCA biplot for the first two principal components in Figure 19 plots each variable of pellet characteristics, represented as blue eigenvectors, and PC scores of each pellet sample A to I. The percent variation explained by PC1 is 38.4% and PC2 is 22.9%. Pellets D and E clustered close to v12 and v24, which were diametrically opposed to pellet I. The chemical components are present in all quadrants

except the first quadrant. The physical properties of pellets are in quadrants II and IV. Density and dry mass are diametrically opposed. The elastic modulus is close to the center but slightly positive in the direction of PC2. The volume eigenvector is the furthest right and close to the x-axis, thus driving the PC1 variability the most in the positive direction.

Bead To Bead Transfer and Scale Up

Attempts to establish B2B transfer and scale-up to spinner flasks are presented in Supplementary Figure 4S and Supplementary Figure 5S. For B2B attempts, cell growth did not differ compared to no B2B addition, both for Cytodex and mycelium carriers. This may be because cells did not have enough time to migrate to newly added beads and thus, sampling time was too short to measure an effect of cell amplification on newly added beads. For spinner flask trials, cell number on microcarriers did not increase over the culture period of six days. In these initial experiments, we utilized Cytodex culturing protocol for mycelium carriers. However, based on these results, methodology is not directly translatable to these novel carriers and additional work and discovery is needed to find an approach that works for these novel mycelium carrier use in spinner flasks and B2B transfer.

Discussion

This study aimed to identify the factors that most impact cell-carrier interaction to further advance mycelium carrier technology for use in cultivated meat production. The significant influence of both fungal strain and growth media on the physical and biochemical properties of mycelium carriers was confirmed, as was their subsequent impact on cell-carrier biocompatibility but this time with bSC, a cell type realistically suited for cultivated meat production for human consumption.

The most impactful mycelium carrier characteristic on bSC compatibility was the pellet's chemical composition. Two regions of the Raman spectra were highly correlated with cell viability in the positive direction. Generally, Raman intensity is proportional to concentration. The first is v12, at Raman shift

1158cm^{-1} -1130 cm^{-1} regions corresponding to C-C and C-O stretching groups, indicating the presence of polysaccharides (Dzurendová et al., 2021). The intensity values of this region were highest in Pellet D and E, which supported bSC viability the best. The second region is v24 at 1576 cm^{-1}–1547 cm^{-1} corresponding to C-N, C-C stretching, and N-H deformation groups for Amide II, indicating the presence of proteins (Saif et al., 2021). The intensity values of this region were also highest in Pellet D and E. Another interesting region was v36, which had the largest positive coefficient while still surpassing the VIP = 1 threshold in Figure 18. This Raman shift is at 1469 cm^{-1}–1402 cm$^{-1,}$ corresponding to CH2 deformation, indicating the presence of lipids. This region was only slightly negatively correlated with bSC metabolic activity (Figure 17) and most likely explains the lipid membrane properties of the mycelium pellets, which can be altered or modified significantly by inactivation methods (Ogawa, Moreno García, et al., 2022).

The molecular vibrations at v12 and v24 hint at the presence of functional groups which can modulate the adsorption of extracellular matrix proteins (ECM) (Karamanos et al., 2021). Although polysaccharide with C-C and C-O stretching is not reported to be directly relevant to cell adhesion, there are increasing reports that polysaccharides, such as chitosan, can increase re-seeding efficiency and support cell growth (Gupta et al., 2018; Jana et al., 2013; Rubio et al., 2019). Chitosan is a deacetylated form of chitin, a major carbohydrate component of the fungal cell wall. It is structurally similar to the proxy structure of glycosaminoglycan (GAG) which is a main component of native ECMs in tissue and is thought to create a biomimetic environment for cells and tissue, thereby favorable for cell attachment and growth (Bhattarai et al., 2010; Kean & Thanou, 2010). For v24, Amide II bond is a characteristic vibrational mode found in all proteins, including ECM proteins. A study by Reid and colleagues 2020 reported enhanced adhesive properties of endothelial cells with scaffolds that had stronger Amide II peaks (Reid et al., 2020). Strong signals from Amide II can be caused by collagen and elastin, both ECM proteins that bind to cell integrins and directly contribute to cell attachment (X. Wang & Cooper, 2013).

Reports of collagen production in fungal species have been documented (Celerin et al., 1996; Wanderley et al., 2016), although not in the specific species used in this study. Nonetheless, these regions positively influenced bSC growth and could serve as markers for identifying mycelial pellets with a high ability to support cell growth.

The pellet's physical characteristics studied here, which were dry weight, volume, density, and elastic modulus, also contributed to the mycelium carrier's performance in bSC attachment. The size of the pellet, measured by its volume, had the most impact on cell viability, even more so than most of the chemical attributes (Supplementary Figure 3S). This was an interesting finding, especially because the carriers in this study are much larger (over 1mm in diameter) than conventional microcarriers which typically range from 200 to 1000 μm in diameter. The optimal size of microcarriers remains controversial however, with some reports showing better attachment on larger carriers of up to 3000 μm while smaller carriers increased growth rate, possibility due to increased shear stress (Sart et al., 2013; Schmidt et al., 2011). The overall trend seen for physical characteristics of mycelium carriers that performed well were smaller, lighter pellets that were less dense. These characteristics would also be favorable for using these carriers in a bioreactor because less agitation will be needed to keep the carriers afloat, meaning less shear force and stress experienced by the cells (Bodiou et al., 2020). Density of the pellets is also essential to consider when developing methodology for dynamic cultures such as in spinner flasks and bioreactors because it directly impacts the rate at which carriers settle. Interestingly, the elastic modulus did not have a significant effect on cell attachment and growth. The elastic modulus is a measurement of the stiffness of the material and helps to determine cell fate via mechanotransduction (Choquet et al., 1997). In vivo, different tissue types are found in specific ranges of stiffness. For example, adipose tissue and the brain are soft, ranging from approximately 0.2 to 1.0 kPa, skeletal muscle has intermediate stiffness around 10 kPa, and bone is hard, ranging from 30 to 45 kPa (Engler et al., 2006; Guvendiren & Burdick, 2012). This study demonstrated that pellet stiffness can

range from 0.13 to 7.1 kPa, which is ideal for fat and muscle cells, the cell types most needed to be produced in abundance for cultivated meat.

This study marks the first application of Raman spectroscopy to analyze the material properties of mycelium carriers and their correlation with animal cell biocompatibility. Future work on mycelium carrier development should focus on refining the selection of fungal strains and growth media to produce carriers with optimal properties for the growth of specific cells. In the case of bSC and mycelium compatibility, smaller, lighter, and less dense pellets generally favored supporting bSC metabolic activity. This study also utilized Raman spectroscopy to identify key molecular variations related to high cell compatibility with C-C and C-O stretching and N-H deformation positively influencing bSC cell-carrier interaction. Utilizing this information, it would be interesting in subsequent experiments to identify and quantify the concentration of chitosan and/or ECM-like proteins on mycelium pellet surface and correlate this information with bSC viability. For chitosan, this can be achieved using spectroscopic methods such as Nuclear Magnetic Resonance (NMR) and Fourier Transform Infrared (FTIR) and complimented with chromatographic methods such as High-Performance Liquid Chromatography (HPLC) upon successful hydrolysis of the pellet. For adhesion-mediating proteins of interest, a mass spectrometry-based proteomics to identify ECM-like proteins in the cell wall could reveal adhesion-related proteins. A complementary approach could use blocking antibodies against candidate adhesion proteins to see if they inhibit adhesion. Nonetheless, the Raman spectroscopy data presented here is informative because it has advanced capabilities beyond what was presented here. Its versatility extends from spatial cellular imaging with a confocal Raman microscope to in-situ monitoring of bioprocesses in bioreactors using a Raman fiber-optic probe (Bergholt et al., 2019; Esmonde-White et al., 2011). This is particularly useful as these processes, from microcarrier production to cell amplification on microcarriers, are scaled up. Attempts to scale this technology are underway, with preliminary results shown in Supplementary Figure 4S and Supplementary Figure 5S. At this current

stage, successful B2B potential and cell growth on mycelium carriers at the spinner flask scale have not been confirmed. However, in this study we have identified a number of factors influencing that mycelium-cell interactions as well as a high-throughput screening method to accelerate future studies for scalability and B2B potential. This advancement brings us closer to creating an edible carrier that performs well in cultivated meat production, enhancing the feasibility of large-scale applications in this emerging industry.

Tables and Figures

Table 4. Fungal species and strains used in this study, with the growth media used to grow each fungi and the collection they originate from. Filamentous fungal pellet medium (FPM) consisted of 6% (w/v) glucose, 0.3% (w/v) yeast extract, 0.3% (w/v) $NaNO_3$, 0.1% (w/v) K_2HPO_4, 0.05% (w/v) $MgSO_4$, 0.05% (w/v) KCl, and 0.001% (w/v) $FeSO_4$. Potato dextrose broth (PDB), consists of 2.4% potato dextrose broth (which consists of dextrose 2% (w/v) and potato infusion 0.4% (w/v)).

Sample	Species	Strain	Growth Media	Average pellet diameter	Origin
A	*Aspergillus oryzae*	FST 76-2	FPM	1.2 mm	1
B	*Aspergillus oryzae*	FST 76-2	PDB	3.5 mm	1
C	*Aspergillus awamori*	FST 40-400	FPM	2.9 mm	1
D	*Aspergillus nishimurae*	UCD15	FPM	1.2 mm	2
E	*Aspergillus sojae*	FST 76-1	FPM	1.7 mm	1
F	*Aspergillus sojae*	FST 76-1	PDB	2.0 mm	1
G	*Aspergillus tubingensis*	UCD12	FPM	2.1 mm	2
H	*Penicillium chrysogenum*	H3	FPM	2.3 mm	3
I	*Rhizopus oligosporus*	FST 72-2	FPM	8* mm	1
J	*Aspergillus oryzae*	UCD8	FPM	3.1 mm	3
K	*Aspergillus oryzae*	UCD8	PDB	3.2 mm	3

1: UC Davis Phaff Culture Collection, Davis, CA, USA

2: UC Davis Viticulture and Enology Culture Collection, Davis, CA, USA

3: University of Cordoba, Department of Microbiology, Spain

*note that this species' geometry was not spherical but cylindrical (disk-like)

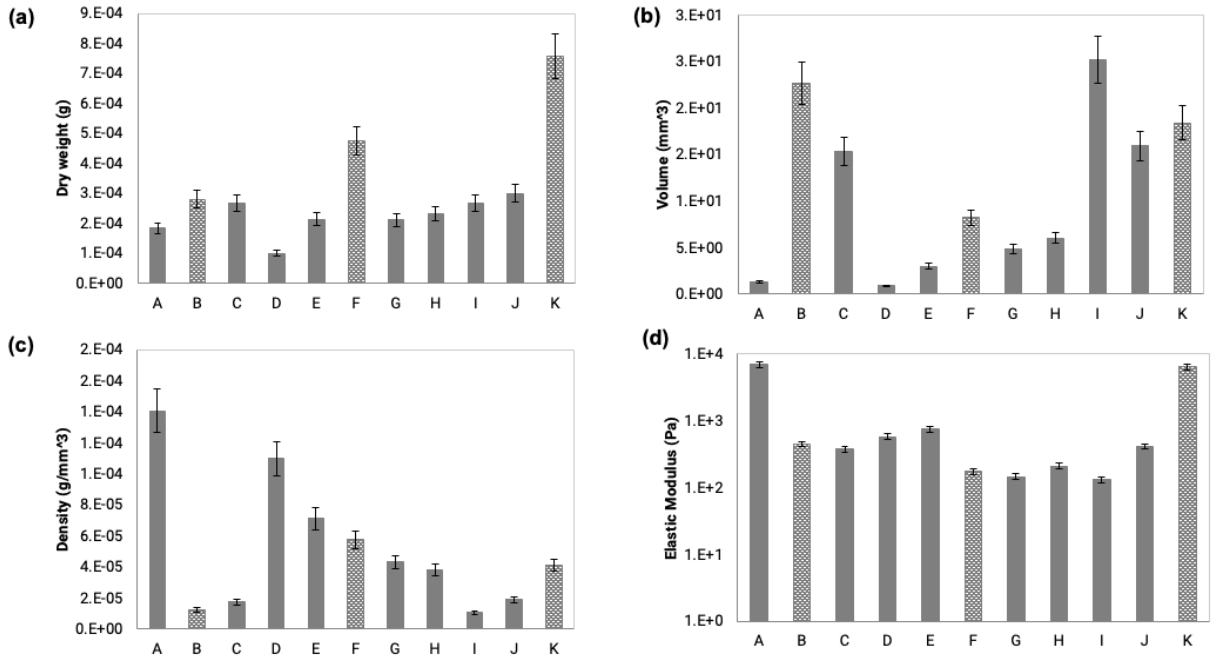

Figure 14. Physical characteristics of mycelial pellets per pellet. (a) Dry weight, (b) Volume, (c) Density, (d) Elastic Modulus. Error bars represent standard deviations.

Table 5. Assignments of infrared and Raman bands: str.—stretching and def.—deformation for filamentous fungi

v#	Wavenumbers (cm^{-1})	Cell Component	Molecular Vibration	Reference
1	1680 - 1620	Carbohydrates	-C=O str. (Amide I, chitin)	Duzurendova et al 2021
2	1755	Carbohydrates	-C=O str. (glucuronan)	Duzurendova et al 2021
3	1620 - 1570	Carbohydrates	NH2 def. (chitosan)	Duzurendova et al 2021
4	1460 - 1440	Carbohydrates	CH2 and CH3 def	Duzurendova et al 2021
5	1377	Carbohydrates	CH2, CH, COH def	Duzurendova et al 2021
6	1327	Carbohydrates	CH2, CH, COH def	Duzurendova et al 2021
7	1256	Carbohydrates	C-C, C-O, CH, CH2	Duzurendova et al 2021
8	1200 - 1150	Carbohydrates	C-O-C str.	Duzurendova et al 2021
9	1150 - 1050	Carbohydrates	C-N str. and C-C str	Duzurendova et al 2021
10	950 - 850	Carbohydrates	C-C str. and C-O-C str. and def, COH def.	Duzurendova et al 2021
11	715	Carbohydrates	O-C-O st. and CH def	Duzurendova et al 2021
12	1158 - 1130	Carbohydrates	C-C,C-O str.	Saif et al 2021
13	999 - 902	Carbohydrates	C-O-C str	Saif et al 2021
14	896 - 840	Carbohydrates	C-C str.	Saif et al 2021
15	567 - 461	Carbohydrates	COC glycosidic ring, CCC def. (chitin)	Saif et al 2021
16	424 - 413	Carbohydrates	beta(1,3)-D-glucan	Saif et al 2021
17	1660	Protein	-C=O str. (Amide 1)	Duzurendova et al 2021
18	1620 - 1580	Protein	NH2 def	Duzurendova et al 2021
19	1605	Protein	C=C str (phynl ring)	Duzurendova et al 2021
20	1460 - 1440	Protein	CH2 and CH3 def	Duzurendova et al 2021
21	1310 - 1250	Protein	C-N-H def, (Amide III)	Duzurendova et al 2021
22	1005	Protein	phenyl ring def.	Duzurendova et al 2021
23	1639 - 1609	Protein	C-N str. C-C str. (Amide I)	Saif et al 2021
24	1576 - 1547	Protein	N-H def (Amide II)	Saif et al 2021
25	1302	Protein	Amide III	Saif et al 2021
26	1313	Protein	Amide III	Saif et al 2021

27	1314	Protein	Amide III	Saif et al 2021
28	1287 - 1214	Protein	Amide III	Saif et al 2021
29	670 - 622	Protein	Adenine, Cytosine, thymine, phosphodiester band in DNA and RNA	Saif et al 2021
30	835 - 702	Protein	Adenine, Cytosine, thymine, phosphodiester band in DNA and RNA	Saif et al 2021
31	1750	Lipid	C=O str.	Duzurendova et al 2021
32	1660	Lipid	C=C str.	Duzurendova et al 2021
33	1460 - 1460	Lipid	CH2 and CH3 def	Duzurendova et al 2021
34	1305	Lipid	CH2 def	Duzurendova et al 2021
35	1080 - 1060	Lipid	C-C str. C-O str.	Duzurendova et al 2021
36	1469 - 1402	Lipid	CH2 def.	Saif et al 2021

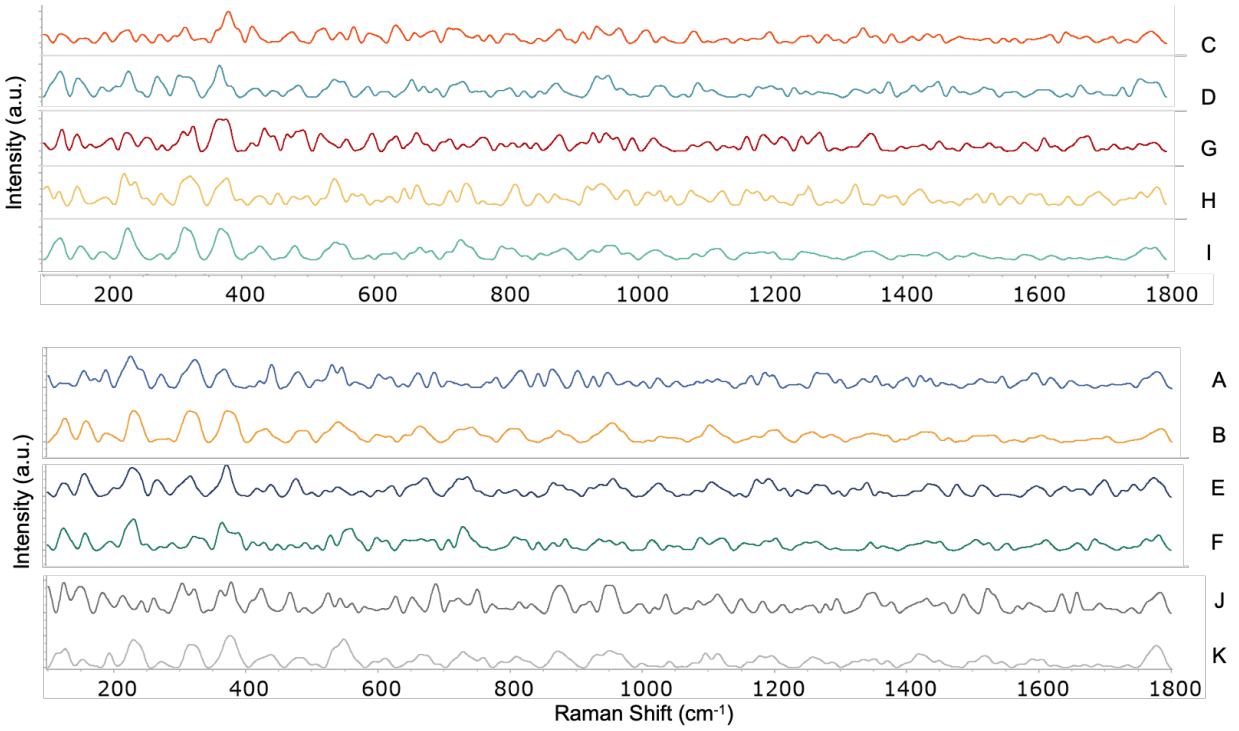

Figure 15. Raman spectra fingerprinting of each pellet samples A to K from raman shift 1800 cm^{-1} - 100 cm^{-1}. (Top) Spectras of C, D, G, H, and I which are pellets of different species made under the same fermentation conditions. (Bottom) Spectras of A&B, E&F, and J&K which are pairs of pellets of the same fungal strain, but made with Filamentous Fungal Pellet Medium (A, E, J) or Potato Dextrose Broth (B, F, K).

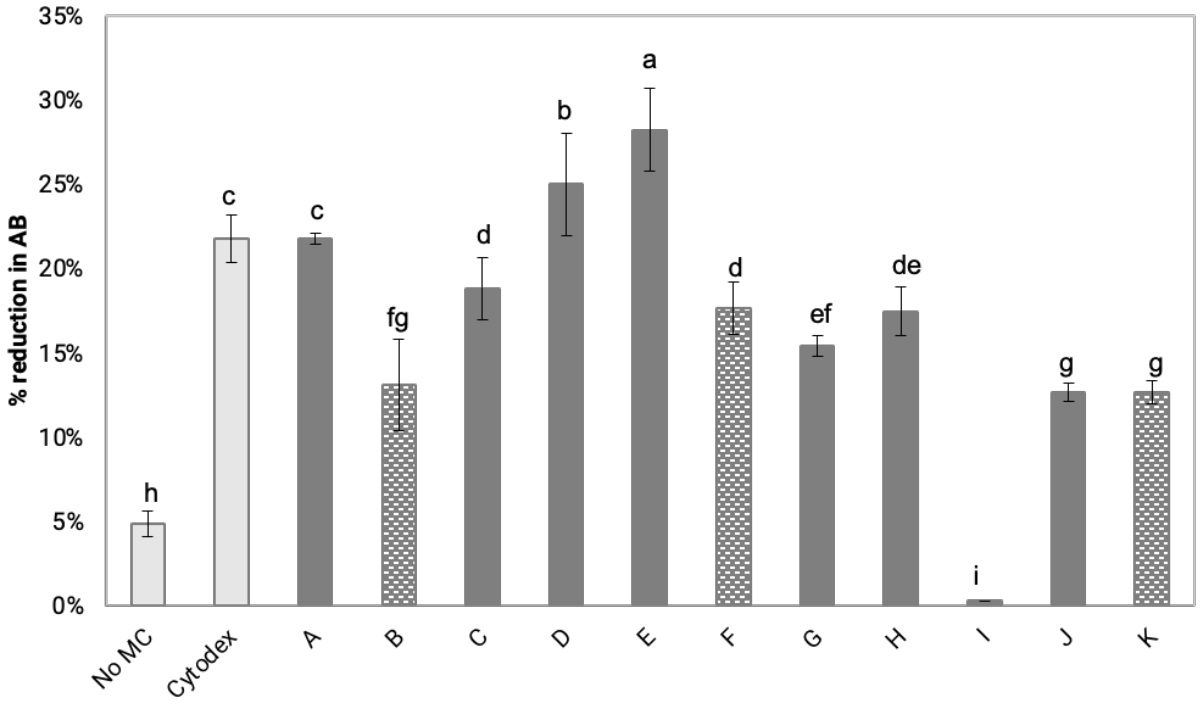

Figure 16. Metabolic activity presented as percent reduction of alamarblue (AB) of bSC cells attached to microcarriers (MC). No MC are cells forced to grow in suspension without any support. Superscript letters (a–c) indicate statistically significant homogenous groups differing in the parameters among the strains ($p < 0.05$, F-test). Error bars represent standard deviations.

Table 6. PLS holdback cross validation with proportion=0.333 using SIMPLS with Fast SVD

Number of factors	Root Mean PRESS		van der Voet T^2	Prob > van der Voet T^2	Q^2	Cumulative Q^2	R^2X	Cumulative R^2X	R^2Y	Cumulative R^2Y
0	1.100000		0.000023	0.9910	-0.210000	-0.210000	0.000000	0.000000	0.000000	0.000000
1	1.221034		0.703399	0.4270	-0.490923	-0.490923	0.480913	0.480913	0.464697	0.464697
2	1.098716		0.000000	1.0000	-0.207177	-0.799809	0.357838	0.838751	0.226157	0.690854
3	1.168383		0.475101	0.6330	-0.365118	-1.456951	0.082264	0.921015	0.116817	0.807671
4	1.545632		2.273375	0.0010*	-1.388978	-4.869603	0.029954	0.950969	0.051418	0.859089
5	2.391228		2.681942	0.0030*	-4.717973	-32.56223	0.017025	0.967994	0.070386	0.929474
6	2.590523		2.476405	0.0120*	-5.710808	-224.2297	0.016093	0.984087	0.036764	0.966238
7	2.598266		2.805721	0.0060*	-5.750987	-1519.523	0.008146	0.992233	0.022003	0.988241
8	2.892003		2.436915	0.0100*	-7.363682	-12716.17	0.005009	0.997242	0.010018	0.998259
9	2.885148		2.366848	0.0180*	-7.324082	-105857.7	0.002758	1.000000	0.001741	1.000000
10	2.885148		2.366848	0.0100*	-7.324082	-881175.8	0.000000	1.000000	0.000000	1.000000
11	2.885148		2.366848	0.0130*	-7.324082	-7334987	0.000000	1.000000	0.000000	1.000000

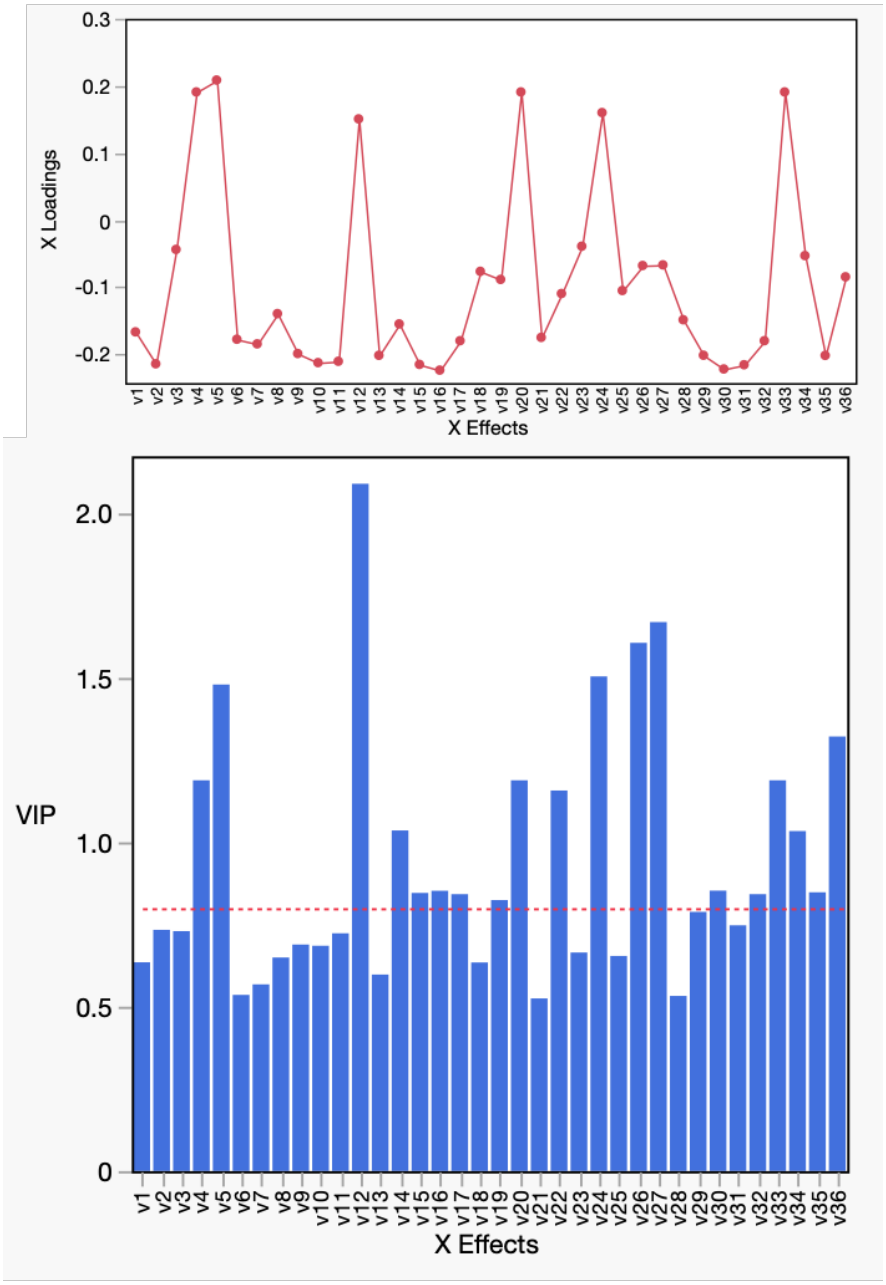

Figure 17. Partial least squares regression analysis of Raman data (a) X loadings plot, (b) VIP plot The measured Raman intensities for each Raman shift corresponding to cellular components of filamentous fungi were used to perform PLS to reveal potential correlations between cellular components and bSC culture performance using percent reduction of alamarblue as a measure of attachment and viability. (a) top figure is X-effects loadings plot for the first factor in the model, indicating the relative correlation of each measured raman shift on bSC attachment, with points in the positive y-axis direction being positively correlated and points in the negative y-axis direction being negatively correlated. (b) bottom graph shows the variable importance plot of the x-effects in the model. This indicates the relative importance of each raman shift in explaining the variability in bSC attachment. The dotted line denotes the conventional threshold of 0.8 which can be used to select x-effects to create a pruned model.

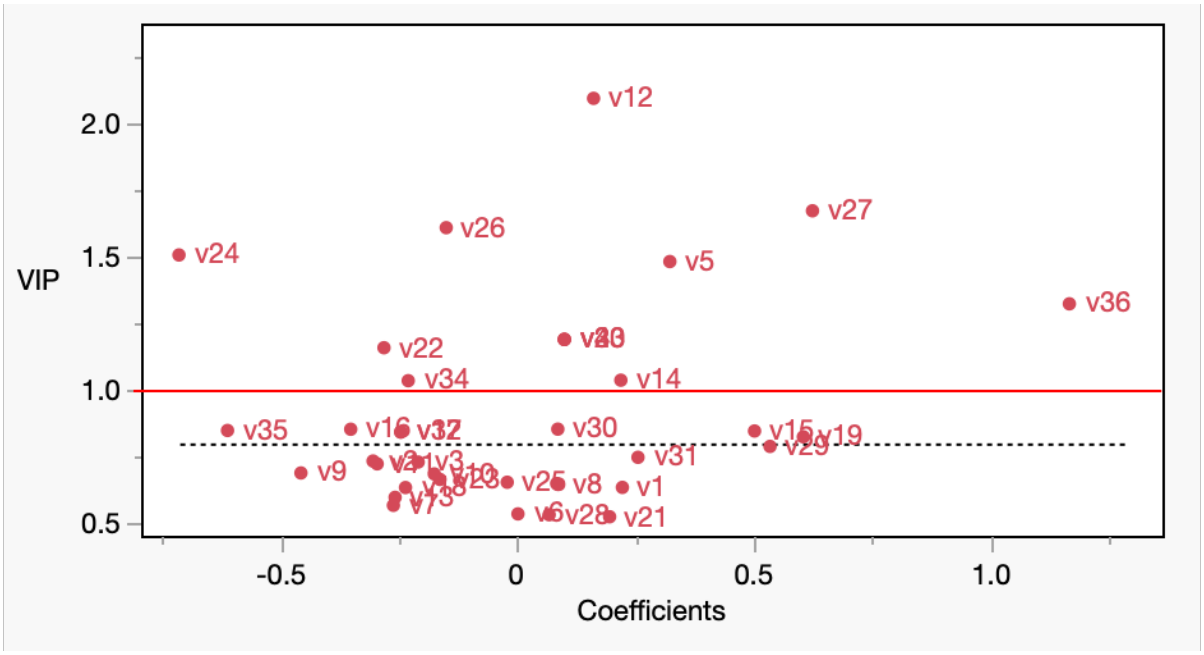

Figure 18. VIP vs Coefficient values. The calculated variable importance plot (VIP) statistics for each X-effect (% reduction of alamarblue) used in the partial least squares regression analysis (PLS) of the (centered and scaled) Raman spectrography data are plotted versus their respective model coefficient values. Components with both a low VIP and coefficient value are candidates for pruning from the PLS model. The dotted line represents the VIP threshold value of 0.8, the lowest acceptable threshold. This study used VIP=1 as the cutoff threshold, indicated by the solid red line

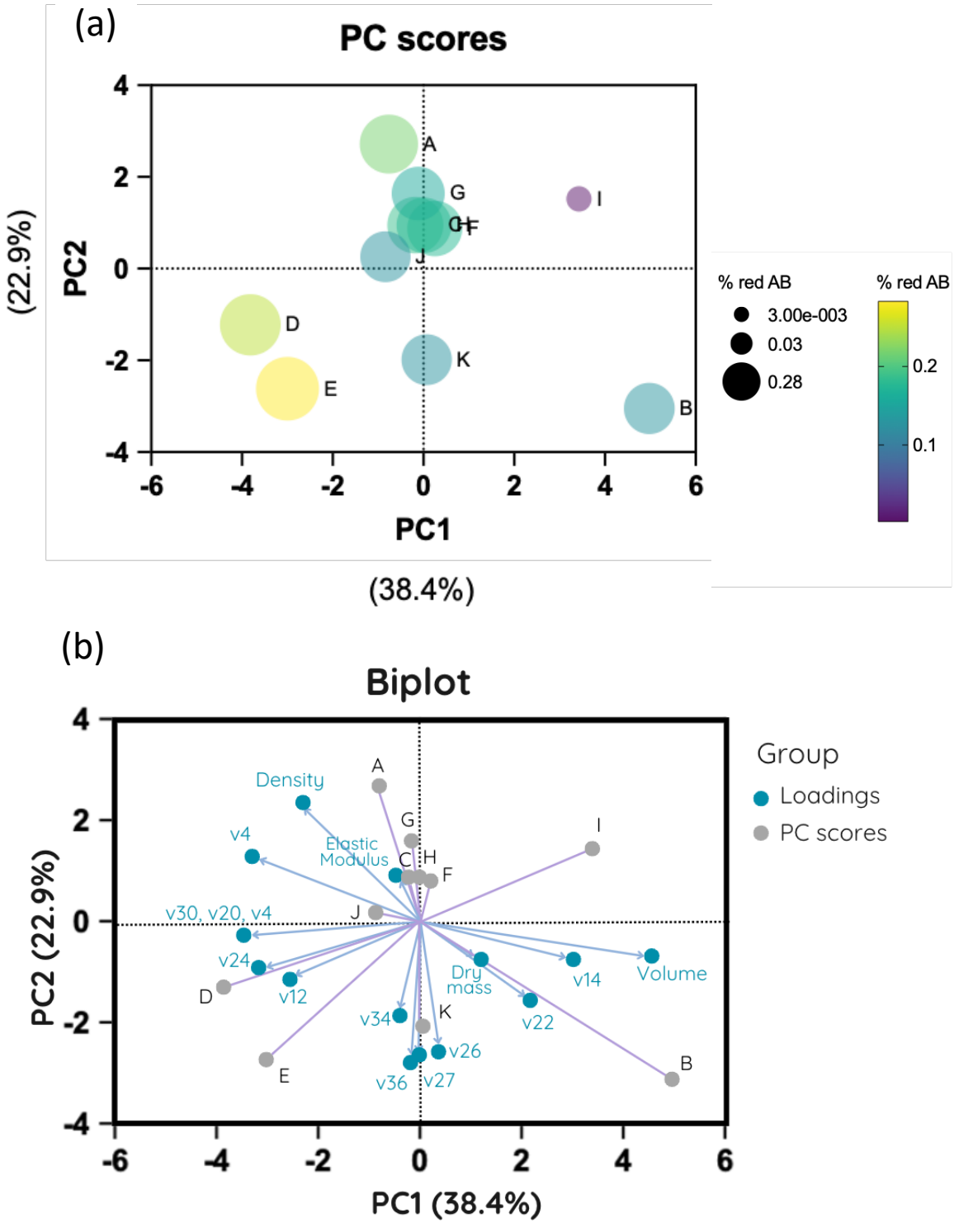

Figure 19. Principal component analysis (PCA) of pellet characteristics presented as variables in blue with samples A to K in gray (a) top graph is PCA scores plot where circle size and color corresponding to the percentage reduction of alamarblue (AB), (b) bottom plot is Biplot

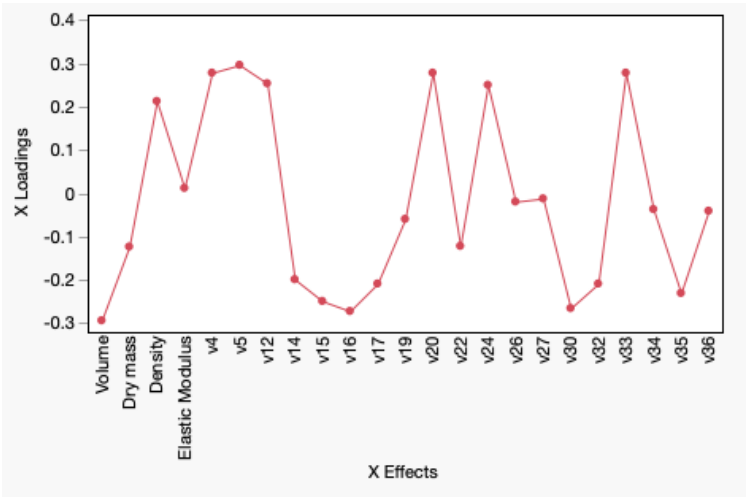

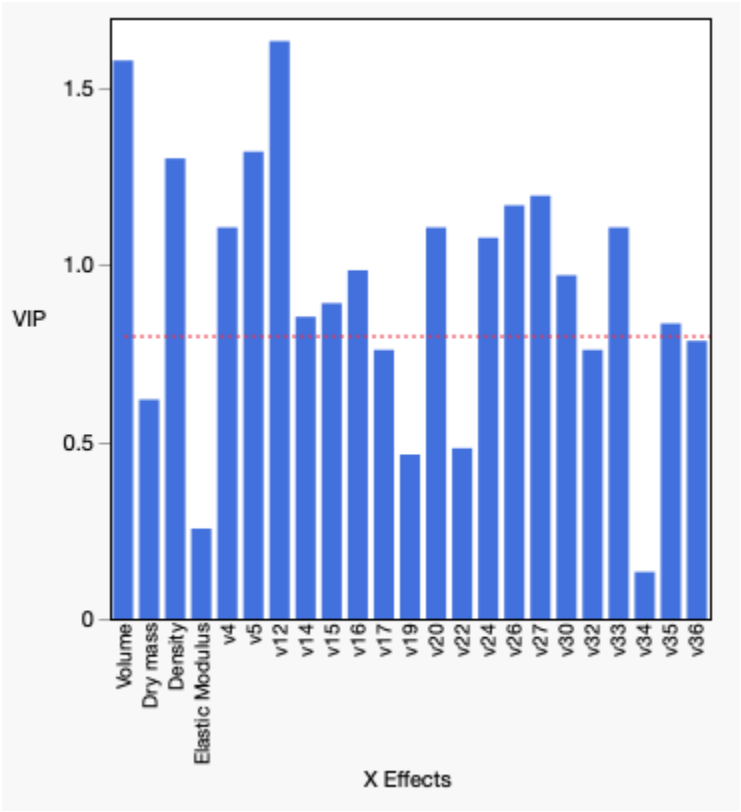

Supplementary Figure 3S. Partial least squares regression analysis of Raman data which had a VIP greater than or equal to 1 and physical characteristics of the mycelial pellets. (a) top figure is X-effects loadings plot for the first factor in the model, indicating the relative correlation of each measured variable on bSC attachment, with points in the positive y-axis direction being positively correlated and points in the negative y-axis direction being negatively correlated. (b) Bottom figure indicates the relative importance of each variable in explaining the variability in bSC attachment. The dotted line denotes the conventional threshold of 0.8 which can be used to select x-effects to create a pruned model.

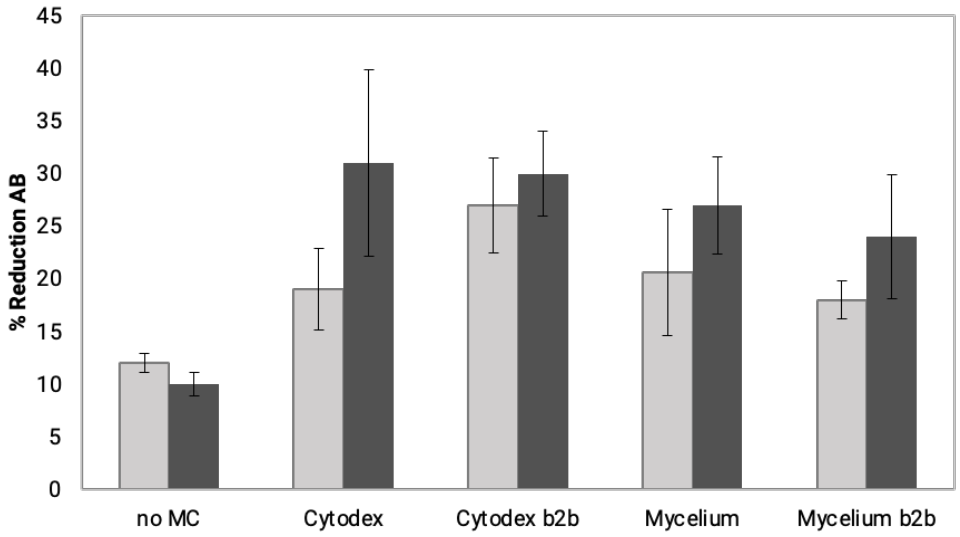

Supplementary Figure 4S. Bead-to-bead (b2b) transfer potential. Gray bars represent samples at 24 hours from seeding and dark gray bars are samples taken at 72 hours from seeding. b2b conditions added new beads to the culture at 48 hours after seeding. Error bars represent standard deviations.

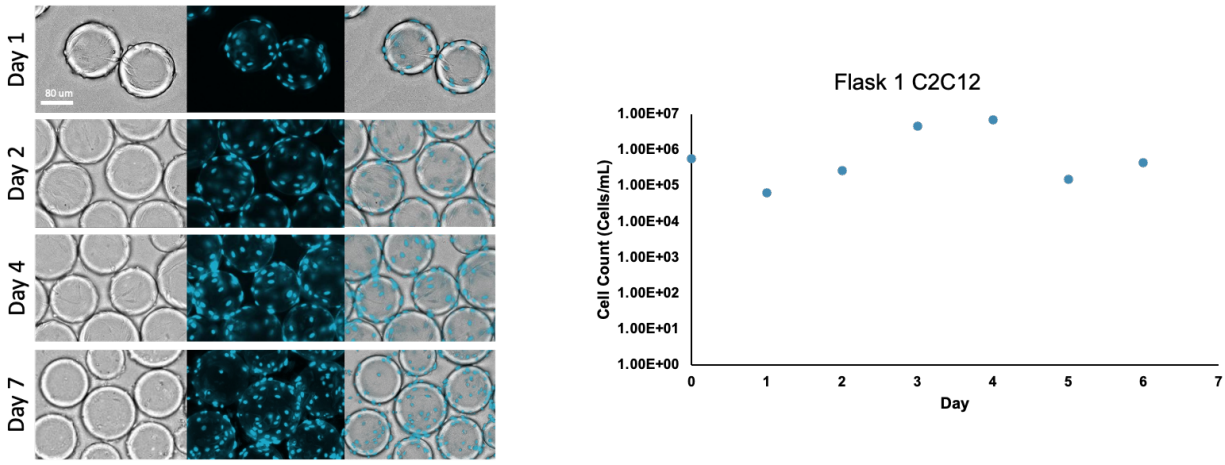

Supplementary Figure 5S. Scale up attempts of C2C12 on microcarriers. Microcarriers in photos are Cytodex 3 with C2C12 cells stained with Hoechst (blue).

CHAPTER 5: Conclusions and Future Directions

This work focused on developing an edible mycelium carrier specifically for cultivated meat applications. The pressing need to overcome the challenges associated with the large-scale commercialization of cultivated meat, driven by the global demand for high-quality dietary protein, has been the primary motivation behind this work. By navigating the complexities of creating innovative tools to support cultivated meat production, the findings of this study not only influence the future direction of cultivated meat but also impact the broader field of alternative proteins and novel food products.

The findings presented in this dissertation serve as necessary first steps in exploring the potential of using mycelium biomass as an edible carrier. However, this research underscores several critical areas that require further development. These include determining the optimal time to achieve animal cell confluence on microcarriers and refining the bead-to-bead transfer process. Successful scale-up is essential to utilize this technology for cell proliferation at commercial scales. Producing at the spinner flask scale is also necessary for the R&D phase to produce sample sizes large enough for the comprehensive sensory trials necessary for assessing taste, texture, and culinary changes, given that the mycelium carrier will be part of the final product. While this research primarily focused on cell attachment and growth, it also aligns with the growing interest in utilizing mycelium as a scaffold to create larger, more structured meat products, such as those resembling steak. This opens up promising avenues for further advancements in cultivated meat production.

A significant challenge experienced during the development of mycelium carriers was determining the direct cell count on carriers. Through my own experiments and discussions with companies selling microcarriers and users of microcarriers, I discovered that direct cell count is nearly impossible because cells do not dissociate properly from carriers and that this issue is widespread in all types of microcarriers. While at the production scale, this is not a problem for edible carriers—since there is no need to separate the carrier from the cell in the production process—it poses difficulties during the investigation and development phases. Several iterations of cell counting were performed. Using various amounts of trypsin and longer contact time with the protease did not separate cells from the carriers. Visually counting using fluorescent and confocal microscope approaches was extremely difficult due to the autofluorescence of the mycelium. Quantifying DNA was challenging because the fungal DNA overwhelmed the DNA in the sample, and the assay was not sensitive enough to detect differences due to the animal cells on the surface. This left indirect measurement approaches as the most compatible, with the alamarBlue proliferation assay emerging as the most reliable method.

Since the start of this project, recent discoveries have opened exciting avenues for improving this system. A recently published paper that describes a novel CRISPR-Cas9 genetically modified *Aspergillus oryzae* could be used to enhance the biomass properties (Q. Li et al., 2023; Maini Rekdal et al., 2024). This toolbox for a longstanding, edible species such as *A. oryzae* is an exciting advance

because it allows for modifications of the fungi that can not be achieved by using the native, wild strain. For example, it would be beneficial to not inactivate the fungi and instead leverage the biological activity of fungi in some cases. As mentioned in the introduction, inactivation of the fungi can lead to loss of beneficial metabolites and changes to the structure of the mycelium that are undesired, making this material hard to control. Genetic modifications could make tuning this biomaterial more effective. It opens several possibilities, such as the upregulation of secreted antibiotics from the fungi that could serve as a natural anti-contamination agent for cells. Metabolites such as glutamic acid, which gives the umami flavor, can be upregulated. Adhesion compounds and characteristics like those discovered in Chapter 4 of this dissertation can be controlled more efficiently, increasing cell attachment and proliferation, as well as providing more control for differentiation. The possibilities are infinite when using biological organisms such as filamentous fungi as the support.

The broader impact of this research extends beyond cultivated meat. The methodologies and insights developed here serve as a model for natural biomaterial development and optimization in various other sectors, including biotechnology and medicine. For instance, animal cell growth on mycelium has been applied to biomedical applications, such as tissue regeneration and cartilage and bone engineering. *Aspergillus*-derived freeze-dried mycelial mats promote superior adhesion and proliferation of human keratinocytes compared to traditional 2D culture methods (Narayanan et al., 2020). Mycelia have also shown potential as a promising candidate for wound care due to their similarities to native mammalian extracellular matrix proteins and favorable oxygen transport properties (Ruggeri et al., 2023). Components of fungi, such as chitosan, have shown potential to support the adhesion and proliferation of human adipose-derived stem cells (Rubio et al., 2019). Combined with the discovery of air pores in *Armillaria luteobubalina* that allow for oxygen transport, the mycelium-derived biomaterial is showing more promising features for medical-grade scaffolding tools, as well as cell culture in general (Pareek et al., 2006).

In conclusion, this dissertation addresses a key challenge in cultivated meat development, providing a foundational understanding for ongoing edible carrier development. The experiments explored the challenges and opportunities of using diverse cell types and fungal species, pointing towards future research avenues. The insights gained from this work are poised to inform carrier formulation in various biotechnological applications, potentially leading to improved efficiencies and technological breakthroughs across multiple industries. As the world faces increasing environmental and ethical challenges associated with traditional animal agriculture, the innovations presented in this dissertation offer a promising pathway toward more sustainable and humane food production systems. The integration of mycelium-based carriers into the cultivated meat industry represents a critical step toward achieving these goals, paving the way for a future where high-quality, environmentally friendly protein sources are accessible to all.

References

Ahmad, K., Shaikh, S., Chun, H. J., Ali, S., Lim, J. H., Ahmad, S. S., Lee, E. J., & Choi, I. (2023). Extracellular matrix: The critical contributor to skeletal muscle regeneration—a comprehensive review. *Inflammation and Regeneration*, *43*, 58. https://doi.org/10.1186/s41232-023-00308-z

Andreassen, R. C., Rønning, S. B., Solberg, N. T., Grønlien, K. G., Kristoffersen, K. A., Høst, V., Kolset, S. O., & Pedersen, M. E. (2022). Production of food-grade microcarriers based on by-products from the food industry to facilitate the expansion of bovine skeletal muscle satellite cells for cultured meat production. *Biomaterials*, *286*, 121602. https://doi.org/10.1016/j.biomaterials.2022.121602

Antinori, M. E., Contardi, M., Suarato, G., Armirotti, A., Bertorelli, R., Mancini, G., Debellis, D., & Athanassiou, A. (2021). Advanced mycelium materials as potential self-growing biomedical scaffolds. *Scientific Reports*, *11*(1), 12630. https://doi.org/10.1038/s41598-021-91572-x

Asfour, H. A., Allouh, M. Z., & Said, R. S. (2018). Myogenic regulatory factors: The orchestrators of myogenesis after 30 years of discovery. *Experimental Biology and Medicine*, *243*(2), 118–128. https://doi.org/10.1177/1535370217749494

Bach, A. D., Stem-Straeter, J., Beier, J. P., Bannasch, H., & Stark, G. B. (2003). Engineering of muscle tissue. *Clinics in Plastic Surgery*, *30*(4), 589–599. https://doi.org/10.1016/s0094-1298(03)00077-4

Baptista, C., Cóias, J. M. A., Oliveira, A. C. M., Oliveira, N. M. C., Rocha, J. M. S., Dempsey, M. J., Lannigan, K. C., & Benson, P. S. (2006). Natural immobilisation of microorganisms for continuous ethanol production. *Enzyme and Microbial Technology*, *40*(1), Article 1.

Baraniak, P. R., Cooke, M. T., Saeed, R., Kinney, M. A., Fridley, K. M., & McDevitt, T. C. (2012). Stiffening of human mesenchymal stem cell spheroid microenvironments induced by incorporation of

gelatin microparticles. *Journal of the Mechanical Behavior of Biomedical Materials*, *11*, 63–71. https://doi.org/10.1016/j.jmbbm.2012.02.018

Barzee, T. J., Cao, L., Pan, Z., & Zhang, R. (2021). Fungi for future foods. *Journal of Future Foods*, *1*(1), 25–37. https://doi.org/10.1016/j.jfutfo.2021.09.002

Barzee, T. J., El Mashad, H. M., Cao, L., Chio, A., Pan, Z., & Zhang, R. (2022). Cell-cultivated food production and processing: A review. *Food Bioengineering*, *1*(1), 4–25. https://doi.org/10.1002/fbe2.12009

Berger, R. G., Bordewick, S., Krahe, N.-K., & Ersoy, F. (2022). Mycelium vs. Fruiting Bodies of Edible Fungi-A Comparison of Metabolites. *Microorganisms*, *10*(7). https://doi.org/10.3390/microorganisms10071379

Bergholt, M. S., Serio, A., & Albro, M. B. (2019). Raman Spectroscopy: Guiding Light for the Extracellular Matrix. *Frontiers in Bioengineering and Biotechnology*, *7*, 303. https://doi.org/10.3389/fbioe.2019.00303

Bhattarai, N., Gunn, J., & Zhang, M. (2010). Chitosan-based hydrogels for controlled, localized drug delivery. *Advanced Drug Delivery Reviews*, *62*(1), 83–99. https://doi.org/10.1016/j.addr.2009.07.019

Bi, J., Jing, H., Zhou, C., Gao, P., Han, F., Li, G., & Zhang, S. (2022). Regulation of skeletal myogenesis in C2C12 cells through modulation of Pax7, MyoD, and myogenin via different low-frequency electromagnetic field energies. *Technology and Health Care : Official Journal of the European Society for Engineering and Medicine*, *30*(S1), 371–382. https://doi.org/10.3233/THC-THC228034

Biggs, R., Schlüter, M., & Schoon, M. L. (Eds.). (2015). *Principles for Building Resilience: Sustaining Ecosystem Services in Social-Ecological Systems*. Cambridge University Press. https://doi.org/10.1017/CBO9781316014240

Block, D., & Ogawa, M. (2024). *Compositions including filamentous fungal biomass and cultured animal cells, and methods of forming and using* (United States Patent US20240074478A1). https://patents.google.com/patent/US20240074478A1/en

Blüml, G. (2007). Microcarrier cell culture technology. In R. Pörtner (Ed.), *Animal Cell Biotechnology* (Vol. 24, pp. 149–178). Humana Press. https://doi.org/10.1007/978-1-59745-399-8_5

Bodiou, V., Moutsatsou, P., & Post, M. J. (2020). Microcarriers for upscaling cultured meat production. *Frontiers in Nutrition*, *7*, 10. https://doi.org/10.3389/fnut.2020.00010

Bomkamp, C., Skaalure, S. C., Fernando, G. F., Ben-Arye, T., Swartz, E. W., & Specht, E. A. (2022). Scaffolding biomaterials for 3D cultivated meat: Prospects and challenges. *Advanced Science (Weinheim, Baden-Wurttemberg, Germany)*, *9*(3), e2102908. https://doi.org/10.1002/advs.202102908

Boonen, K. J. M., Rosaria-Chak, K. Y., Baaijens, F. P. T., van der Schaft, D. W. J., & Post, M. J. (2009). Essential environmental cues from the satellite cell niche: Optimizing proliferation and differentiation. *American Journal of Physiology. Cell Physiology*, *296*(6), C1338-45. https://doi.org/10.1152/ajpcell.00015.2009

Caruso, S. R., Orellana, M. D., Mizukami, A., Fernandes, T. R., Fontes, A. M., Suazo, C. A. T., Oliveira, V. C., Covas, D. T., & Swiech, K. (2014). Growth and functional harvesting of human mesenchymal stromal cells cultured on a microcarrier-based system. *Biotechnology Progress*, *30*(4), 889–895. https://doi.org/10.1002/btpr.1886

Celerin, M., Ray, J. M., Schisler, N. J., Day, A. W., Stetler-Stevenson, W. G., & Laudenbach, D. E. (1996). Fungal fimbriae are composed of collagen. *The EMBO Journal*, *15*(17), 4445–4453.

Cha, S. H., Lee, H. J., & Koh, W.-G. (2017). Study of myoblast differentiation using multi-dimensional scaffolds consisting of nano and micropatterns. *Biomaterials Research*, *21*, 1. https://doi.org/10.1186/s40824-016-0087-x

Chacón-Navarrete, H., Martín, C., & Moreno-García, J. (2021). Yeast immobilization systems for second-generation ethanol production: Actual trends and future perspectives. *Biofuels, Bioproducts and Biorefining*, *15*(5), 1549–1565. https://doi.org/10.1002/bbb.2250

Chen, A. K.-L., Chen, X., Lim, Y. M., Reuveny, S., & Oh, S. K. W. (2014). Inhibition of ROCK–Myosin II Signaling Pathway Enables Culturing of Human Pluripotent Stem Cells on Microcarriers Without Extracellular Matrix Coating. *Tissue Engineering Part C: Methods*, *20*(3), 227–238. https://doi.org/10.1089/ten.tec.2013.0191

Chen, J., Leng, L., Ye, C., Lu, Q., Addy, M., Wang, J., Liu, J., Chen, P., Ruan, R., & Zhou, W. (2018). A comparative study between fungal pellet- and spore-assisted microalgae harvesting methods for algae bioflocculation. *Bioresource Technology*, *259*, 181–190. https://doi.org/10.1016/j.biortech.2018.03.040

Choquet, D., Felsenfeld, D. P., & Sheetz, M. P. (1997). Extracellular matrix rigidity causes strengthening of integrin-cytoskeleton linkages. *Cell*, *88*(1), 39–48. https://doi.org/10.1016/s0092-8674(00)81856-5

Clemmensen, K. E., Bahr, A., Ovaskainen, O., Dahlberg, A., Ekblad, A., Wallander, H., Stenlid, J., Finlay, R. D., Wardle, D. A., & Lindahl, B. D. (2013). Roots and associated fungi drive long-term carbon sequestration in boreal forest. *Science*, *339*(6127), 1615–1618. https://doi.org/10.1126/science.1231923

Cooper, A., Jana, S., Bhattarai, N., & Zhang, M. (2010). Aligned chitosan-based nanofibers for enhanced myogenesis. *Journal of Materials Chemistry*, *20*(40), 8904–8911. https://doi.org/10.1039/C0JM01841D

Cosenza, Z. A. (2022). *Sequential Learning Methods for the Experimental Optimization of Cell Culture Media for Cellular Agriculture* [UC Davis]. https://escholarship.org/uc/item/119489fc

Cosenza, Z., Block, D. E., Baar, K., & Chen, X. (2023). Multi-objective Bayesian algorithm automatically discovers low-cost high-growth serum-free media for cellular agriculture application. *Engineering in Life Sciences*, *23*(8), e2300005. https://doi.org/10.1002/elsc.202300005

Cukierman, E., Pankov, R., Stevens, D. R., & Yamada, K. M. (2001). Taking cell-matrix adhesions to the third dimension. *Science*, *294*(5547), 1708–1712. https://doi.org/10.1126/science.1064829

De Gelder, J., De Gussem, K., Vandenabeele, P., & Moens, L. (2007). Reference database of Raman spectra of biological molecules. *Journal of Raman Spectroscopy*, *38*(9), 1133–1147. https://doi.org/10.1002/jrs.1734

Derakhti, S., Safiabadi-Tali, S. H., Amoabediny, G., & Sheikhpour, M. (2019). Attachment and detachment strategies in microcarrier-based cell culture technology: A comprehensive review. *Materials Science & Engineering. C, Materials for Biological Applications*, *103*, 109782. https://doi.org/10.1016/j.msec.2019.109782

Derbyshire, E. (2022). Food-Based Dietary Guidelines and Protein Quality Definitions-Time to Move Forward and Encompass Mycoprotein? *Foods*, *11*(5). https://doi.org/10.3390/foods11050647

DiEdwardo, C. A., Petrosko, P., Acarturk, T. O., DiMilla, P. A., LaFramboise, W. A., & Johnson, P. C. (1999). Muscle Tissue Engineering. *Clinics in Plastic Surgery*, *26*(4), 647–656. https://doi.org/10.1016/S0094-1298(20)32663-8

Duarte, J. C., Rodrigues, J. A. R., Moran, P. J. S., Valença, G. P., & Nunhez, J. R. (2013). Effect of immobilized cells in calcium alginate beads in alcoholic fermentation. *AMB Express*, *3*(1), 31. https://doi.org/10.1186/2191-0855-3-31

Dyachuk, V. (2013). Extracellular matrix is required for muscle differentiation in primary cell cultures of larval Mytilus trossulus (Mollusca: Bivalvia). *Cytotechnology*, *65*(5), 725–735. https://doi.org/10.1007/s10616-013-9577-z

Dzurendová, S., Shapaval, V., Tafintseva, V., Kohler, A., Byrtusová, D., Szotkowski, M., Márová, I., & Zimmermann, B. (2021). Assessment of Biotechnologically Important Filamentous Fungal Biomass by Fourier Transform Raman Spectroscopy. *International Journal of Molecular Sciences*, *22*(13), Article 13. https://doi.org/10.3390/ijms22136710

Edwards, D. G., & Cummings, J. H. (2010). The protein quality of mycoprotein. *Proceedings of the Nutrition Society*, *69*(OCE4). https://doi.org/10.1017/S0029665110001400

Engler, A. J., Sen, S., Sweeney, H. L., & Discher, D. E. (2006). Matrix elasticity directs stem cell lineage specification. *Cell*, *126*(4), 677–689. https://doi.org/10.1016/j.cell.2006.06.044

Eshel, G., Shepon, A., Makov, T., & Milo, R. (2014). Land, irrigation water, greenhouse gas, and reactive nitrogen burdens of meat, eggs, and dairy production in the United States. *Proceedings of the National Academy of Sciences*, *111*(33), 11996–12001. https://doi.org/10.1073/pnas.1402183111

Esmonde-White, K. A., Esmonde-White, F. W. L., Morris, M. D., & Roessler, B. J. (2011). Fiber-optic Raman spectroscopy of joint tissues. *Analyst*, *136*(8), 1675–1685. https://doi.org/10.1039/C0AN00824A

Fish, K. D., Rubio, N. R., Stout, A. J., Yuen, J. S. K., & Kaplan, D. L. (2020). Prospects and challenges for cell-cultured fat as a novel food ingredient. *Trends in Food Science & Technology*, *98*, 53–67. https://doi.org/10.1016/j.tifs.2020.02.005

Frisch, S. M., & Screaton, R. A. (2001). Anoikis mechanisms. *Current Opinion in Cell Biology*, *13*(5), 555–562. https://doi.org/10.1016/S0955-0674(00)00251-9

Fu, Y.-Q., Yin, L.-F., Zhu, H.-Y., Jiang, R., Li, S., & Xu, Q. (2014). Effects of pellet characteristics on L-lactic acid fermentation by R. oryzae: Pellet morphology, diameter, density, and interior structure. *Applied Biochemistry and Biotechnology*, *174*(6), 2019–2030. https://doi.org/10.1007/s12010-014-1146-1

Füting, P., Barthel, L., Cairns, T. C., Briesen, H., & Schmideder, S. (2021). Filamentous fungal applications in biotechnology: A combined bibliometric and patentometric assessment. *Fungal Biology and Biotechnology*, *8*(1), 23. https://doi.org/10.1186/s40694-021-00131-6

GARCÍA, J. M., Ogawa, M., Nitin, N., RAI, R., VIGARA, J. J. M., MAURICIO, J. C. G., MARTÍNEZ, M. T. G., & Amores, R. P. (2024). *Method for the production of microbial biocapsules, microbial biocapsules obtained by said method and uses thereof* (World Intellectual Property Organization Patent WO2024068943A1). https://patents.google.com/patent/WO2024068943A1/en?oq=PCT%2fEP2023%2f077088

García-Martínez, T., Moreno, J., Mauricio, J. C., & Peinado, R. (2015). Natural sweet wine production by repeated use of yeast cells immobilized on Penicillium chrysogenum. *LWT - Food Science and Technology*, *2*(61), 503–509. https://doi.org/10.1016/j.lwt.2014.12.029

García-Martínez, T., Peinado, R. A., Moreno, J., García-García, I., & Mauricio, J. C. (2011). Co-culture of Penicillium chrysogenum and Saccharomyces cerevisiae leading to the immobilization of yeast. *Journal of Chemical Technology & Biotechnology*, *86*(6), 812–817. https://doi.org/10.1002/jctb.2593

García-Martínez, T., Puig-Pujol, A., Peinado, R. A., Moreno, J., & Mauricio, J. C. (2012). Potential use of wine yeasts immobilized on Penicillium chrysogenum for ethanol production. *Journal of Chemical Technology & Biotechnology*, *87*(3), 351–359. https://doi.org/10.1002/jctb.2725

GE Healthcare/Amersham Biosciences. (2005). *Microcarrier Cell Culture: Principles and Methods*. https://www.scribd.com/document/364986081/Microcarrier-Cell-Culture-Principles-and-Methods

Goh, T. K.-P., Zhang, Z.-Y., Chen, A. K.-L., Reuveny, S., Choolani, M., Chan, J. K. Y., & Oh, S. K.-W. (2013). Microcarrier culture for efficient expansion and osteogenic differentiation of human fetal

mesenchymal stem cells. *BioResearch Open Access*, *2*(2), 84–97. https://doi.org/10.1089/biores.2013.0001

Gray, C. J., & Dowsett, J. (1988). Retention of insulin in alginate gel beads. *Biotechnology and Bioengineering*, *31*(6), 607–612. https://doi.org/10.1002/bit.260310613

Groboillot, A., Boadi, D. K., Poncelet, D., & Neufeld, R. J. (1994). Immobilization of cells for application in the food industry. *Critical Reviews in Biotechnology*, *14*(2), 75–107. https://doi.org/10.3109/07388559409086963

Gupta, S. K., Mishra, N. C., & Dhasmana, A. (2018). Decellularization Methods for Scaffold Fabrication. *Methods in Molecular Biology (Clifton, N.J.)*, *1577*, 1–10. https://doi.org/10.1007/7651_2017_34

Guvendiren, M., & Burdick, J. A. (2012). Stiffening hydrogels to probe short- and long-term cellular responses to dynamic mechanics. *Nature Communications*, *3*, 792. https://doi.org/10.1038/ncomms1792

Handorf, A. M., Zhou, Y., Halanski, M. A., & Li, W.-J. (2015). Tissue stiffness dictates development, homeostasis, and disease progression. *Organogenesis*, *11*(1), 1–15. https://doi.org/10.1080/15476278.2015.1019687

Huang, N. F., Patel, S., Thakar, R. G., Wu, J., Hsiao, B. S., Chu, B., Lee, R. J., & Li, S. (2006). Myotube Assembly on Nanofibrous and Micropatterned Polymers. *Nano Letters*, *6*(3), 537–542. https://doi.org/10.1021/nl060060o

Huling, R. (2023). Applications of fungi for alternative protein. In T. Satyanarayana & S. K. Deshmukh (Eds.), *Fungi and fungal products in human welfare and biotechnology* (pp. 365–395). Springer Nature Singapore. https://doi.org/10.1007/978-981-19-8853-0_13

Jana, S., Cooper, A., & Zhang, M. (2013). Chitosan Scaffolds with Unidirectional Microtubular Pores for Large Skeletal Myotube Generation. *Advanced Healthcare Materials*, *2*(4), 557–561. https://doi.org/10.1002/adhm.201200177

Jeennor, S., Anantayanon, J., Panchanawaporn, S., Chutrakul, C., & Laoteng, K. (2019). Morphologically engineered strain of Aspergillus oryzae as a cell chassis for production development of functional lipids. *Gene*, *718*, 144073. https://doi.org/10.1016/j.gene.2019.144073

Karamanos, N. K., Theocharis, A. D., Piperigkou, Z., Manou, D., Passi, A., Skandalis, S. S., Vynios, D. H., Orian-Rousseau, V., Ricard-Blum, S., Schmelzer, C. E. H., Duca, L., Durbeej, M., Afratis, N. A., Troeberg, L., Franchi, M., Masola, V., & Onisto, M. (2021). A guide to the composition and functions of the extracellular matrix. *The FEBS Journal*, *288*(24), 6850–6912. https://doi.org/10.1111/febs.15776

Karel, S. F., Libicki, S. B., & Robertson, C. R. (1985). The immobilization of whole cells: Engineering principles. *Chemical Engineering Science*, *40*(8), 1321–1354. https://doi.org/10.1016/0009-2509(85)80074-9

Kean, T., & Thanou, M. (2010). Biodegradation, biodistribution and toxicity of chitosan. *Advanced Drug Delivery Reviews*, *62*(1), 3–11. https://doi.org/10.1016/j.addr.2009.09.004

Kim, J. H., Seol, Y.-J., Ko, I. K., Kang, H.-W., Lee, Y. K., Yoo, J. J., Atala, A., & Lee, S. J. (2018). 3D Bioprinted Human Skeletal Muscle Constructs for Muscle Function Restoration. *Scientific Reports*, *8*(1), 12307. https://doi.org/10.1038/s41598-018-29968-5

Kimura, A., Katoh, O., Hyodo, H., Kusumi, S., & Kuramoto, A. (1991). Autocrine and/or paracrine mechanism operate during the growth of human bone marrow fibroblasts. *British Journal of Haematology*, *78*(4), 469–473. https://doi.org/10.1111/j.1365-2141.1991.tb04474.x

Kirsch, M., Morales-Dalmau, J., & Lavrentieva, A. (2023). Cultivated meat manufacturing: Technology, trends, and challenges. *Engineering in Life Sciences*, *23*(12), e2300227. https://doi.org/10.1002/elsc.202300227

Kong, Y., Ong, S., Liu, M. H., Yu, H., & Huang, D. (2022). Functional composite microbeads for cell-based meat culture: Effect of animal gelatin coating on cell proliferation and differentiation. *Journal of Physics D: Applied Physics*, *55*(34), 345401. https://doi.org/10.1088/1361-6463/ac7011

Kwee, B. J., & Mooney, D. J. (2017). Biomaterials for skeletal muscle tissue engineering. *Current Opinion in Biotechnology*, *47*, 16–22. https://doi.org/10.1016/j.copbio.2017.05.003

Kyriakou, M., Chatziiona, V. K., Costa, C. N., Kallis, M., Koutsokeras, L., Constantinides, G., & Koutinas, M. (2019). Biowaste-based biochar: A new strategy for fermentative bioethanol overproduction via whole-cell immobilization. *Applied Energy*, *242*, 480–491. https://doi.org/10.1016/j.apenergy.2019.03.024

Leber, J., Barekzai, J., Blumenstock, M., Pospisil, B., Salzig, D., & Czermak, P. (2017). Microcarrier choice and bead-to-bead transfer for human mesenchymal stem cells in serum-containing and chemically defined media. *Process Biochemistry*. https://doi.org/10.1016/j.procbio.2017.03.017

Lee, S. J., & Yang, S. (2012). Micro glass ball embedded gels to study cell mechanobiological responses to substrate curvatures. *The Review of Scientific Instruments*, *83*(9), 094302. https://doi.org/10.1063/1.4751869

Letcher, S. M., Rubio, N. R., Ashizawa, R. N., Saad, M. K., Rittenberg, M. L., McCreary, A., Ali, A., Calkins, O. P., Trimmer, B. A., & Kaplan, D. L. (2022). In vitro Insect Fat Cultivation for Cellular Agriculture Applications. *ACS Biomaterials Science & Engineering*, *8*(9), 3785–3796. https://doi.org/10.1021/acsbiomaterials.2c00093

Li, B., Wang, X., Wang, Y., Gou, W., Yuan, X., Peng, J., Guo, Q., & Lu, S. (2015). Past, present, and future of microcarrier-based tissue engineering. *Journal of Orthopaedic Translation*, *3*(2), 51–57. https://doi.org/10.1016/j.jot.2015.02.003

Li, L., Liang, T., Liu, W., Liu, Y., & Ma, F. (2020). A comprehensive review of the mycelial pellet: Research status, applications, and future prospects. *Industrial & Engineering Chemistry Research*, *59*(39), 16911–16922. https://doi.org/10.1021/acs.iecr.0c01325

Li, Q., Lu, J., Zhang, G., Zhou, J., Li, J., Du, G., & Chen, J. (2023). CRISPR/Cas9-Mediated Multiplexed Genome Editing in Aspergillus oryzae. *Journal of Fungi (Basel, Switzerland)*, *9*(1), 109. https://doi.org/10.3390/jof9010109

Li, Z. J., Shukla, V., Fordyce, A. P., Pedersen, A. G., Wenger, K. S., & Marten, M. R. (2000). Fungal morphology and fragmentation behavior in a fed-batchAspergillus oryzae fermentation at the production scale. *Journal of Biochemical and Microbiological Technology and Engineering*, *70*(3), 300–312. https://doi.org/10.1002/1097-0290(20001105)70:3<300::AID-BIT7>3.0.CO;2-3

Liu, M., Qin, X., & Wu, X. (2022). Study on the technology of brewing red raspberry wine by using new immobilized yeast technology. *Scientific Reports*, *12*(1), 21344. https://doi.org/10.1038/s41598-022-25410-z

Liu, Y., Wang, R., Ding, S., Deng, L., Zhang, Y., Li, J., Shi, Z., Wu, Z., Liang, K., Yan, X., Liu, W., & Du, Y. (2022). Engineered meatballs via scalable skeletal muscle cell expansion and modular micro-tissue assembly using porous gelatin micro-carriers. *Biomaterials*, *287*, 121615. https://doi.org/10.1016/j.biomaterials.2022.121615

López de Lerma, N., Peinado, R. A., Puig-Pujol, A., Mauricio, J. C., Moreno, J., & García-Martínez, T. (2018). Influence of two yeast strains in free, bioimmobilized or immobilized with alginate forms on the aromatic profile of long aged sparkling wines. *Food Chemistry*, *250*, 22–29. https://doi.org/10.1016/j.foodchem.2018.01.036

Lopez, M. J., & Mohiuddin, S. S. (2023). Biochemistry, essential amino acids. In *StatPearls*. StatPearls Publishing. https://www.ncbi.nlm.nih.gov/pubmed/32496725

López-Menchero, J. R., Ogawa, M., Mauricio, J. C., Moreno, J., & García, J. M. (2021). Effect of calcium alginate coating on the cell retention and fermentation of a fungus-yeast immobilization system. *LWT*, 111250. https://doi.org/10.1016/j.lwt.2021.111250

Lu, Y., Liu, T., Bai, R., Jia, Y., Chen, W., Zhao, J., & Liu, Y. (2024). Potential application of grape endophytic fungus (*Alternaria alternata* MG1) as bio-adjunct and immobilization carrier of *S. cerevisiae* in improving aroma quality, polyphenol profiles, antioxidant activity and color stability of Merlot red wine. *LWT*, *198*, 116034. https://doi.org/10.1016/j.lwt.2024.116034

Lu, Y., Ogawa, M., García, J. M., & Nitin, N. (2024). Filamentous fungal pellets as a novel and sustainable encapsulation matrix for exogenous bioactive compounds. *Food & Function*, *15*(6), 3087–3097. https://doi.org/10.1039/D3FO04425D

Maini Rekdal, V., van der Luijt, C. R. B., Chen, Y., Kakumanu, R., Baidoo, E. E. K., Petzold, C. J., Cruz-Morales, P., & Keasling, J. D. (2024). Edible mycelium bioengineered for enhanced nutritional value and sensory appeal using a modular synthetic biology toolkit. *Nature Communications*, *15*(1), 2099. https://doi.org/10.1038/s41467-024-46314-8

Mattick, C. S., Landis, A. E., Allenby, B. R., & Genovese, N. J. (2015). Anticipatory Life Cycle Analysis of In Vitro Biomass Cultivation for Cultured Meat Production in the United States. *Environmental Science & Technology*, *49*(19), 11941–11949. https://doi.org/10.1021/acs.est.5b01614

Mauro, A. (1961). Satellite cell of skeletal muscle fibers. *The Journal of Biophysical and Biochemical Cytology*, *9*, 493–495. https://doi.org/10.1083/jcb.9.2.493

McKee, C., & Chaudhry, G. R. (2017). Advances and challenges in stem cell culture. *Colloids and Surfaces. B, Biointerfaces*, *159*, 62–77. https://doi.org/10.1016/j.colsurfb.2017.07.051

McMurtrey, R. J. (2016). Analytic Models of Oxygen and Nutrient Diffusion, Metabolism Dynamics, and Architecture Optimization in Three-Dimensional Tissue Constructs with Applications and Insights

in Cerebral Organoids. *Tissue Engineering. Part C, Methods*, *22*(3), 221–249. https://doi.org/10.1089/ten.TEC.2015.0375

Mehrotra, T., Dev, S., Banerjee, A., Chatterjee, A., Singh, R., & Aggarwal, S. (2021). Use of immobilized bacteria for environmental bioremediation: A review. *Journal of Environmental Chemical Engineering*, *9*(5), 105920. https://doi.org/10.1016/j.jece.2021.105920

Metz, B., & Kossen, N. W. F. (1977). The growth of molds in the form of pellets-a literature review. *Journal of Biochemical and Microbiological Technology and Engineering*, *19*(6), 781–799. https://doi.org/10.1002/bit.260190602

Moreira, M. T., Sanromán, A., Feijoo, G., & Lema, J. M. (1996). Control of pellet morphology of filamentous fungi in fluidized bed bioreactors by means of a pulsing flow. Application to Aspergillus niger and Phanerochaete chrysosporium. *Enzyme and Microbial Technology*, *19*(4), 261–266. https://doi.org/10.1016/0141-0229(95)00244-8

Moreno-García, J., García-Martínez, T., Mauricio, J. C., & Moreno, J. (2018). Yeast immobilization systems for alcoholic wine fermentations: Actual trends and future perspectives. *Frontiers in Microbiology*, *9*, 241. https://doi.org/10.3389/fmicb.2018.00241

Moreno-García, J., García-Martinez, T., Moreno, J., Mauricio, J. C., Ogawa, M., Luong, P., & Bisson, L. F. (2018). Impact of Yeast Flocculation and Biofilm Formation on Yeast-Fungus Coadhesion in a Novel Immobilization System. *American Journal of Enology and Viticulture*, *69*(3), 278–288. https://doi.org/10.5344/ajev.2018.17067

Moreno-García, J., Martín-García, F. J., Ogawa, M., García-Martínez, T., Moreno, J., Mauricio, J. C., & Bisson, L. F. (2018). FLO1, FLO5 and FLO11 Flocculation Gene Expression Impacts Saccharomyces cerevisiae Attachment to Penicillium chrysogenum in a Co-immobilization Technique. *Frontiers in Microbiology*, *9*, 2586. https://doi.org/10.3389/fmicb.2018.02586

Moritz, M. S. M., Verbruggen, S. E. L., & Post, M. J. (2015). Alternatives for large-scale production of cultured beef: A review. *Journal of Integrative Agriculture*, *14*(2), 208–216. https://doi.org/10.1016/S2095-3119(14)60889-3

Murugan, P., Yap, W. S., Ezhilarasu, H., Suntornnond, R., Le, Q. B., Singh, S., Seah, J. S. H., Tan, P. L., Zhou, W., Tan, L. P., & Choudhury, D. (2024). Decellularised plant scaffolds facilitate porcine skeletal muscle tissue engineering for cultivated meat biomanufacturing. *Npj Science of Food*, *8*(1), 25. https://doi.org/10.1038/s41538-024-00262-1

Narayanan, K. B., Zo, S. M., & Han, S. S. (2020). Novel biomimetic chitin-glucan polysaccharide nano/microfibrous fungal-scaffolds for tissue engineering applications. *International Journal of Biological Macromolecules*, *149*, 724–731. https://doi.org/10.1016/j.ijbiomac.2020.01.276

Nedović, V., Gibson, B., Mantzouridou, T. F., Bugarski, B., Djordjević, V., Kalušević, A., Paraskevopoulou, A., Sandell, M., Šmogrovičová, D., & Yilmaztekin, M. (2015). Aroma formation by immobilized yeast cells in fermentation processes. *Yeast*, *32*(1), 173–216. https://doi.org/10.1002/yea.3042

Negulescu, P. G., Risner, D., Spang, E. S., Sumner, D., Block, D., Nandi, S., & McDonald, K. A. (2023). Techno-economic modeling and assessment of cultivated meat: Impact of production bioreactor scale. *Biotechnology and Bioengineering*, *120*(4), 1055–1067. https://doi.org/10.1002/bit.28324

Ng, E. X., Wang, M., Neo, S. H., Tee, C. A., Chen, C.-H., & Van Vliet, K. J. (2021). Dissolvable Gelatin-Based Microcarriers Generated through Droplet Microfluidics for Expansion and Culture of Mesenchymal Stromal Cells. *Biotechnology Journal*, *16*(3), e2000048. https://doi.org/10.1002/biot.202000048

Nijdam, D., Rood, T., & Westhoek, H. (2012). The price of protein: Review of land use and carbon footprints from life cycle assessments of animal food products and their substitutes. *Food Policy*, *37*(6), 760–770. https://doi.org/10.1016/j.foodpol.2012.08.002

Noothalapati, H., Sasaki, T., Kaino, T., Kawamukai, M., Ando, M., Hamaguchi, H., & Yamamoto, T. (2016). Label-free Chemical Imaging of Fungal Spore Walls by Raman Microscopy and Multivariate Curve Resolution Analysis. *Scientific Reports*, *6*, 27789. https://doi.org/10.1038/srep27789

Norris, S. C. P., Kawecki, N. S., Davis, A. R., Chen, K. K., & Rowat, A. C. (2022). Emulsion-templated microparticles with tunable stiffness and topology: Applications as edible microcarriers for cultured meat. *Biomaterials*, *287*, 121669. https://doi.org/10.1016/j.biomaterials.2022.121669

Nyman, J., Lacintra, M. G., Westman, J. O., Berglin, M., Lundin, M., Lennartsson, P. R., & Taherzadeh, M. J. (2013). Pellet formation of zygomycetes and immobilization of yeast. *New Biotechnology*, *30*(5), 516–522. https://doi.org/10.1016/j.nbt.2013.05.007

Odintsova, N. A., Dyachuk, V. A., & Nezlin, L. P. (2010). Muscle and neuronal differentiation in primary cell culture of larval Mytilus trossulus (Mollusca: Bivalvia). *Cell and Tissue Research*, *339*(3), 625–637. https://doi.org/10.1007/s00441-009-0918-3

Ogawa, M. (2024). *Edible Mycelium Carriers as Proliferation And Differentiation Support for Anchorage Dependent Animal Cells in Cultivated Meat Production*.

Ogawa, M., Bisson, L. F., García-Martínez, T., Mauricio, J. C., & Moreno-García, J. (2019). New insights on yeast and filamentous fungus adhesion in a natural co-immobilization system: Proposed advances and applications in wine industry. *Applied Microbiology and Biotechnology*, *103*(12), 4723–4731. https://doi.org/10.1007/s00253-019-09870-4

Ogawa, M., Carmona-Jiménez, P., García-Martínez, T., Jorrín-Novo, J. V., Moreno, J., Rey, M. D., & Moreno-García, J. (2022). Use of yeast biocapsules as a fungal-based immobilized cell technology for Indian Pale Ale-type beer brewing. *Applied Microbiology and Biotechnology*, *106*(22), 7615–7625. https://doi.org/10.1007/s00253-022-12239-9

Ogawa, M., Moreno García, J., Nitin, N., Baar, K., & Block, D. E. (2022). Assessing edible filamentous fungal carriers as cell supports for growth of yeast and cultivated meat. *Foods*, *11*(19), 3142. https://doi.org/10.3390/foods11193142

Oh, D.-C., Kauffman, C. A., Jensen, P. R., & Fenical, W. (2007). Induced production of emericellamides A and B from the marine-derived fungus Emericella sp. In competing co-culture. *Journal of Natural Products*, *70*(4), 515–520. https://doi.org/10.1021/np060381f

Okada, M., Smith, N. I., Palonpon, A. F., Endo, H., Kawata, S., Sodeoka, M., & Fujita, K. (2012). Label-free Raman observation of cytochrome c dynamics during apoptosis. *Proceedings of the National Academy of Sciences of the United States of America*, *109*(1), 28–32. https://doi.org/10.1073/pnas.1107524108

O'Neill, E. N., Cosenza, Z. A., Baar, K., & Block, D. E. (2021). Considerations for the development of cost-effective cell culture media for cultivated meat production. *Comprehensive Reviews in Food Science and Food Safety*, *20*(1), 686–709. https://doi.org/10.1111/1541-4337.12678

Pajčin, I., Knežić, T., Savic Azoulay, I., Vlajkov, V., Djisalov, M., Janjušević, L., Grahovac, J., & Gadjanski, I. (2022). Bioengineering outlook on cultivated meat production. *Micromachines*, *13*(3). https://doi.org/10.3390/mi13030402

Papagianni, M. (2004). Fungal morphology and metabolite production in submerged mycelial processes. *Biotechnology Advances*, *22*(3), 189–259. https://doi.org/10.1016/j.biotechadv.2003.09.005

Pareek, M., Allaway, W. G., & Ashford, A. E. (2006). Armillaria luteobubalina mycelium develops air pores that conduct oxygen to rhizomorph clusters. *Mycological Research*, *110*(Pt 1), 38–50. https://doi.org/10.1016/j.mycres.2005.09.006

Park, S., Lee, M., Jung, S., Lee, H., Choi, B., Choi, M., Lee, J. M., Yoo, K. H., Han, D., Lee, S. T., Koh, W.-G., Bang, G., Hwang, H., Lee, S., & Hong, J. (2024). Rice grains integrated with animal cells: A

shortcut to a sustainable food system. *Matter*, *7*(3), 1292–1313. https://doi.org/10.1016/j.matt.2024.01.015

Pastor-Vega, N., Carbonero-Pacheco, J., Mauricio, J. C., Moreno, J., García-Martínez, T., Nitin, N., Ogawa, M., Rai, R., & Moreno-García, J. (2023). Flor yeast immobilization in microbial biocapsules for Sherry wine production: Microvinification approach. *World Journal of Microbiology and Biotechnology*, *39*(10), 271. https://doi.org/10.1007/s11274-023-03713-1

Pathak, V. M. & Navneet. (2017). Review on the current status of polymer degradation: A microbial approach. *Bioresources and Bioprocessing*, *4*(1), 15. https://doi.org/10.1186/s40643-017-0145-9

Peinado Amores, R., & Garcia Mauricio, J. C. (n.d.). *Method of obtaining yeast biocapsules, biocapsules thus obtained and applications of same* (Patent WO2004029240A1). Retrieved May 12, 2022, from https://patents.google.com/patent/WO2004029240A1/en

Peinado, R. A., Moreno, J. J., Villalba, J. M., González-Reyes, J. A., Ortega, J. M., & Mauricio, J. C. (2006). Yeast biocapsules: A new immobilization method and their applications. *Enzyme and Microbial Technology*, *40*(1), 79–84. https://doi.org/10.1016/j.enzmictec.2005.10.040

Post, M., & van der Weele, C. (2014). Principles of tissue engineering for food. In *Principles of tissue engineering* (pp. 1647–1662). Elsevier. https://doi.org/10.1016/B978-0-12-398358-9.00078-1

Puig-Pujol, A., Bertran, E., García-Martínez, T., Capdevila, F., Mínguez, S., & Mauricio, J. C. (2013). Application of a new organic yeast immobilization method for sparkling wine production. *American Journal of Enology and Viticulture*, *64*(3), 386–394. https://doi.org/10.5344/ajev.2013.13031

Rafiq, Q. A., Coopman, K., & Hewitt, C. J. (2013). Scale-up of human mesenchymal stem cell culture: Current technologies and future challenges. *Current Opinion in Chemical Engineering*, *2*(1), 8–16. https://doi.org/10.1016/j.coche.2013.01.005

Raman, C. V., & Krishnan, K. S. (1928). A New Type of Secondary Radiation. *Nature*, *121*(3048), 501–502. https://doi.org/10.1038/121501c0

Ravi Kumar, M. N. V. (2000). A review of chitin and chitosan applications. *Reactive and Functional Polymers*, *46*(1), 1–27. https://doi.org/10.1016/S1381-5148(00)00038-9

Reid, J. A., McDonald, A., & Callanan, A. (2020). Modulating electrospun polycaprolactone scaffold morphology and composition to alter endothelial cell proliferation and angiogenic gene response. *PLOS ONE*, *15*(10), e0240332. https://doi.org/10.1371/journal.pone.0240332

Rodrigues, A. L., Rodrigues, C. A. V., Gomes, A. R., Vieira, S. F., Badenes, S. M., Diogo, M. M., & Cabral, J. M. S. (2019). Dissolvable Microcarriers Allow Scalable Expansion And Harvesting Of Human Induced Pluripotent Stem Cells Under Xeno-Free Conditions. *Biotechnology Journal*, *14*(4), 1800461. https://doi.org/10.1002/biot.201800461

Rojas López-Menchero, J., Ogawa, M., Mauricio, J., Moreno, J., & Moreno-García, J. (2021). Effect of calcium alginate coating on the cell retention and fermentation of a fungus-yeast immobilization system. *LWT*, *144*, 111250. https://doi.org/10.1016/j.lwt.2021.111250

Rosenberg, M., Gutnick, D., & Rosenberg, E. (1980). Adherence of bacteria to hydrocarbons: A simple method for measuring cell-surface hydrophobicity. *FEMS Microbiology Letters*, *9*(1), 29–33. https://doi.org/10.1111/j.1574-6968.1980.tb05599.x

Rowley, J., Abraham, E., Campbell, A., Brandwein, H., & Oh, S. (2012). Meeting Lot-Size Challenges of Manufacturing Adherent Cells for Therapy. *Journal BioProcess Int*. https://www.semanticscholar.org/paper/Meeting-Lot-Size-Challenges-of-Manufacturing-Cells-Rowley-Abraham/30725a7fde9538213672bc9ea969f8ae8558e0c3

Rubio, N. R., Fish, K. D., Trimmer, B. A., & Kaplan, D. L. (2019). In Vitro Insect Muscle for Tissue Engineering Applications. *ACS Biomaterials Science & Engineering*, *5*(2), 1071–1082. https://doi.org/10.1021/acsbiomaterials.8b01261

Ruggeri, M., Miele, D., Contardi, M., Vigani, B., Boselli, C., Icaro Cornaglia, A., Rossi, S., Suarato, G., Athanassiou, A., & Sandri, G. (2023). Mycelium-based biomaterials as smart devices for skin wound healing. *Frontiers in Bioengineering and Biotechnology*, *11*, 1225722. https://doi.org/10.3389/fbioe.2023.1225722

Saif, F. A., Yaseen, S. A., Alameen, A. S., Mane, S. B., & Undre, P. B. (2021). Identification and characterization of Aspergillus species of fruit rot fungi using microscopy, FT-IR, Raman and UV-Vis spectroscopy. *Spectrochimica Acta. Part A, Molecular and Biomolecular Spectroscopy*, *246*, 119010. https://doi.org/10.1016/j.saa.2020.119010

Sakurai, A., Nishida, Y., Saito, H., & Sakakibara, M. (2000). Ethanol production by repeated batch culture using yeast cells immobilized within porous cellulose carriers. *Journal of Bioscience and Bioengineering*, *90*(5), 526–529. https://doi.org/10.1016/s1389-1723(01)80034-7

Sart, S., Agathos, S. N., & Li, Y. (2013). Engineering stem cell fate with biochemical and biomechanical properties of microcarriers. *Biotechnology Progress*, *29*(6), 1354–1366. https://doi.org/10.1002/btpr.1825

Schindelin, J., Arganda-Carreras, I., Frise, E., Kaynig, V., Longair, M., Pietzsch, T., Preibisch, S., Rueden, C., Saalfeld, S., Schmid, B., Tinevez, J.-Y., White, D. J., Hartenstein, V., Eliceiri, K., Tomancak, P., & Cardona, A. (2012). Fiji: An open-source platform for biological-image analysis. *Nature Methods*, *9*(7), 676–682. https://doi.org/10.1038/nmeth.2019

Schmidt, J. J., Jeong, J., & Kong, H. (2011). The interplay between cell adhesion cues and curvature of cell adherent alginate microgels in multipotent stem cell culture. *Tissue Engineering. Part A*, *17*(21–22), 2687–2694. https://doi.org/10.1089/ten.tea.2010.0685

Schuster, K. C., Urlaub, E., & Gapes, J. R. (2000). Single-cell analysis of bacteria by Raman microscopy: Spectral information on the chemical composition of cells and on the heterogeneity in a culture.

Journal of Microbiological Methods, *42*(1), 29–38. https://doi.org/10.1016/s0167-7012(00)00169-x

Shigeto, S., & Takeshita, N. (2022). Raman Micro-spectroscopy and Imaging of Filamentous Fungi. *Microbes and Environments*, *37*(6). https://doi.org/10.1264/jsme2.ME22006

State of the Industry Reports—The Good Food Institute. (2024, April 16). https://gfi.org/state-of-the-industry-reports/

Steam Sterilization | Disinfection & Sterilization Guidelines | Guidelines Library | Infection Control | CDC. (n.d.). Retrieved May 11, 2022, from https://www.cdc.gov/infectioncontrol/guidelines/disinfection/sterilization/steam.html

Steinfeld, H., Gerber, P., Wassenaar, T., Castel, V., Rosales, M., & de Haan, C. (2006). *Livestock's long shadow*. https://www.fao.org/4/a0701e/a0701e00.htm

Stöckel, S., Kirchhoff, J., Neugebauer, U., Rösch, P., & Popp, J. (2016). The application of Raman spectroscopy for the detection and identification of microorganisms. *Journal of Raman Spectroscopy*, *47*(1), 89–109. https://doi.org/10.1002/jrs.4844

Sun, Z., Guo, S. S., & Fässler, R. (2016). Integrin-mediated mechanotransduction. *Journal of Cell Biology*, *215*(4), 445–456. https://doi.org/10.1083/jcb.201609037

Thomas, K., Engler, A. J., & Meyer, G. A. (2015). EXTRACELLULAR MATRIX REGULATION IN THE MUSCLE SATELLITE CELL NICHE. *Connective Tissue Research*, *56*(1), 1–8. https://doi.org/10.3109/03008207.2014.947369

Tomiyama, A. J., Kawecki, N. S., Rosenfeld, D. L., Jay, J. A., Rajagopal, D., & Rowat, A. C. (2020). Bridging the gap between the science of cultured meat and public perceptions. *Trends in Food Science & Technology*, *104*, 144–152. https://doi.org/10.1016/j.tifs.2020.07.019

Truong, Q. T., Miyata, N., & Iwahori, K. (2004). Growth of Aspergillus oryzae during treatment of cassava starch processing wastewater with high content of suspended solids. *Journal of Bioscience and Bioengineering*, *97*(5), 329–335. https://doi.org/10.1016/S1389-1723(04)70214-5

Tsuruwaka, Y., & Shimada, E. (2022). Reprocessing seafood waste: Challenge to develop aquatic clean meat from fish cells. *Npj Science of Food*, *6*(1), 7. https://doi.org/10.1038/s41538-021-00121-3

Tuomisto, H. L., & Teixeira de Mattos, M. J. (2011). Environmental Impacts of Cultured Meat Production. *Environmental Science & Technology*, *45*(14), 6117–6123. https://doi.org/10.1021/es200130u

Pitchbook. *US approval of lab-grown meat to unleash "stifled" sector*. Retrieved September 19, 2024, from https://pitchbook.com/news/articles/lab-grown-cultivated-meat-usda-vc-deals

van der Weele, C., & Tramper, J. (2014). Cultured meat: Every village its own factory? *Trends in Biotechnology*, *32*(6), 294–296. https://doi.org/10.1016/j.tibtech.2014.04.009

van de Velde, F., Lourenço, N. D., Pinheiro, H. M., & Bakker, M. (2002). Carrageenan: A Food-Grade and Biocompatible Support for Immobilisation Techniques. *Advanced Synthesis & Catalysis*. https://onlinelibrary.wiley.com/doi/10.1002/1615-4169(200209)344:8%3C815::AID-ADSC815%3E3.0.CO;2-H

Vasilieva, S., Lobakova, E., Grigoriev, T., Selyakh, I., Semenova, L., Chivkunova, O., Gotovtsev, P., Antipova, C., Zagoskin, Y., Scherbakov, P., Lukyanov, A., Lukanina, K., & Solovchenko, A. (2020). Bio-inspired materials for nutrient biocapture from wastewater: Microalgal cells immobilized on chitosan-based carriers. *Journal of Water Process Engineering*, 101774. https://doi.org/10.1016/j.jwpe.2020.101774

Veiter, L., Rajamanickam, V., & Herwig, C. (2018). The filamentous fungal pellet-relationship between morphology and productivity. *Applied Microbiology and Biotechnology*, *102*(7), 2997–3006. https://doi.org/10.1007/s00253-018-8818-7

Verbruggen, S., Luining, D., van Essen, A., & Post, M. J. (2018). Bovine myoblast cell production in a microcarriers-based system. *Cytotechnology*, *70*(2), 503–512. https://doi.org/10.1007/s10616-017-0101-8

Verstrepen, K. J., Derdelinckx, G., Verachtert, H., & Delvaux, F. R. (2003). Yeast flocculation: What brewers should know. *Applied Microbiology and Biotechnology*, *61*(3), 197–205. https://doi.org/10.1007/s00253-002-1200-8

Verstrepen, K. J., & Klis, F. M. (2006). Flocculation, adhesion and biofilm formation in yeasts. *Molecular Microbiology*, *60*(1), 5–15. https://doi.org/10.1111/j.1365-2958.2006.05072.x

Wanderley, M. C. de A., Neto, J. M. W. D., Filho, J. L. de L., Lima, C. de A., Teixeira, J. A. C., & Porto, A. L. F. (2016). Collagenolytic enzymes produced by fungi: A systematic review. *Brazilian Journal of Microbiology*, *48*(1), 13–24. https://doi.org/10.1016/j.bjm.2016.08.001

Wang, H.-T., Yang, J.-T., Chen, K.-I., Wang, T.-Y., Lu, T.-J., & Cheng, K.-C. (2019). Hydrolyzation of mogrosides: Immobilized β-glucosidase for mogrosides deglycosylation from Lo Han Kuo. *Food Science & Nutrition*, *7*(2), 834–843. https://doi.org/10.1002/fsn3.932

Wang, X., & Cooper, S. (2013). Adhesion of Endothelial Cells and Endothelial Progenitor Cells on Peptide-Linked Polymers in Shear Flow. *Tissue Engineering. Part A*, *19*(9–10), 1113–1121. https://doi.org/10.1089/ten.tea.2011.0653

Wang, Z., Zhang, X., Xue, L., Wang, G., Li, X., Chen, J., Xu, R., & Xu, T. (2023). A controllable gelatin-based microcarriers fabrication system for the whole procedures of MSCs amplification and tissue engineering. *Regenerative Biomaterials*, *10*, rbad068. https://doi.org/10.1093/rb/rbad068

Westhoek, H., Lesschen, J. P., Rood, T., Wagner, S., De Marco, A., Murphy-Bokern, D., Leip, A., van Grinsven, H., Sutton, M. A., & Oenema, O. (2014). Food choices, health and environment: Effects of cutting Europe's meat and dairy intake. *Global Environmental Change*, *26*, 196–205. https://doi.org/10.1016/j.gloenvcha.2014.02.004

Williams, D., & Munnecke, D. M. (1981). Production of ethanol by immobilized yeast cells. *Biotechnol. Bioeng.; (United States)*, *23:8*. https://doi.org/10.1002/bit.260230809

Yablonka-Reuveni, Z. (2011). The skeletal muscle satellite cell: Still young and fascinating at 50. *The Journal of Histochemistry and Cytochemistry*, *59*(12), 1041–1059. https://doi.org/10.1369/0022155411426780

Yan, X., Zhang, K., Yang, Y., Deng, D., Lyu, C., Xu, H., Liu, W., & Du, Y. (2020). Dispersible and Dissolvable Porous Microcarrier Tablets Enable Efficient Large-Scale Human Mesenchymal Stem Cell Expansion. *Tissue Engineering Part C: Methods*, *26*(5), 263–275. https://doi.org/10.1089/ten.tec.2020.0039

Yousif, E., & Haddad, R. (2013). Photodegradation and photostabilization of polymers, especially polystyrene: Review. *SpringerPlus*, *2*(1), 398. https://doi.org/10.1186/2193-1801-2-398

Zeng, Y., Chen, E., Zhang, X., Li, D., Wang, Q., & Sun, Y. (2022). Nutritional Value and Physicochemical Characteristics of Alternative Protein for Meat and Dairy-A Review. *Foods (Basel, Switzerland)*, *11*(21), 3326. https://doi.org/10.3390/foods11213326

Zhang, J., & Zhang, J. (2016). The filamentous fungal pellet and forces driving its formation. *Critical Reviews in Biotechnology*, *36*(6), 1066–1077. https://doi.org/10.3109/07388551.2015.1084262

Zhang, J., Zhao, W., Zhang, H., Wang, Z., Fan, C., & Zang, L. (2018). Recent achievements in enhancing anaerobic digestion with carbon- based functional materials. *Bioresource Technology*, *266*, 555–567. https://doi.org/10.1016/j.biortech.2018.07.076

Zhang, N., Mendieta-Esteban, J., Magli, A., Lilja, K. C., Perlingeiro, R. C. R., Marti-Renom, M. A., Tsirigos, A., & Dynlacht, B. D. (2020). Muscle progenitor specification and myogenic differentiation are associated with changes in chromatin topology. *Nature Communications*, *11*(1), 6222. https://doi.org/10.1038/s41467-020-19999-w

Zhou, W., Cheng, Y., Li, Y., Wan, Y., Liu, Y., Lin, X., & Ruan, R. (2012). Novel fungal pelletization-assisted technology for algae harvesting and wastewater treatment. *Applied Biochemistry and Biotechnology*, *167*(2), 214–228. https://doi.org/10.1007/s12010-012-9667-y

Zhu, Y. (2007). Immobilized cell fermentation for production of chemicals and fuels. In *Bioprocessing for Value-Added Products from Renewable Resources* (pp. 373–396). Elsevier. https://doi.org/10.1016/B978-044452114-9/50015-3

Žnidaršič-Plazl, P. (2021). Biocatalytic process intensification via efficient biocatalyst immobilization, miniaturization, and process integration. *Current Opinion in Green and Sustainable Chemistry*, *32*, 100546. https://doi.org/10.1016/j.cogsc.2021.100546